# MORPHOMETRIC HISTOPATHOLOGY OF THE PHYSIOLOGICALLY FIXED KERATOCONIC CORNEA

By

Jessica H. Mathew, O.D.

DISSERTATION

In partial satisfaction of the requirements for the degree of

DOCTOR OF PHILOSOPHY

in

PHYSIOLOGICAL OPTICS

Presented to the Graduate Faculty of the

College of Optometry
University of Houston

August 2010

Approved:

Jan P.G. Bergmanson, O.D., Ph.D., D.Sc (Chair)

John D. Goosey, M.D.

Norman E. Leach, O.D., M.S.

William L. Miller, O.D., Ph.D.

Michael D. Twa, O.D., Ph.D.

Committee in Charge

## Dedication

This work is dedicated to my parents, Gary and Bessie Horne, for their eternal belief in me, for always being so proud of me and for my mom doing all the worrying for me so I did not have to! I could not have accomplished so much without their love and support and their Godly example in my life.

**Acknowledgments**

Advisor/Committee Chair:

Jan PG Bergmanson, OD, PhD, PhD h.c., Dsc
*Thank you for all of your encouragement, guidance and tutelage along this cultivating journey. You have been an exceptional mentor, colleague and friend!*

Committee Members:

John D. Goosey, MD
Norman E. Leach, OD, MS
William L. Miller, OD, PhD
Michael D. Twa, OD, PhD
Yaron S. Rabinowitz, MD (Consultant)

Graduate Studies Dean: Laura Frishman, PhD

Graduate Studies Administrator: Michele Murphy

The Faculty and Staff at the University of Houston College of Optometry

Audio Visual Department at the University of Houston College of Optometry
*Special Thanks to Kim Thompson*

Funding and Support

Texas Eye Research and Technology Center
*for providing continual financial and travel support for this research*

John D. Goosey, MD; Houston Eye Associates
*for providing the necessary keratoconic and eye bank tissue and for offering clinical, surgical and intellectual input*

Eye Birth Defects Research Foundation
UHCO NEI Core Grant P30 EY07551
American Optometric Foundation's Ezell Fellowship
NIH Loan Repayment Grant

My Family

…and especially,
My husband and best friend, Danny

# MORPHOMETRIC HISTOPATHOLOGY OF THE PHYSIOLOGICALLY FIXED KERATOCONIC CORNEA

by

Jessica Horne Mathew, OD

**DISSERTATION**

In partial satisfaction of the requirements for the degree of

**DOCTOR OF PHILOSOPHY**

**in**

**PHYSIOLOGICAL OPTICS & VISION SCIENCE**

Presented to
the Graduate Faculty of the

College of Optometry
University of Houston

Houston, Texas

August, 2010

# General Abstract

**Purpose:** Clinically, keratoconus is a condition associated with corneal ectasia, thinning, steepening and scarring, and sometimes necessitates transplant surgery. Exactly where this corneal pathology starts, what structures are involved and what is lost in the thinning process is poorly defined in literature. The purpose of this study was to investigate the etiology, pathophysiology and the structural collapse leading to ectasia by utilizing a histopathological approach.

**Methods:** A total of 15 surgically removed keratoconic corneas and 7 eye bank control corneas were used. The corneas were fixed in 2% glutaraldehyde in 80mM sodium cacodylate (pH 7.4, 320 to 340 mOsm/kg) and prepared for transverse sectioning with light (Olympus BX51 digital) and transmission electron microscopy (Jeol 100C, initially, and the Tecnai G2 12 twin). Serial electron micrographs were taken of the geometric center of normal corneas and the central cone region of keratoconic corneas. Montages were created for full stromal thickness lamellar counts and for assessment of the anterior limiting lamina (ALL)/stromal interface. Lamellar counts adhered to a specific set of criteria, while a morphometric approach was utilized to define the features of the ALL/stromal interface. The central cone and mid-peripheral regions of the keratoconic cornea were evaluated using light microscopy (LM) and larger anatomical and pathological structures were quantified with the aid of NIH image software.

**Results:** The normal cornea contained 242$\pm$4 lamellae, while the keratoconic cornea averaged 319$\pm$105 but, if an extremely thinned keratoconic cornea was excluded, the

average was 360±22. In the keratoconic cornea, the middle and, to a degree, posterior lamellae had broken up into smaller units. In the normal cornea**,** the ALL and stromal layers showed some shallow overlapping of <1µm in either direction. The anterior stromal lamellae were delicate and interweaved extensively. In central and peripheral LM assessments of the keratoconic cornea, the ALL was thinned or lost over 60% of the area examined and the thin anterior lamellae were absent. Anterior lamellae in central control cornea appeared, at intervals, to terminate surrounded by dense staining particles. This unreported stromal feature was termed electron dense formation and was not observed in the keratoconic cornea. The epithelial thickness varied greatly across the keratoconic cornea (14-92µm), while the epithelium in normal maintained a uniform thickness. Keratoconic specimens contained densely stained, distorted epithelial cells and in 58%, a grossly thickened basement membrane. Stroma in the normal cornea contained predominantly one cell type, the keratocyte, along with the occasional Schwann cell and neuron, but in keratoconus, other cells were present in areas where apparent stromal and ALL disassembling occurred.

**Conclusions:** The keratoconic stroma had paradoxically 50% more lamellae than the normal and this was explained by the fragmentation of lamellae – not an actual increase in lamellae, but rather the breaking apart of lamellae, which has not been described elsewhere. The complete loss of anterior interweaving lamellae in the keratoconic corneas examined likely contributes to the thinning of the keratoconic corneas seen clinically. The terminating lamellae in the normal central cornea suggests that stromal lamellae do not span the full width of the cornea, which is in contradiction to existing

literature. The present study reported a clear and well-defined epithelial contribution to pathological changes in keratoconus, but this work does not establish which layer - the epithelium or stroma – is affected first. The extensive destruction of ALL reported here is in contrast to previous statements in literature. It appears that the removal of ALL and anterior lamellae is accomplished by stromal cells that may have been recruited from outside the cornea.

This morphometric, ultrastructural study has demonstrated the anterior focus of keratoconus and the epithelial involvement in the disease, all of which is of importance to contact lens practitioners and surgeons. The new knowledge on the normal human cornea, e.g. number of lamellae and anterior structural integration, generated by this work has multiple surgical and clinical applications. The loss and disintegration of lamellar structure in keratoconus appears to be an important factor in provoking ectasia and its accompanying devastating effect on vision.

# Table of Contents

# List of Figures

# List of Tables

# Chapter 1 - General Introduction

## Background and Significance

Keratoconus is a non-inflammatory condition leading to ectasia, steepening, thinning and scarring of the cornea (Nottingham, 1854; Rabinowitz, 1998; Zadnik et al., 1998, Barr et al., 2000), causing the cornea to take on a conical shape. This conical shape is typically concentrated to an inferior paracentral area (Leibowitz & Morello, 1998; Zadnik et al., 1998; Woodward and Rubinstein, 2007; Patel et al., 2009) and referred to as the cone region. Although keratoconus is described as a bilateral condition, occurring in both eyes, the severity of the disease is usually asymmetric between the two eyes (Nichols et al., 2004). Keratoconus is usually manifest in youth or adolescence, affects all ethnic groups worldwide and has no preference for gender (Rabinowitz, 1998). It is typically an isolated disease, but can be associated with other pathological conditions such as Down's Syndrome, Leber's Congenital Amaurosis and connective tissue disorders (Rabinowitz, 1998).

Keratoconus results in considerable visual impairment due to anterior corneal surface distortions causing irregular myopic astigmatism (Duke-Elder and Leigh, 1965; Mahmoud et al., 2008). Although keratoconus is a relatively uncommon disease, with an incidence of 1 in 2000 and a prevelance of 54.5 in 100,000 (Kennedy et al., 1986; Rabinowitz, 1998), there is a significant clinical importance because the quality of life for individuals afflicted with keratoconus can be quite severe and devastating. These patients are faced with an increasingly blurred or distorted retinal image, a lifetime of, likely uncomfortable, contact lens dependence, the threat of major ocular surgery and possible limitations in career choice, all of which will have a profound affect on quality of life.

Kymes and colleagues (2004) indicated that, "because it affects young adults [who are in the prime of their life], the magnitude of its public health impact is disproportionate to its prevalence." Furthermore, keratoconus is the most common corneal disease leading to corneal transplantation (Maeno et al., 2000), penetrating keratoplasty being the most common (Pramanik et al., 2006), with as many as 20% of keratoconic patients requiring it (Rabinowitz, 1998).

Challenges of the irregular cornea (i.e. irregular astigmatism) have long been an issue for practitioners in managing the keratoconic patient, since a spectacle prescription will not provide optimal vision. In fact, these challenges became evident as early as the late 1800's and, in large part, motivated the development of the first contact lenses, which was undertaken by Fick and Kalt (Fick, 1988; Brachner A, 1988; Pearson, 1989; Albert, 1996).

Keratoconus was first described over 150 years ago (Nottingham, 1854), and yet the etiology of this disease is still debated. Several proposed etiologies exist in literature (Table 1.1) including inflammation, atopy, collagen matrix breakdown, eye rubbing and genetic factors (Teng, 1963; Hartstein, 1968; Karsearas and Ruben, 1976; Berman, 1991; Kim et al., 1999; Kenney et al., 2000; Krachmer, 2004; McMonnies, 2009). Opinions are also divided on whether keratoconus is a dystrophy (Cintron, 1994; Arffa, 1997; Yanoff and Sassani, 2009) or degeneration (Maguire, 1998) while some are undecided (Duke-Elder and Leigh, 1965; Casey & Sharif, 1991; Feder & Kshettry, 2005; McMahon & Szczotka-Flynn, 2005) (Table 1.2). There are also conflicting opinions as to which corneal layer this disease first affects (Teng 1963; Karsearas and Ruben, 1976; Kim et al., 1999; Kenney et al., 2000). It seems reasonable that there may be multiple causes or

types of keratoconus (Karsearas and Ruben, 1976; Sherwin & Brookes, 2004), but this lack of agreement demonstrates how incomplete our understanding is.

The cornea is classically defined by five distinct anatomical layers (Figure 1.1), and becomes thinner in keratoconus. Corneal thinning is perhaps the clinical sign that is always present in this disease, but a systematic evaluation of the structural alterations that occur in keratoconus has not been described in detail in the scientific literature. There are literature reports of breaks, interruptions, tears or ruptures in the ALL of keratoconic corneas (Duke-Elder, 1943; Duke-Elder & Leigh, 1965; Chi et al., 1956; McPherson and Kiffney, 1968; Shapiro et al., 1986; Kaas-Hansen, 1993, Arffa, 1997; Leibowitz and Morello, 1998; Maguire, 1998; Sawaguchi et al., 1998; Eagle, 1999; Sugar, 2004; Feder and Kshettry, 2005; Nakamura et al., 2005; Rabinowitz, 2005; Krachmer and Palay, 2006; Yanoff and Sassani, 2009). According to Morishige (et al., 2007) and Hayes (et al., 2007), the keratoconic cornea is characterized by "less lamellar interweaving and marked reduction or loss of [anterior] inserting lamellae". However, the posterior cornea appears to be unaffected until late stages when ectasia may provoke hydrops formation (Thota et al., 2006). The body of available literature appears to indicate that keratoconus is an anterior disease process, at least initially, but which layer is affected first is not resolved. Microscopic alterations in the keratoconic cornea are also not well-defined in literature and thus, structural changes observed clinically are not well understood. One objective of this research was to systematically measure and quantify corneal changes in the keratoconic cornea to determine which corneal layers are truly affected by the disease.

Duke-Elder and Leigh (1965) stated that, "pathological investigations have provided little to add to the biomicroscopic appearances" of keratoconus. Most accounts

in literature since are descriptive, involve few eyes and do not utilize the resolution of the transmission electron microscope (TEM). More critically, these studies utilized fixative that causes substantial tissue shrinkage (McPherson et al., 1968; Scroggs and Proia 1992; Kaas-Hansen, 1993; Sawaguchi et al., 1998; Rohrback et al., 2006). Subsequent distortion of the already distorted keratoconic cornea further obscures the investigation of the cornea, and leads to confusion about what is truly an effect of the disease and what is a product of tissue preparation.

By using the high resolution of TEM and a morphometric approach on physiologically fixed tissue, the intent of this research was to define the locus and pathophysiology of keratoconus, determine the exact structures and components that are lost in corneal thinning and gain insights on the mechanism of events leading to ectasia. To accomplish these goals, it was also necessary to first advance current knowledge of stromal architecture in the normal cornea. It is important to understand these pathological changes that occur in keratoconus and to recognize which layers are affected before a cure for keratoconus in the future can even be considered.

# Specific Aims

## ***Specific Aim I:***

It is generally believed that corneal thinning in keratoconus has primarily occurred in the stromal tissue. Leibowitz and Morello (1998) state that, “collagen fibers are said to be normal, with thinning attributable to a decrease in the number of collagen lamellae”. The loss of lamellae as an explanation to corneal thinning is also proposed by other sources (Apple & Rabb, 1998; Sugar, 2004; Morshige et al., 2007). However, no systematic studies have provided full thickness lamellar counts to support these claims. By counting the number of lamellae, as defined in the chapters to follow, and investigating stromal characteristics in normal versus keratoconus, one aspect of the keratoconic stroma will be defined and better understood.

The research described here addressed this issue by defining the number of lamellae across the entire thickness of keratoconic corneas removed by penetrating keratoplasty (PKP). However, since the number of lamellae, in a cross section, forming the normal human cornea has never been established, a lamellar count in normal eyes was required first. My hypothesis was that the number of countable stromal lamellae in the keratoconic cornea are reduced when compared to the normal eye.

***Specific Aim II:***

Bron (et al., 2001) reported that "a proportion of the anterior lamellae are known to be inserted directly into Bowman's layer" in the normal human cornea. Sir William Bowman (1847), a distinguished anatomist and ophthalmologist in the mid-nineteenth century, also implied in his diagrams, a similar relationship between anterior limiting lamina (ALL) and stromal lamellae. Bron (et al., 2001**)** went further to suggest that keratoconus is a case of disinsertion of stromal lamellae from the ALL. The implication of this notion is that the breakdown of the stromal-ALL interface is an important aspect of the keratoconus disease process. Based on my previous qualitative observations, I propose that the border between the two corneal layers is relatively well defined in normal eyes and lacks stromal lamellae traversing it. The hypothesis for the second research question was that, other than a limited overlapping of the two tissues, this interface in the normal human cornea contains no full thickness lamellar insertions into the ALL, nor is it structurally modified to accommodate extensive insertions as seen with extraocular muscle insertions into the sclera (Bergmanson, 2010).

***Specific Aim III:***

As stated above, keratoconus is the most common ophthalmic pathology requiring corneal transplant surgery (Maeno et al., 2000) with 10-20% of patients requiring it (Rabinowitz, 1998; Pramanik et al., 2006), making these excised keratoconic corneas relatively accessible for research. Surprisingly, there are no systematic research studies assessing the ultrastructural characteristics of the keratoconic cornea with multiple

samples of tissue. This is especially important in a disease with such heterogenous clinical manifestations.

The third part of this dissertation work involved a general histopathological assessment of the keratoconic cornea utilizing light and transmission electron microscopy. This effort involved morphometry of multiple keratoconic corneas in order to systematically evaluate which corneal layers are involved in the keratoconus disease process. An important aspect of the study was that, unlike previous studies, these corneas were preserved with little or no induced preparation artifacts since the fixative better matches that of normal corneal physiology. The hypothesis for this research effort was that the epithelial, ALL and stromal layers, in their full thickness, are all involved in the disease process, but with a focal point centered in the cone region and the more peripheral corneal regions affected to a lesser degree.

## Figures and Tables

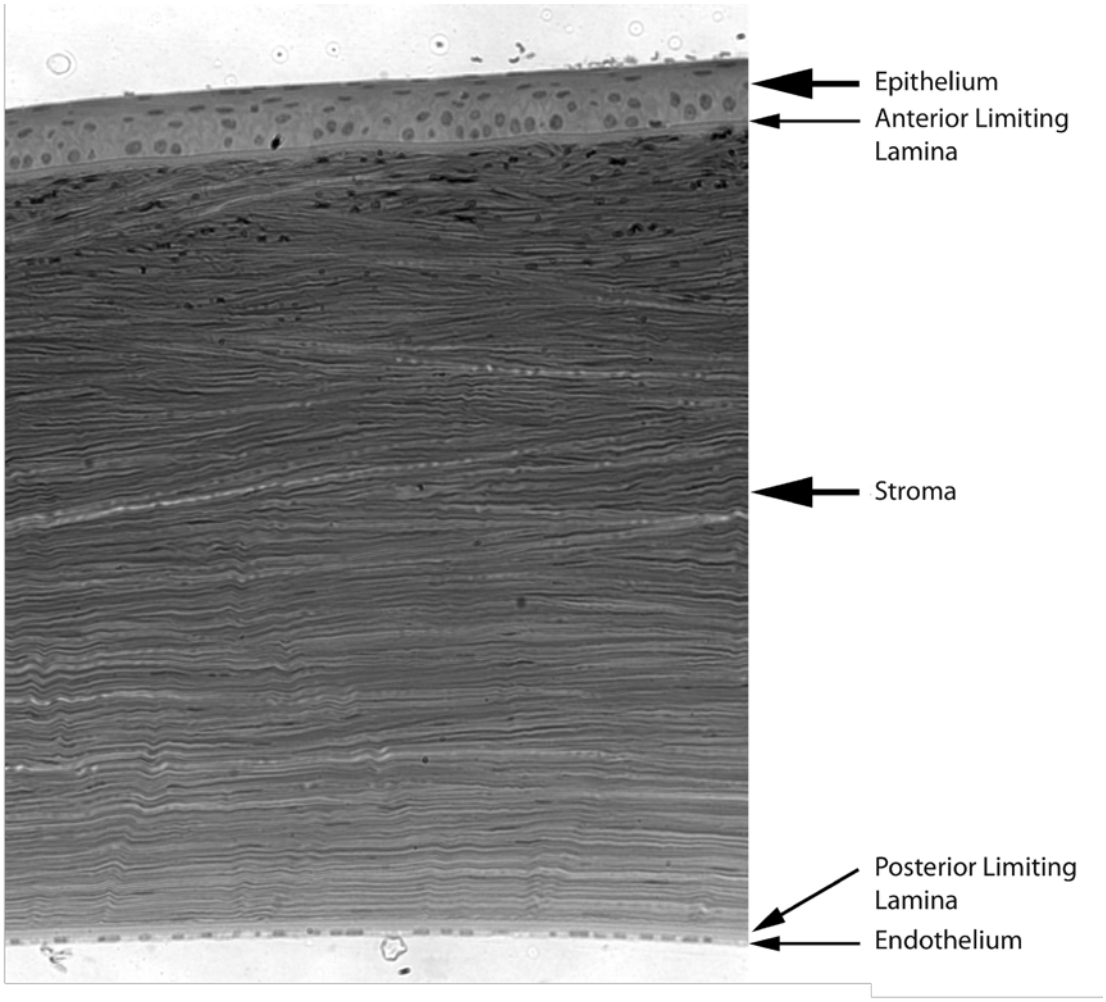


**Figure 1.1: Transverse Section of the Normal Primate Cornea**

The five layers of the normal cornea are indicated. Magnification approximately 100X. Light microscopy. (image from: Bergmanson, 2010)

**Table 1.1: Multiple suggested etiologies of keratoconus in literature**

| Proposed Etiology | Author |
|---|---|
| 1. Proteolytic or autolytic enzymes released by dead or dying basal corneal epithelial cells which may attack posterior tissues | Teng, 1956 |
| 2. PMMA hard contact lenses | Harstein, 1968 |
| 3. Forceful eye rubbing or oculodigital reflex | Karseras & Ruben, 1976<br>Krachmer, 2004<br>McMonnies, 2009 |
| 4. Faulty regulation of collagen turnover | Berman, 1991 |
| 5. Increased keratocyte apoptosis | Kim et al., 1999 |
| 6. Ultraviolet Radiation – UVB wavelength | Kenney et al., 2000 |

**Table 1.2: Dystrophy versus Degeneration in Literature**

| Dystrophy | Degeneration | Undecided/Ectatic |
|---|---|---|
| • Cintron, 1994<br>• Arffa, 1997<br>• Yanoff and Sasanni, 2009 | • Maguire, 1998 | • Duke-Elder and Leigh, 1965<br>• Casey & Sharif, 1991<br>• Feder & Kshettry, 2005<br>• McMahon, & Szczotka-Flynn, 2005 |

# Chapter 2 - General Methods

## Subjects

Normal corneas were obtained from Human Eye Banks – National Disease of Research Interchange (Philadelphia, PA), Lions Eye Bank (Houston or Dallas, TX) or North Carolina Eye bank (Winston Salem, NC). These corneas were determined, by the source, as unsuitable for transplant surgery. The source maintained that these corneas were free of active disease and lacked a history of such events. On arrival to our laboratory and before processing the tissue, these eyes were evaluated under a dissection microscope using a bright light source and were determined, in this manner, to be healthy. Keratoconic corneas were surgically removed for penetrating (PKP) or lamellar (LKP) keratoplasty by Dr. John D. Goosey at Houston Eye Associates (Houston, TX). Only subjects diagnosed with keratoconus were included, and the diagnosis was defined by the manifestation of one or more specific keratoconic clinical signs – abnormal thinning, Fleischer's ring, Vogt striae, or corneal topography with an area of >45D steepening (Barr et al., 2006). Subjects 18 years of age and older were included. Informed consent was obtained for both clinical measurements and donation of surgically removed tissue. The surgeon and patient together determined the most suitable type and timing of surgery. The protocol was in accordance with the guidelines of the Declaration of Helsinki regarding research on human tissue. Confidentiality of the patients was maintained. Eye bank corneas (n=7) ranged in age from 42-82 (mean age: 59), while recruited keratoconic subjects (n=15) ranged in age from 18-70 (mean age: 47).

For obvious and ethical reasons, it was not possible to be selective in the choice of corneas assessed and, therefore, age between normal and keratoconic corneas was not controlled. Eye bank corneas came from individuals who were relatively older than the

keratoconic subjects and the eye bank corneas were fixed several days post-mortem, while keratoconic corneas were fixed immediately following removal by the surgeon. However, all corneas examined came from adults and there are no known major histological differences between the young and aging corneas except, endothelial cell loss, thickening of posterior limiting lamina, and thickening of the epithelial basement membrane (Bergmanson, 2010). Only the age-related thickening of the basement membrane may be considered to have an impact on the findings on the present work and, indeed, such consideration was given to this issue (see chapter 6).

The surgeon's decision on whether to choose the PKP or LKP procedure for the keratoconic patient was essentially dependent on the patient's age and the thickness of the cornea. A very thin cornea, in an older patient, was an indication for the PKP procedure. In general, a cornea requiring PKP has a more advanced stage of the disease than and a LKP, although this is not necessarily always the case. As previously mentioned, there may be more than one type of keratoconus, but differences between varying presentations are not well defined in literature (Sherwin & Brookes, 2004). No attempt was made to classify the assessed corneas into different groups. In addition, severity of the disease, based on base curvature, was not classified.

## General Histological Methodology

Normal corneas were delivered to the laboratory within 72 hours after death, in an iced container and individually immersed in an eye bank storage medium (Optisol GS; Bausch and Lomb, Irvine, CA). The tissue was then thoroughly rinsed with 0.1 M sodium cacodylate buffer (pH 7.4) and immersed overnight at 4°C in a fixative solution of 2% glutaraldehyde in 80 mM sodium cacodylate (pH 7.4, 320–340 mOsm/kg). This formulation was based on an established protocol, from our laboratory, developed to minimize tissue distortion and dimensional change (Doughty et al, 1997; Doughty et al, 2001; Bergmanson et al, 2005;). Removed keratoconic corneas were immediately placed in the same fixative formulation by the surgeon and stored on ice.

After primary fixation, small analogous pieces (1 x 3 mm) were cut from the region of interest of each cornea using an unused, degreased razor blade. Regions of interest included: 1) the geometric center of normal corneas, 2) the center of the cone, within the visible Fleischer ring of keratoconic corneal buttons, 3) or the periphery of button, outside of Fleischer ring and opposite to the cone, in keratoconic corneas. The tissue pieces were then rinsed in cacodylate buffer at room temperature and subsequently postfixed by immersion for 1 hour, under subdued lighting, in a freshly prepared 1% solution of osmium tetroxide ($OsO_4$) in 0.1 M cacodylate buffer. The samples were again washed in buffer and then dehydrated through a graded alcohol series (30% to 100% in six steps) at room temperature. Then the samples were infiltrated with propylene oxide (three changes at 10 minute intervals) and followed by a 2:1 vol/vol mixture of propylene oxide and Spurr's or Araldite resin for 3 hours. Subsequently, the specimens were

immersed overnight in a 1:1 vol/vol mixture of propylene oxide and Spurr's or Araldite resin, followed by transfer to 100% Spurr's or Araldite resin overnight. The tissue samples were then oriented in embedding molds and left for overnight polymerization at 60°C.

The corneal samples were prepared for light microscopy by first cutting thick transverse sections (0.5–1 µm) and then staining with toluidine blue. For electron microscopy, parallel bar copper grids (product number 2440C-XA or product no. 2415C-XA SPI Supplies, West Chester, PA) with a 80µm or 125µm spacing were used, and ultrathin sections (60–90nm) were stained first in 3.5% uranyl acetate (dissolved in water) for 20 minutes at 60°C, followed by Reynold's lead citrate for 10 minutes at room temperature. The grids were examined in a transmission electron microscope (TEM) (JEOL 100C USA, Peabody, MA, operating at 60kV or Tecnai G2 12twin, FEI Company, Hillsboro, OR, operating at 100kV).

## Montaging

In 2007, the Jeol 100C TEM was upgraded to the more modern digital Tecnai G2 12 twin TEM. Work on normal corneas was performed on the Jeol using standard film photography, while work on keratoconic corneas was conducted on the new Tecnai using digital technology. For normal corneas, a continuous sequence of slightly overlapping film micrographs were taken at 2,600X magnification across the entire thickness of the corneal stroma or at 6,600x magnification along the ALL–stroma interface. The negatives were developed and printed on photographic paper to a final magnification of 3,640X or 10,204X, respectively, and were manually assembled to form a continuous montage of photographs. For keratoconic (and control) corneas, a sequence of overlapping digital micrographs was taken at 860X across the entire thickness of the corneal stroma. A seamless digital montage was created using PanaVue ImageAssembler 3 software and was then printed (Roland FJ-52) on photo quality paper at a final magnification of 5000X.

Due to the updated digital quality of the new Tecnai TEM, it was necessary to develop a new system for creating continuous corneal montages. Just as with the Jeol TEM, the individual micrographs for each montage were captured manually before being pieced together. Each montage consisted of approximately 18-25 micrographs. Since the micrographs were in a digital format, it was desirable to form the montage digitally as well. However, because of the large file size of each digital micrograph, and the even larger file size after putting them all together, a new system for doing this had to be created. After some research, it was determined that the PanaVue ImageAssembler

software would accomplish this objective. Although labor intensive, the PanaVue software provided a seamless digital montage that was then easily printed with high-resolution quality.

# Chapter 3 - Assessment of the Number of Lamellae in the Central Region of the Normal Human Corneal Stroma at the Resolution of the Transmission Electron Microscope

This work has been peer-reviewed and published:

Bergmanson JPG, Horne J, Doughty MJ, et al. Assessment of the number of lamellae in the central region of the human corneal stroma, at the resolution of the transmission electron microscope. *Eye Contact Lens.* 2005; 31(6):281–287.

## Abstract

**Purpose:** To determine the total number of lamellae within the central region of the human corneal stroma by using a continuous section through the corneal stroma and at the ultrastructural resolution of the electron microscope.

**Methods:** Six human eye bank corneas, from individuals aged between 42 and 82 years, were received in corneal storage medium (Optisol GS) and then processed for transmission electron microscopy with buffered 2% glutaraldehyde fixation. Thin sections were mounted on parallel bar copper grids for an uninterrupted full corneal thickness observation. A sequence of overlapping micrographs were taken at 2,600X magnification, printed at a final magnification of 3,640X, and assembled as a montage. The number of lamellae were counted across the corneal stromal strip by three observers, independently, by using a pre-agreed set of criteria for identifying individual lamella.

**Results:** The average number of lamellae per stroma was determined to be 242 ± 4 (range, 234–247). In the more anterior region of the stroma, the density of the lamellae was 50% greater than in the posterior stroma (mean, 57 ± 12 per 100 µm anteriorly vs. 38 ± 5 per 100 µm posteriorly). Interobserver differences were modest and generally less than the intersample variance.

**Conclusions:** When assessed at the resolution of the transmission electron microscope, the number of stromal lamellae in the central region of the human cornea were higher (at approximately 240 per cornea) than most previous estimates reported from light microscopy studies.

## Introduction

The human cornea is composed of five distinct layers, namely the epithelium, anterior limiting lamina (Bowman's membrane), stroma, posterior limiting lamina (Desçemet's membrane), and the endothelium (Bergmanson & Doughty, 2004; Maurice, 1984). Based on clinical observations and experimental studies, it can be considered to be largely transparent to visible light at wavelengths greater than 400 nm (Maurice, 1984; Freegard, 1997). The optics underlying this transparency have been considered in detail, with most attention being given to the organization of the collagen fibrils that make up the corneal stroma (Maurice, 1984; Clarke, 2001). Overall, the optical transparency can be considered to be the result of a unique combination of the organization of these fibrils and their minimal light scattering properties (Clarke, 2001). This transparency is associated with a certain hydration of the collagen fibrils and their associated proteoglycans, and thus on the overall thickness of the corneal stroma (Maurice, 1984). For the nominally normal human cornea, the overall thickness has a predictable range of values (Doughty & Zaman, 2000). However, it can be noted that this range is rather wide, with a meta-analysis yielding a 95% confidence interval between 0.473 and 0.597 mm for normal thickness (Doughty & Zaman, 2000). The reason for this range of values is unknown, but factors such as gender, age, ethnic origin, and refractive error have all been considered as possible causes of fundamental differences in central corneal thickness.

It is well known that certain corneal degenerative diseases, such as keratoconus and pellucid marginal degeneration, are associated with a progressive reduction in central or peripheral corneal thickness, with an overall thinning of the corneal stroma being the

dominant feature (Pouliquen et al., 1987; Takahashi et al., 1990; Rabinowitz, 1998). In addition, however, there have been considerations that extended wear of contact lenses may also reduce the thickness of the corneal stroma, at least in some patients (Myrowitz, 2002). In more recent years, there has been renewed interest in this fundamental characteristic of the cornea. These interests have arisen with the advent of refractive surgery and with the consideration of the importance of corneal thickness in measurements of intraocular pressure (Doughty & Zaman, 2000). A case can be made, however that, in reality, relatively little information is available on these fundamental properties of the corneal stroma, namely its thickness and the factors that may result in changes in its thickness beyond acute physiologic or toxic changes (Doughty, 2003).

It is well known, as based on various texts on ophthalmology or the anatomy and physiology of the eye or cornea, that the corneal stroma is principally composed of collagen fibrils organized into thin flattened sheets, generally referred to as lamellae (Thomas, 1955; Duke-Elder & Wybar, 1961; Hogan et al., 1971; Marshall & Grindle, 1978; Newell, 1982; Pouliquen, 1985; Pouliquen, 1987; Fatt & Weissman, 1992; Huff, 1997; Bron et al., 1997; Arffa, 1997; Trinkaus-Randall et al., 1998; Klyce & Beuerman, 1998; Oyster, 1999; Edelhauser & Ubels, 2003). Such texts also provide, often repeated, statements on the number of lamellae within the central region of the corneal stroma, although the origins of these counts are generally unclear and the methodology by which they were obtained is rarely mentioned. Overall, these various sources indicate that the number of lamellae in the human cornea could be anywhere between 60 and 500.

Beyond the textbook and review sources, there have been a number of fairly detailed, but largely qualitative, studies on the organization of the lamellae of the human

corneal stroma (Komai & Ushiki, 1991; Radner et al., 1998; Ojeda et al., 2001; Muller et al., 2001). To the best of the authors' knowledge, only three substantial published reports have contained specific details of investigations designed to assess the number of lamellae in the human corneal stroma (Takahashi et al., 1990; Pouliquen, 1985; Hamada, 1972). It must be noted that these assessments were limited to three specimens (Takahashi et al., 1990), two specimens (Pouliquen, 1985; Pouliquen, 1987), or just one specimen (Hamada et al., 1972). Two of the reports involved the assessment of thick sections from the central corneal stroma, stained with toluidine blue and examined under high magnification by polarized light microscopy and adding the counts made from different regions of the stroma (Hamada et al., 1972) or making a total count across the entire corneal section (Pouliquen, 1985). The other study used transmission electron microscopy but likely extrapolated counts from part of the stroma to the entire stromal thickness, because it was not clearly indicated what proportion of the stroma was used for the counting (Takahashi et al., 1990).

The goal of the current study was not only to assess the total number of lamellae in a larger number of human corneal specimens than assessed in previous studies, but also to perform this count from a continuous strip of images across the entire thickness of the corneal stroma and use the resolution of the electron microscope (rather than a polarizing light microscope). Because the visualization and demarcation of the actual boundaries of the individual lamellae will likely depend on the quality of the sample and perception of the observer, part of the goal of the current study was to apply a set of criteria for the counting and to assess how much the estimates of the number of lamellae was subject to inter-observer differences.

## Materials and Methods

The eyes, unsuitable for corneal transplantation, were obtained in accordance with the guidelines of the Declaration of Helsinki regarding research on human tissue and were provided by the National Disease Research Interchange (Philadelphia, PA) and Lions Eye Bank (Houston and Dallas, TX). The eyes were from six separate individuals, aged 42 to 82 years. All of the eyes had been rejected as unsuitable for corneal transplant for reasons other than corneal disease.

The eyes were delivered to the laboratory within 72 hours after death and were then processed for electron microscopy on the same day. The corneas were shipped in an iced container, were immersed in an eye bank storage solution (Optisol GS, Bausch & Lomb, Irvine, CA), and included a rim of scleral tissue. These preparations were first thoroughly rinsed with 0.1 mol/L sodium cacodylate buffer (pH 7.4) and then immersed in a fixative solution overnight at 4°C. The fixative, specifically developed for studies on rabbit corneas (Doughty et al., 1997; Doughty and Bergmanson, 2004), consisted of 2% glutaraldehyde in 80 mM sodium cacodylate, pH 7.4, 320 to 340 mOsm/kg. With the cornea now thoroughly fixed, small analogous pieces (1 X 3 mm) were cut from the geometric center region, then rinsed in cacodylate buffer at room temperature, and subsequently postfixed by immersion for 1 hour, under subdued lighting, in a freshly prepared 1% solution of osmium tetroxide in 100 mM cacodylate buffer. The samples were again washed in cacodylate buffer and then dehydrated through a graded alcohol series (30%–100% in 6 steps) at room temperature. The tissue samples were then first infiltrated with propylene oxide (three changes at 10-minute intervals) and then with a

3:1 v/v mixture of propylene oxide and Spurr's resin (product number 4300, Electron Microscopy Sciences, Fort Washington, PA) for 3 hours. This was followed by overnight immersion in a 1:1 v/v mixture of propylene oxide and Spurr's resin, followed by transfer to 100% Spurr's resin overnight. The tissue samples were then oriented in embedding molds and left for overnight polymerization at 60°C.

Thick transverse sections (0.5–1 μm) of the cornea were cut and stained with toluidine blue, for light microscopic observations and to determine tissue orientation. Ultrathin sections were then obtained and mounted on parallel bar copper grids (115 μm bar spacing) (product number 2415C-XA, SPI Supplies, West Chester, PA). The sections were double-stained first in 3.5% uranyl acetate (dissolved in water) for 20 minutes at 60°C, followed by Reynold's lead citrate for 10 minutes at room temperature.

The grids were examined in a Jeol 100C (Tokyo, Japan) transmission electron microscope operating at 60 kV. A portion of the grid was selected where there was an uninterrupted high-contrast section while avoiding regions with pronounced lamellar undulations. Once located, a continuous sequence of slightly overlapping micrographs were taken at 2,600X magnification across the entire thickness of the corneal stroma. The negatives were printed to a final magnification of 3,640X and then assembled to form a continuous montage (Fig. 3.1) of each cornea.

Starting at the anterior aspect of the montage, the number of lamellae were counted with the strip placed on a flat surface under cool fluorescent lighting. The count was carried out, independently, by three different observers following a pre-agreed set of specified criteria (Table 3.1). These criteria were that the distinction between adjacent lamellae would be made on the basis of an obvious difference in contrast, usually

associated with a distinct change in the fibril orientation as a result of the lamellae being cut at a slightly different angle. If, within the width of the micrograph (approximately 60 µm), there was an obvious branch or bifurcation of lamellae, care was taken not to double-count such lamellae branches. Conversely, in regions of the micrograph where variation in contrast was subtle, the presence of nearby projections from keratocytes or the presence of thin glancing sections through the edges of such projections were used to decide whether the lamella should be counted as one or two; that is, the presence of keratocyte projections running through the plane of a lamella was an indication of an interlamellar border. Lastly, a decision was made not to include in the count those lamellae that appeared to be extremely thin (i.e., less than 0.2 µm in thickness). This decision was made because other contemporary investigators have considered this value to be the minimum thickness of the lamellae (Komai & Ushiki, 1991; Radner et al., 1998).

In addition to making the overall counts of the lamellae, the montages were then marked to define the most anterior 100 µm proximal to the anterior limiting lamina (ALL) and the most posterior 100 µm proximal to the posterior limiting lamina (PLL). In this manner, the stroma was subdivided into three regions.

All the data were entered into a statistics software package (Systat version 8.0, Systat, Inc., Evanston, IL) for generation of descriptive statistics.

## Results

From each of the six corneas, a montage was obtained that was between 9 and 12 feet long (Fig. 3.1). The overall corneal stromal thickness, from stromal interface with the ALL to the stromal interface with the PLL, was measured from the montages. These values for the stromal thickness ranged from 0.493 to 0.605 mm (mean, 0.556 mm). Within any particular section at 3,640X magnification, the numerous lamellae were generally reasonably well demarcated. Successive layers of lamellae could be distinguished using the criteria outlined (see Materials and Methods).

Figure 3.2 shows the interface between the ALL and the array of collagen bundles located immediately posteriorly. The ALL is approximately 8 to 14 μm thick (Bergmanson & Doughty, 2004; Horne et al., 2002). In this region immediately posterior to the ALL, the collagen fibers are disorganized and only sometimes formed into distinct flattened bundles. Where these were present, they appeared to be highly interwoven and branched. In discrete locations, the lamellae appeared to be compact (i.e., formed into darkly staining dense arrays with distinct borders), whereas others appeared far less dense and could even be spread out into small groups of fibrils or microfibrils. In this particular example, the zone was less than 1 μm thick, whereas in others, it was up to 2.5 μm thick. This most anterior zone, regardless of its thickness, then rather abruptly gave way to a more organized array of flattened lamellae that were generally running mostly parallel to the ALL. This transition was emphasized by the keratocytes that, in this region, tended to be slender but with the cell processes running parallel to the ALL (Fig. 3.2). In some

corneas, the processes of slender keratocytes were seen to extend into the zone immediately under the ALL after the oblique course of the dense lamellae.

Deeper into the more anterior stroma, the lamellae appeared to be well organized into discrete flattened sheets with well defined borders (Fig. 3.3). This organization was again highlighted by the orientation of the keratocytes, which were generally seen to be parallel to the ALL and much more substantial in thickness. However, despite the general organization into flattened sheets, three important features were noted for the lamellae of the anterior stroma. These need to be considered for any attempt being made to count the number of lamellae. First, as evident at several locations in the micrograph (Fig. 3.3), some of the lamellae cross through the stroma at rather different angles. Within the regions where these lamellae contact others, which run parallel to the ALL, there was often considerable heterogeneity to the internal finer structure of the lamellae. In the lower region of the micrograph, just posterior to the junction between two dark staining lamellae, a lighter staining zone can be seen that is subtly different from the main bulk of the lamella posterior to the junction between the lamellae. In this example, this lighter region extends only part of the way across the micrograph and has variable thickness (up to 0.8 μm), so depending on where the count was made, it could be considered as a separate feature. If the differences in contrast were sufficient, such features could be counted but might well have been missed if there was a lower contrast from the original micrograph or on the print. Second, and a related issue to the first one, is whether some of the apparent lamellae were actually several sheets of similarly oriented collagen fibrils that were lying immediately on top of one another, as opposed to each successive lamellae being made of fibrils running at slightly different angles. In this example (Fig.

3.3), as in the others, there were several locations where there were fine and usually slightly darker lines running through the lamellae and generally parallel to the anterior and posterior borders of these lamellae. Depending on the contrast of the print and on lighting conditions under which such features were observed, these fine lines were not necessarily that evident. In some cases, the presence of such lines could have been taken as indicating that the thicker lamellae were actually composed of two or more discrete lamellae, whereas in other cases these could have been overlooked. The latter scenario was more likely if, as illustrated, these fine lines appeared to converge and disappear, perhaps because they represented a bifurcation or fusion of lamellae. If these lines were overlooked, the count of lamellae in that region could have been underestimated. The third aspect of the objective evaluation of the micrographs that must be considered is where there were thin lamellae. As can be seen in Figure 3.3, there were several extremely thin (less than 0.2 μm) and dark staining bands. At this resolution, these could have been distinct and flattened lamellae or the extreme edges (ends) of lamellae that were considerably thicker in adjacent regions of the stroma. Alternatively, these dark staining bands could be the edge of a lamella that, for some reason, stained more intensely (see Discussion). Whatever the reason for the appearance, a decision was made not to count these thin features as lamellae, whether in the anterior stroma or more posterior regions.

An example of mid stroma lamellae is shown in Figure 3.4. As compared to the bulk of the anterior stroma (Fig. 3.3), the lamellae were generally distinctly thicker, and there was little evidence of any interweaving. Most lamellae, but not all, were simply arranged as flattened sheets running parallel to the ALL. As with the anterior stroma,

some fine darker lines can be seen running through some of the lamellae. As noted earlier, these may or may not have been distinct enough to warrant a decision being made that a thicker lamella was in fact composed of two or more distinct sheets.

Lastly, an example is shown (Fig. 3.5) of lamellae in the most posterior 100 µm of the stroma. As with the mid stroma, the lamellae were generally well demarcated and formed thicker flat sheets running essentially parallel to the ALL and PLL. As with the mid stroma, there were again some faint darker lines running through some lamellae, which may or may not have been taken as the borders between adjacent lamellae. There were also some fine dark staining bands that were less than 0.2 µm in thickness that were not included in the count.

Based on the appearance described earlier and with the caveats that any distinctions made between adjacent lamellae will depend on the resolution of the printed image and the contrast of the print, several strategies may be adopted to analyze the outcome of the counts of lamellae. These strategies will be presented to provide an overall outcome and indicate the potential sources of error in the counting process. Overall, taking the average of three counts (one from each of the observers), the total number of lamellae, with a thickness exceeding 0.2 µm, ranged from 234 to 247 with a group mean value of 242 ± 4 per stroma. A similar overall outcome was obtained if the data from each observer were analyzed. Observer one generated individual counts between 225 and 259 lamellae for the six corneas (mean, 240 ± 12 lamellae). Observer two generated counts between 237 and 254 lamellae (mean, 246 ± 6 lamellae), whereas the counts from observer three ranged from 229 to 248 lamellae (mean, 239 ± 6 lamellae). The inter-observer error can be considered, in its simplest sense, as variance

between counts. So, for example, for cornea 1, the three values were 259, 254, and 229 to give an average of 247 lamellae per stroma. The standard error on the counts was thus 1.73, which is equivalent to a coefficient of variation of just 0.7%. Across the six corneas, the standard error on the counts ranged from 0.47 to 6.95 (mean, 2.63) for an overall coefficient of variation of 1.08%.

The inter-observer agreement was less when discrete regions of the corneal stroma were assessed. For the anterior 100 µm of the stroma, the lamellae followed a more complex pattern and were less well organized than those found in the posterior 100 µm. For instance, the anterior lamellae often appeared to be more interwoven and not always ran strictly parallel to the epithelial basement membrane. Furthermore, the contrast between the lamellae was generally less than that found in the more posterior aspects of the stroma. From the average of three counts, the number of lamellae in the most anterior stroma was assessed to be between 49 and 78, for a group mean value of 57 ± 12 per 100 µm for the six corneas. The same mean value for anterior lamellae was actually recorded by all three observers for the six corneas, but with a slightly different spread of values: 57 ± 11, 57 ± 9, and 57 ± 12 lamellae per 100 µm. Between observers, the counts for the anterior stroma ranged from 43 to 56 (mean, 50) with the standard error being 3.09 for a coefficient of variation of 6.2%. Overall, the standard error on the anterior lamellae counts ranged from 1.0 to 11.2 for an overall coefficient of variation of 4.98%. For the posterior stroma, fewer lamellae were apparent with a mean count of just 38 ± 5 / 100 µm, with the overall coefficient of variation on these counts being just 2.50%. The sets of average counts were normally distributed, and a paired *t* test indicated that the anterior and posterior counts were statistically different ($P = 0.016$).

For the mid stromal regions, the interobserver variance in the counts was between those for 100 µm segments of the anterior or posterior stroma (Table 3.2). The number of clearly demarcated lamellae was 147 ± 14, and the overall coefficient of variation on these counts was 3.39%.

## Discussion

As based on an extensive literature search, the current study represented the first attempt, at the resolution of the transmission electron microscope, to define the number of lamellae across the entire thickness of the human corneal stroma. Although the overall result (a mean count of 242 per stroma) is within the range of "200 to 250," (Marshall & Grindle, 1978) "about 200 to 250," (Hogan et al., 1971; Edelhauser & Ubels, 2003) and "200 to 300," (Bron et al., 1997; Arffa, 1997) it is rather higher than numerous other statements found in the literature: "probably 100 to 150" (Duke-Elder & Wybar, 1961) and "approximately 200" (Newell, 1982; Huff, 1997; Trinkaus-Randall et al., 1998; Oyster, 1999). The current estimate is substantially higher than the number provided in older notes. An early article on the cornea (Simpson, 1949), states that there are "60 or more corneal lamellae," whereas an earlier text on the cornea considered that there were only "about 60" lamellae (Thomas, 1955). The overall result obtained in the current study, however, is lower than some other statements of "300 to 500" (Klyce & Beuerman, 1998) or "several hundred" (Fatt, 1992).

As noted in the introduction, presented in the various textbooks, many of the statements on the number of lamellae in the corneal stroma do not have a clear origin (i.e., a specific research-based study). Just three systematic studies have been identified, only one of which used the electron microscope. In a study including three normal corneas from younger adults, the average number of lamellae was given as 304 for the central region of the stroma, with a range between 260 and 350 lamellae (Takahashi et al., 1990). It is not entirely clear, from the account provided, exactly how these counts

were obtained. However, it seems likely that these were based on measurements of the thickness of the lamellae visualized in electron micrographs taken at 4,700X magnification, and then a calculation of average thickness and the number of lamellae made with respect to the overall thickness of the corneal stroma. Two other systematic studies have used light microscopy to evaluate corneal sections, but they did not clearly show how they arrived at the total number of corneal lamellae. In an initial study, Hamada et al (1972) examined a single human corneal button from a 26-year-old patient. A count of the lamellae was apparently made by examining the anterior, mid, and posterior portions of toluidine blue–stained thick sections of the corneal tissue at 640X magnification with a polarizing microscope. The number of lamellae were counted, and then the counts were added (i.e., 101 + 99 + 109) for the three portions of the central stroma. It was concluded that there were 309 lamellae in the central corneal region. However, many years later, it was noted that the "methods of measurement" using the polarizing microscope technique could be improved on, and as a result, the original estimate of close to 300 was revised downward to 200 lamellae (Pouliquen, 1987). Further data were also presented for sections from normal corneas of a 17-year-old patient and a 63-year-old patient, as analyzed with the improved polarizing microscope, and for whom the average number of lamellae in the central region of the cornea was stated as being 179 and 161, respectively (Pouliquen, 1985; Pouliquen, 1987), that is, much lower counts than originally presented (Hamada, 1972). Two other points must also be noted. First, in reporting a much lower count for the lamellae, it was noted that "very thin connective bands cannot be detected" (Pouliquen, 1985). It is uncertain what the lower limit of resolution might have been when the sections were viewed through a

polarizing filter, but with a reported magnification of just 250X (Newell, 1982) or even as high as 640X (Hamada, 1972), it seems unlikely that lamellae below 0.5 µm could have been resolved. Second, it was reported that a large number of sections were used for these counts (e.g., 40 and 72 grids for the measures on the 17-year-old and 63-year-old patients), and it is unclear whether the resultant indicator of the variance (e.g., 179 ± 14) was meant to reflect differences between sections and the counts from the entire cornea or differences between sections made across different portions of the cornea (i.e., anterior vs. posterior); the latter interpretation seems more likely.

In the current study, not only were the counts of lamellae made from electron micrographs printed to 3,640X (i.e., high resolution), but a complete montage was prepared across the entire thickness of the stroma (Fig. 1). A strategic decision was made to count only lamellae that had a thickness of at least 0.2 µm. This thinnest value is consistent with the minimum thickness measurements for human corneal lamellae reported by other contemporary researchers (Komai & Ushiki, 1991; Radner et al., 1998). This criterion for a minimum thickness (>=0.2 µm) was selected not only because it was a limit used in these previous reports (Komai & Ushiki, 1991; Radner et al., 1998), but also to avoid the possibility of an overestimate by including in the count some branches of lamellae. Some of the thin (<0.2 µm) flat bundles of fibrils could be fine branches of lamellae or simply the extreme edge of a lamella. However, such thin flat arrays of fibrils exist within the corneal stroma and have been noted previously (Pouliquen, 1985) and illustrated by others. The presence of extremely thin lamellae (0.075 µm) were illustrated and noted in a human corneal stroma (Schwartz & Keyserlingk, 1966) and can be seen in electron micrographs of rabbit stroma (Gallagher & Maurice, 1977). Higher-

magnification electron micrographs can show that, even with the apparent boundaries of a single flat sheet of fibrils, some fibrils can be cut at slightly different orientations (Kuwabara, 1978; Doughty et al., 2001), indicating some degree of heterogeneity even within a single lamella. Therefore, the definition of the boundaries of any individual lamellae are subject to different interpretations. The current study uniquely used a set of criteria for counting the lamellae.

The current study indicated that the total number of lamellae in the human corneal stroma is close to 240 per stroma. The current estimate is presented with the caveat that some thin lamellae may have been omitted, whereas some thicker lamellae may have been considered as a single unit rather than two or more lamellae. Reduction of such errors might have been achieved if a higher magnification had been selected for the strips of micrographs. However, a balance has to be sought between obtaining a lamellar count from a continuous montage across the entire corneal stroma, as achieved in the current study, and having a manageable sequence of micrographs to assess the stroma at higher levels of ultrastructural resolution. The current study is, therefore, presented as a reasonable balance between these two different objectives, and are presented as the most accurate attempt to establish the total number of lamellae in the central region of the normal human cornea.

Although only six corneas were assessed in the current study, this number is more than that in previous studies, and the estimated variance between samples was relatively low. Using the standard deviation from the average counts across the six specimens, a 95% confidence interval would be between 236 and 250 lamellae per stroma for normal corneas. Overall, the results obtained indicate that the application of specific criteria to

define a lamella will result in only minor inter-observer or intra-observer variations for a total lamellar count. Notwithstanding, it is accepted that there are a number of limitations to the regional analyses of the lamellae. These limitations are largely the result of postmortem changes in the tissue, although such changes should have little impact on the total count of the lamellae. Based on measurements of the entire thickness of the stromal montages, the corneas evaluated in the current study were slightly edematous (mean, 0.556 mm) as compared to in vivo human corneas (Doughty & Zaman, 2000); assuming that the epithelium constitutes 10% of the total corneal thickness, the normal stromal thickness would be expected to be between 0.42 and 0.53 mm. The reported stromal thickness was just 0.39 mm for one of the lamellar count studies using light microscopy (Hamada et al, 1972), whereas it was between 0.43 and 0.48 mm for the others (Pouliquen, 1987; Patey et al., 1984). However, a recent study reported that the postmortem stromal thickness values, from light microscopy sections, for human corneas had a mean of approximately 0.6 mm, with values as high as 1 mm being observed (Muller et al., 2001). In another recent study, the overall corneal thickness of a postmortem sample, after formalin fixation, was noted to be approximately 0.8 mm.40 Stromal thickness values of approximately 0.6 mm can be noted for other sections evaluated by light microscopy and made from postmortem human corneas (Marshall & Grindle, 1978). Overall, the resultant thickness of the section would be expected to result from the expected postmortem swelling of the tissue, and some subsequent reduction in stromal thickness as a result of the processing of the tissue for electron microscopy (Muller et al., 2001; Doughty et al., 1997; Merindano et al., 1997). The differences in lamellar counts between the most anterior and posterior regions may be the result of

differences in stromal architecture (Muller et al., 2001) or because the postmortem edema resulted in a proportionately greater swelling of the posterior aspect of the stroma (Muller et al., 2001; Kikkawa & Hirayama, 1971; Lee & Wilson, 1981). Stated another way, the lamellar density in the more anterior region of the corneal stroma might be considered as being closer to those in vivo (because of less postmortem edema developing), whereas the lamellar density in the most posterior zone would be artificially low because of proportionately greater edema that developed after death. Further studies are, however, required to assess the nature of such postmortem changes. Analysis of the counts at different regions of the cornea, between observers and across the different specimens, indicates that total lamellar estimates of as low as 212 or as high as 316 could easily be obtained if only discrete regions of the cornea were analyzed and the counts were then extrapolated to the full corneal thickness.

The current study is an introduction to a systematic attempt to better define the cornea of nominally normal individuals. Because a wide range of corneal thickness values are found in such individuals (Doughty & Zaman 2000), it would be especially useful to be able to assess corneas for which pachymetry data are available shortly before or immediately after death (e.g., by obtaining such data from the eye banks where it might be available if, for example, specular microscopy with pachymetry had been performed on the recently procured specimens). Future studies comparing the central versus peripheral cornea should be helpful in better defining the organization of the lamellae for the entire cornea. Further data are needed to extend the initial observations of Hamada et al. (1972) on the number of lamellae or lamellar branches in the peripheral cornea. If long-term contact lens wear does indeed reorganize the corneal stroma, studies

on corneas from such individuals should be profitable. Most importantly, further studies are also required to provide the data needed for a better understanding of the pathologic changes that occur in conditions such as keratoconus and pellucid marginal degeneration, both of which are characterized by a thinning of the stroma (Pouliquen et al., 1987; Rabinowitz, 1998). Such work will require further assessments of not only the number of lamellae (Pouliquen et al., 1987; Takahashi et al., 1990) and their thickness, but also the composition of the lamellar fibrils and matrix surrounding them.

## Figures and Tables

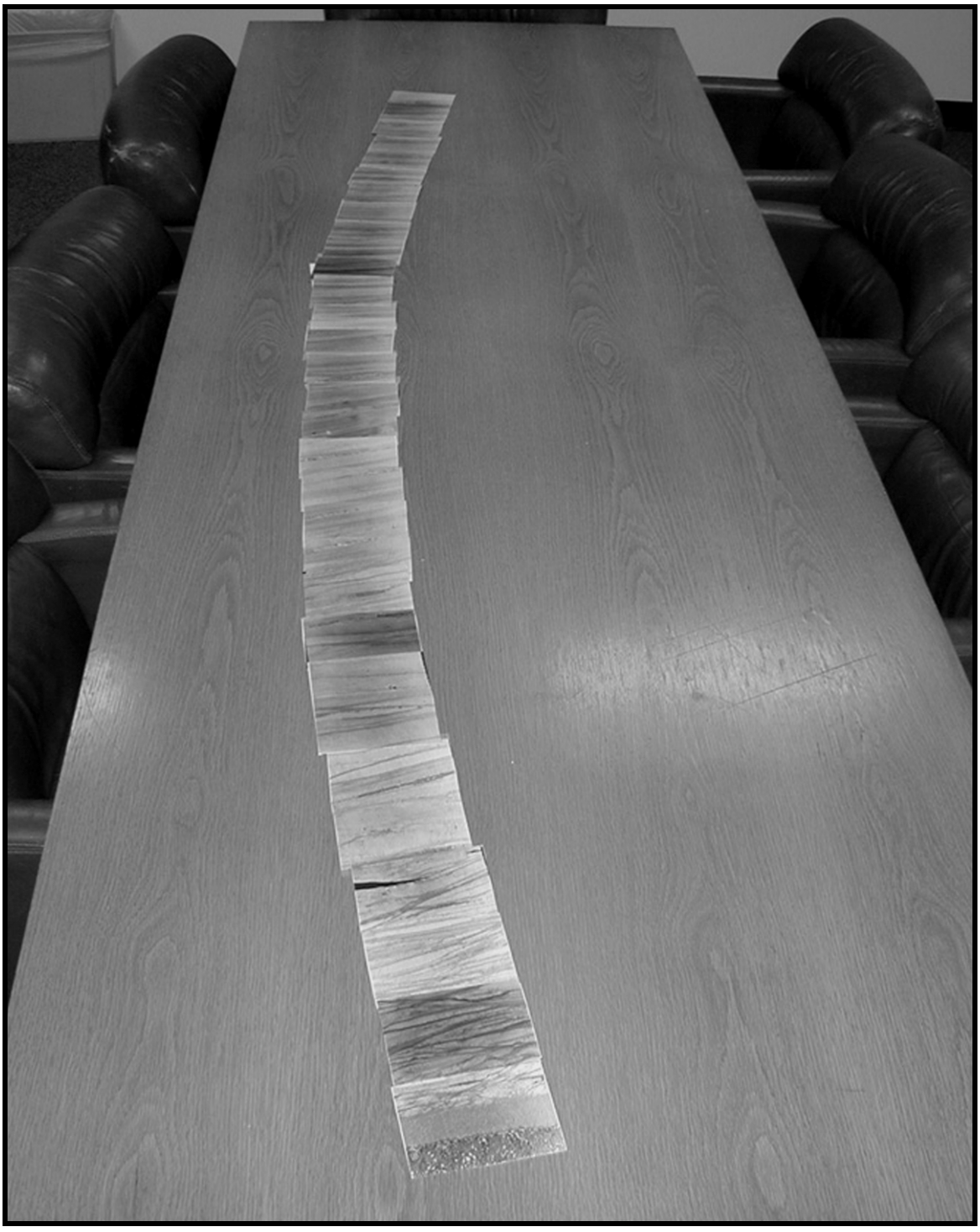

**Figure 3.1**

**Figure 3.1: Assembled full thickness montage of the normal central cornea**

Assembled montage of electron micrographs across the entire thickness of the human corneal stroma (original magnification, 3,640X).

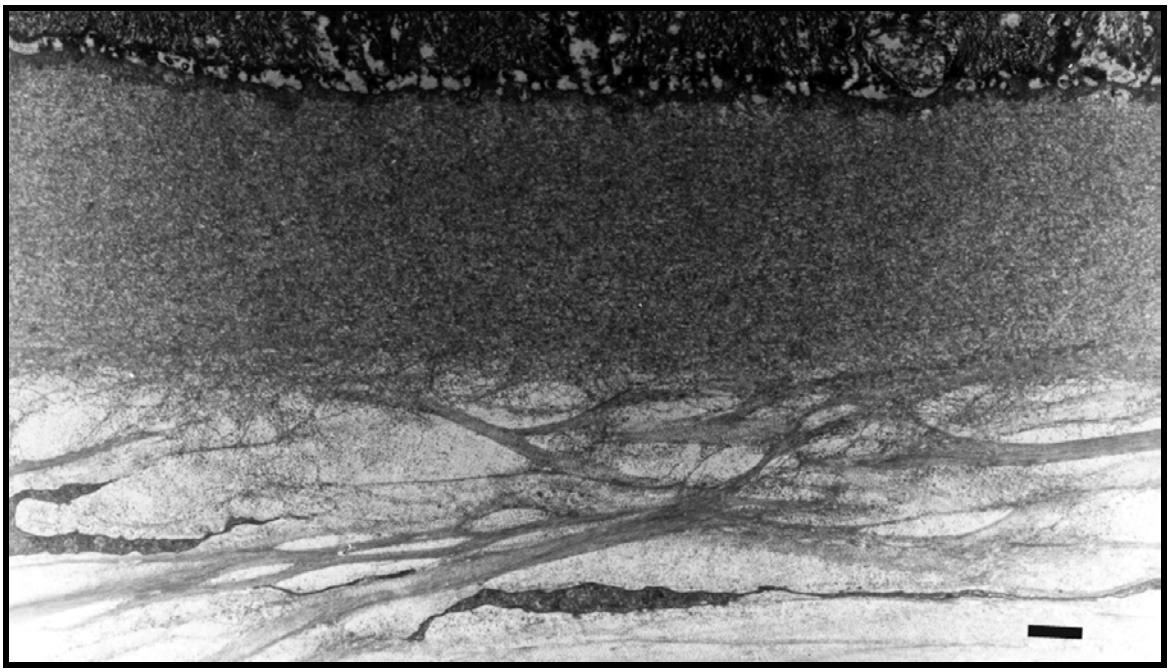

**Figure 3.2: Micrograph of ALL and stromal transitional zone**

Representative transmission electron micrograph showing the transition zone between the anterior limiting lamina and the most anterior aspect of the human corneal stroma. The micrograph was taken at 2,600X magnification and shows highly interwoven and often attenuated lamellae or flattened bundles of collagen fibrils. Scale bar equals 1 µm.

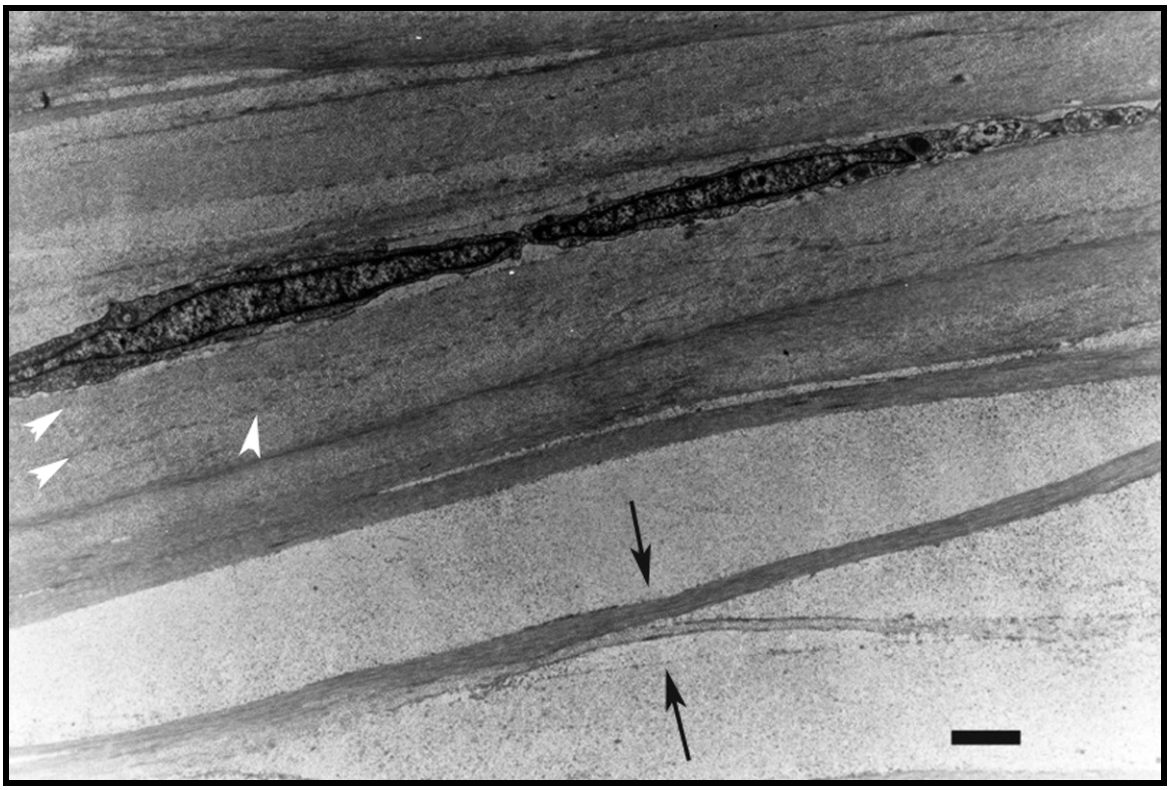

**Figure 3.3: Micrograph of typical features of the anterior corneal stroma**

Representative transmission electron micrograph showing the typical features of the anterior region of the human corneal stroma. The micrograph was taken at 2,600X magnification and shows mainly flattened but generally heterogeneous lamellae. The black arrows show an example of where lamellae apparently split or fuse and where the finer structure of the lamellae was heterogeneous. The white arrowheads show locations of possible borders between lamellae. Scale bar equals 1 μm.

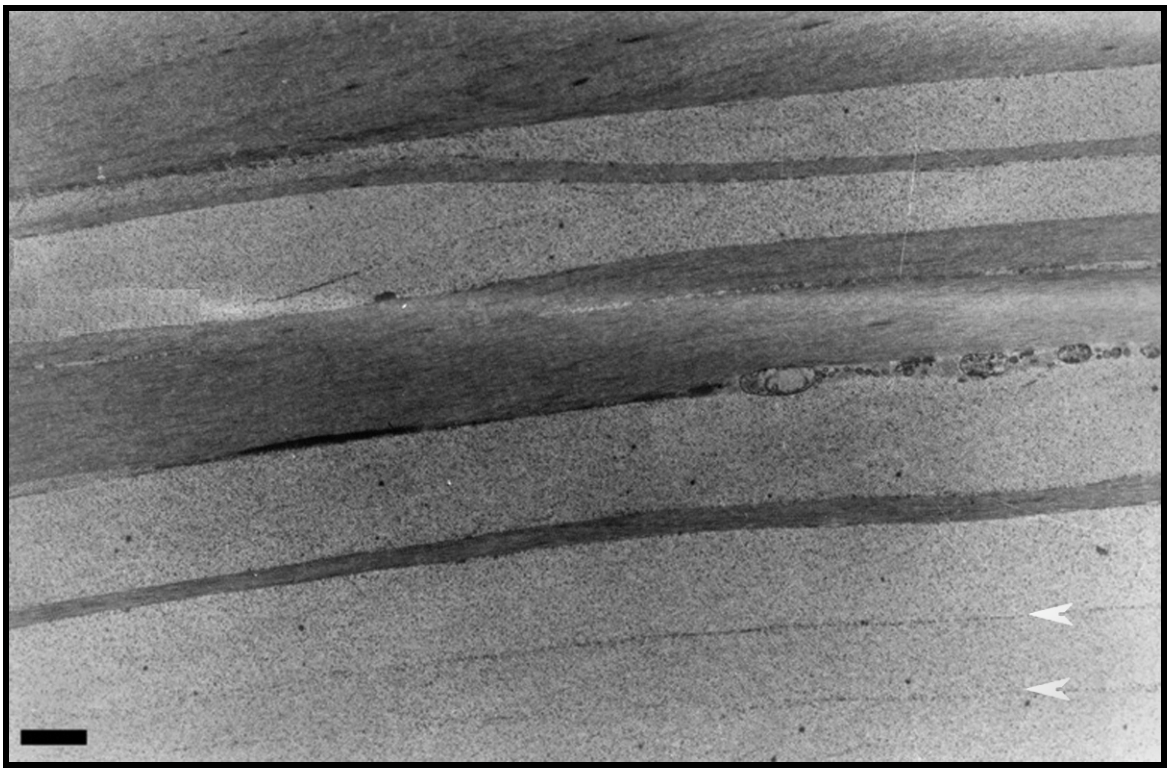

**Figure 3.4: Micrograph of typical features of the mid corneal stroma**

Representative transmission electron micrograph showing the typical features of the mid region of the human corneal stroma. The micrograph was taken at 2,600X magnification and shows flattened but generally homogeneous lamellae. The white arrowheads show locations of possible borders between lamellae. Scale bar equals 1 µm.

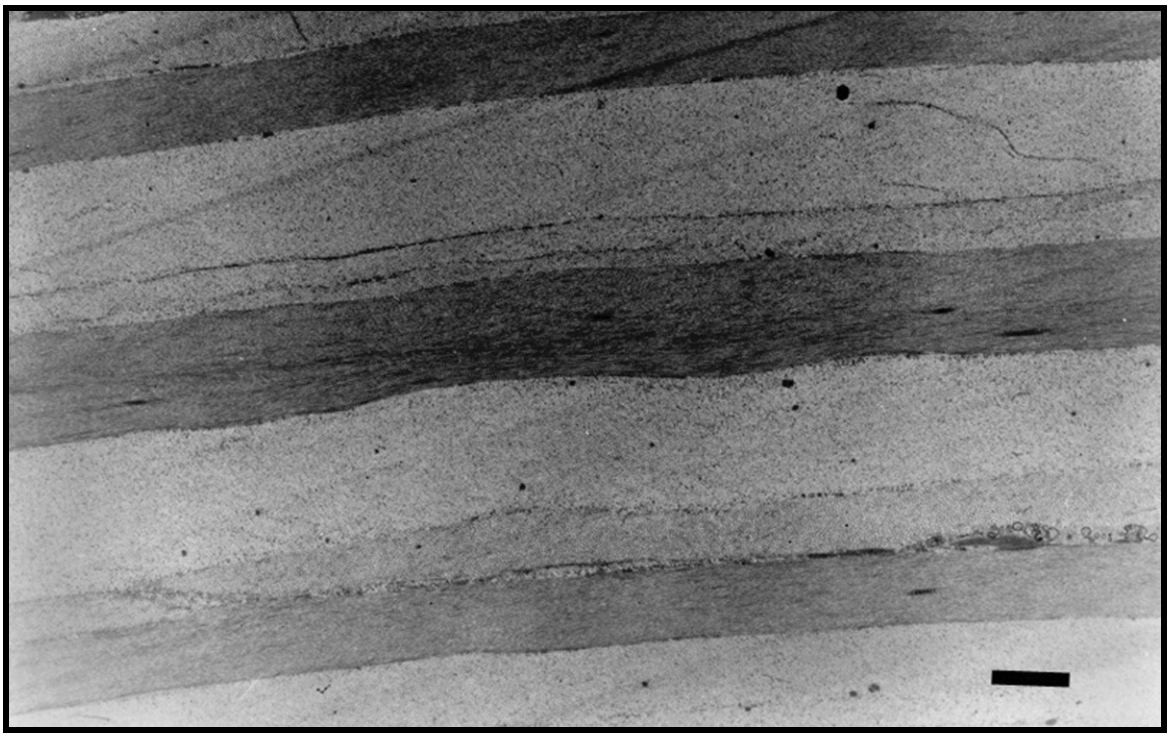

**Figure 3.5: Micrograph of typical features of the posterior corneal stroma**

Representative transmission electron micrograph showing the typical features of the most posterior region of the human corneal stroma. The micrograph was taken at 2,600X magnification and shows flattened but generally homogeneous lamellae. Scale bar equals 1 µm.

**Table 3.1: Criteria used for stromal lamellar counts in normal and keratoconic corneas**

| Lamellar Count Criteria |
| --- |
| • Obvious difference in contrast (change in fibril orientation).<br>• If branching of lamellae occurred within the width of the micrograph, it was counted only once.<br>• Presence of a keratocyte process was considered an interlamellar border.<br>• Lamella <0.2µm were not included. |

**Table 3.2: Assessment of the Number of Lamellae in Different Zones of the Central Region of the Human Corneal Stroma**

| Cornea (Location) | Mean value for lamellae (±SD) | Standard error on counts of lamellae mean (range) | Normalized variance (cov) on counts of lamellae % mean (range) |
|---|---|---|---|
| Entire stroma | 242 ± 4 | 2.63 (0.47 to 6.95) | 1.08 (0.2 to 2.9) |
| Anterior stroma* | 57 ± 12 | 2.60 (1.25 to 4.48) | 4.98 (1.9 to 11.2) |
| Posterior stroma* | 38 ± 5 | 0.93 (0.47 to 1.36) | 2.50 (1.68 to 3.78) |
| Mid-stroma* | 147 ± 14 | 5.08 (0.47 to 12.40) | 3.39 (0.35 to 7.80) |

* counts/100 $\mu$m thickness..

** remaining number of lamellae after subtraction of anterior and posterior counts.

# Chapter 4 - Stromal Lamellar Changes in Keratoconus

## Abstract

**Purpose:** It is known that the keratoconic cornea becomes thinner and ectatic. The purpose of this study was to assess stromal lamellae in the keratoconic cornea to determine whether corneal thinning can be explained by a lamellar drop-out and to identify structural changes that may point to the mechanism of ectasia.

**Methods:** Six surgically removed keratoconic corneal buttons and one normal eye bank control cornea were preserved and processed for transmission electron microscopy using an established corneal protocol, ensuring minimal tissue shrinkage and distortion. A sequence of overlapping digital micrographs spanning the full apical cone thickness was taken at 860X microscope magnification. A seamless digital montage, created using PanaVue ImageAssembler 3 software, was printed (Roland FJ-52) at a final magnification of 5000x. The number of lamellae were counted using an established set of criteria for identifying individual lamellae.

**Results:** The average number of lamellae, in the keratoconic cornea was 319$\pm$105 (range of 109 to 391), but if an extremely thinned keratoconic cornea was excluded, the average was 360$\pm$22. All keratoconic corneas showed clear ultrastructural evidence of lamellar unraveling and a loss of interweaving anterior lamellae. The control cornea contained 241 lamellae.

**Conclusions:** Interestingly, all keratoconic corneas exhibited a dramatic increase in stromal lamellae compared to the control cornea and our previously published data for the normal cornea. Although, it was apparent that the lamellae had not become more numerous, but had rather fragmented into smaller units. A large number of lamellae less than 1µm thick were consistently encountered in all the keratoconic corneas suggesting

that unraveling of the lamellae, most notably anteriorly, is a pathophysiological feature of the keratoconic stroma. The anterior loss of stromal tissue - corneal thinning - together with a generalized fragmentation of lamellae may be dominant factors in provoking corneal ectasia.

## Introduction

Keratoconus is a condition involving corneal steepening, thinning, scarring, and ectasia (Nottingham, 1854; Rabinowitz, 1998; Zadnik et al., 1998, Barr et al., 2000). Scarring in keratoconus is formed by fibroblastic cells or activated keratocytes in the subepithelial or anterior stromal region (Duke Elder & Leigh, 1965; Maguire, 1998, Scroggs & Proia, 1992; Pouliquen et al., 1972; Kenney et al., 2001). The thinning occurring in the keratoconic cornea has been reportedly related to loss of stromal tissue (Eagle, 1999; Leibowitz & Morello, 1998; Rabinowitz, 2005; Shapiro et al., 1986; Morshige et al., 2007). Recent studies have pointed out that the anterior limiting lamina (ALL) and anterior stromal lamellae are lost over large areas **(**Horne et al., 2007**)**. Interestingly, detailed information on the nature of the loss of stromal tissue appears lacking with no consensus on the cause to this thinning. Maguire (1998) summed it up by stating that, "the mechanism of stromal thinning is poorly understood."

Corneal ectasia is associated with keratoconus but may also occur post-surgically after refractive surgery (Binder, 2003; Twa et al., 2004; Holland, 2005; Navas et al., 2007; Dawson et al., 2008). The postsurgical ectasia may manifest itself within a couple of weeks or appear after more than a decade post surgically (Kim H et al., 2006). A recent histopathological analysis (Dawson et al., 2008) of post-PRK and post-LASIK corneas suggested "interlamellar and interfibrillar biomechanical slippage" had occurred and these features were shared with the keratoconic cornea. They also reported a thinning of lamellae and an apparent reduction in the number of lamellae.

Our laboratory assessed the normal central human cornea for number of lamellae and their anterior-posterior distribution, utilizing strict criteria for the count. It was

established that the full thickness human stroma contained 242 lamellae and the individual variation to this number appeared limited. The distribution of lamellae was non-uniform with 50% more lamellae in the anterior than the posterior 100µm (Bergmanson et al., 2005).

The pathological or iatrogenic thinning of the cornea appears to be part of, although not the complete explanation to, the emergence of ectasia. To understand the pathophysiology of keratoconus, we must develop a better appreciation for stromal thinning and its association with the development of ectasia. The purpose of the present study was to establish if stromal thinning can be explained by a reduction in an anterior-to-posterior lamellar count.

## Material and Methods

Six keratoconic corneal buttons were surgically removed by one author (JG) utilizing a penetrating keratoplasty (PKP) procedure. The corneas were from 6 different individuals, aged 38 to 70 years, and all manifested at least one clinical sign for keratoconus, such as Fleischer ring, Vogt striae, Munson sign, abnormal topography, significant corneal thinning and had vision compromised by the disease. All corneas were handled in accordance with the guidelines of the Declaration of Helsinki regarding research on human tissue and appropriate institutional review board approval was obtained. All subjects agreed to the informed consent, which explained that there was no risk involved in donating their tissue. A single control cornea (North Carolina Eye bank) was used in the present study and was transported in a vial containing eye bank medium (Optisol GS, Bausch & Lomb, Irvine, CA) and placed on ice (donor age: 43). This control cornea was in addition and complementary to previous studies on normal human cornea conducted by the authors (Bergmanson et al., 2005).

Immediately following the surgical removal of the keratoconic corneal button, the surgeon placed the tissue into a fixative solution of 2% glutaraldehyde in 80mM sodium cacodylate (pH 7.4, 320 to 340 mOsm/kg). The control cornea, upon arrival, was also immediately placed in the same fixative formulation. For all corneas, the fixative and tissue preparation followed an established protocol developed to minimize tissue distortion and dimensional change (Doughty et al., 1997; Bergmanson et al., 2005). Small analogous pieces (1 x 3 mm) were cut from the geometric center region of the control cornea and from the central cone region within the Fleischer ring, which defines the perimeter of the cone, in keratoconic corneas. These pieces were placed in a freshly

prepared 1% solution of osmium tetroxide (OsO4) in 0.1M cacodylate buffer for post-fixation in subdued lighting. Thereafter, the samples were washed in buffer and then dehydrated through a graded alcohol series (30% to 100% in 6 steps) at room temperature. Then the samples were infiltrated with propylene oxide (3 changes at 10 min intervals) and subsequently with a 2:1 v/v mixture of propylene oxide and Araldite resin (product number 4300, Electron Microscopy Sciences, Fort Washington, PA, USA) for 3 hours. This was followed by overnight immersion in a 1:1 v/v mixture of propylene oxide and Araldite resin, followed by 4-8 hours in 1:3 v/v mixture of propylene oxide and Araldite resin and then transferred to 100% Araldite resin overnight. The tissue samples were oriented in embedding molds and left for overnight polymerization at 60°C.

Thick transverse sections (0.5–1 μm) of the cornea were cut and stained with toluidine blue, for light microscopic observations and to determine tissue orientation. Ultrathin sections (approx. 60-90nm) were then obtained and mounted on parallel bar copper grids (80μm bar spacing) (SPI Supplies, West Chester, PA, USA; product number 2440C-XA). The sections were double-stained first in 3.5% uranyl acetate (dissolved in water) for 20 min at 60°C, followed by Reynold's lead citrate for 10 minutes at room temperature. The grids were examined in a Tecnai G2 12 twin transmission electron microscope (FEI Company, Hillsboro, OR) operating at 100kV. A portion of the grid was selected where there was an uninterrupted high-contrast section while avoiding regions with pronounced lamellar undulations. Once located, a continuous sequence of slightly overlapping digital micrographs was taken at 860X microscope magnification across the entire thickness of the corneal stroma. A seamless montage, created using PanaVue ImageAssembler 3 software, was printed (Roland FJ-52) a single sheet of photo quality

paper at a final magnification of 5000x. Starting at the anterior aspect of the montage, the number of lamellae were counted with the strip placed on a flat surface under cool fluorescent lighting.

The count was carried out by one observer, following a set of pre-established specified criteria (Bergmanson et al., 2005). These criteria specified that the distinction between adjacent lamellae would be made on the basis of an obvious difference in contrast, usually associated with a distinct change in the fibril orientation as a result of the lamellae being cut at a slightly different angle. If, within the width of the micrograph (approximately 28μm), there was an obvious branch or bifurcation of lamellae, care was taken not to double-count such lamellae branches. Conversely, in regions of the micrograph where variation in contrast was subtle, the presence of nearby projections from keratocytes or the presence of thin glancing sections through the edges of such projections were used to decide whether the lamella should be counted as one or two; that is, the presence of keratocyte projections running through the plane of a lamella was an indication of an interlamellar border. Lastly, a decision was made to not include in the count those lamellae that appeared to be extremely thin (i.e., less than 0.2 μm in thickness). This decision was made because other contemporary investigators have considered this value to be the minimum thickness of the lamellae (Komai & Ushiki, 1991; Radner et al., 1998). In addition to making the overall counts of the lamellae, the montages were also marked to define the most anterior 100 μm proximal to the anterior limiting lamina (ALL) and the most posterior 100 μm proximal to the posterior limiting lamina (PLL). In this manner, the stroma was subdivided into three regions.

## Results

All keratoconic corneas exhibited partial or complete losses of ALL over at least a portion of the area surveyed and all specimens also showed a loss of anterior lamellae. The characteristic anterior stroma of the normal cornea, with its branching, interweaving and sometimes terminating lamellae, was absent. As a consequence, the often abnormal epithelial cells, with their thickened basement membrane (BM), were adhering directly onto stromal tissue in places.

The stromal lamellar count, utilizing criteria for inclusion or exclusion in the count, indicated an average number of 319±105 lamellae (range of 109 to 391), which was associated with but not directly dependant on stromal thickness (Figure 4.1). Five of the six keratoconic corneas assessed had lamellar counts in excess of 300 lamellae and had stromal thicknesses of over 350µm. One of the six corneas had just over 100 lamellae, but had only a 212µm thick stroma. By excluding this severely thinned cornea, the average for the keratoconic cornea was 360±22 lamellae. All keratoconic corneas had more lamellae in the anterior versus posterior 100µm, except one, the extremely thin (212µm) cornea where this relationship was reversed.

The lamellae from all of the keratoconic corneas were clearly thin with a high incidence of debris primarily between, but also within, lamellae. This appearance was in stark contrast to the healthy cornea, where lamellae were far thicker and free of debris. Thinned lamellae were predominately present in the anterior to middle regions of the stroma (Figure 4.2 & 4.3), while this phenomenon was present, but less apparent, in the posterior aspects of the cornea (Figure 4.4). A high density of stromal cells was also

apparent (Figure 4.2). Based on cytoplasmic density and nuclear characteristics, these cells appeared to be comprised of keratocytes and cells of another lineage.

Evidence of prominent nerve fibers was lacking. Superficial stroma harbored infrequent, unmyelinated nerve fiber bundles, which appeared abnormal with thin nerve profiles and demonstrating an abnormal relationship with its associated Schwann cell. Posterior cornea, endothelium and posterior limiting lamina, were generally free of abnormalities except for areas of apparent mechanical trauma due to the surgical procedure, where endothelial cells, or portions of them, were absent.

## Discussion

It has long been known that the keratoconic cornea becomes thinned and ectatic (Nottingham, Rabinowitz, Doughty et al., 1997; Bergmanson et al., 2005), but exactly what is lost or the mechanism for developing ectasia has yet to be documented. The present study established the lamellar count in the keratoconic cornea and these results were contrasted to a control cornea and another normal population, which was previously published by our laboratory (Bergmanson et al., 2005). Both studies applied the same criteria for defining a lamella.

The previous study establishing the number of lamellae in the normal human cornea reported that, on average, the cornea had 242 ± 4 lamellae (Bergmanson et al., 2005). The sample (n=6) indicated a narrow variance among individual counts. In addition, when using strict criteria for inclusion or exclusion in the lamellar count, there was little difference between trained observers. Therefore, given the minor inter-observer variation in lamellar counts, only one experienced observer undertook the counting.

All keratoconic corneas in this study, except for one, had a total count of lamellae that was greater than that found in the normal cornea. The average for the six keratoconic corneas assessed was 319 lamellae, which is noticeably more than the control cornea (241) and the 242 lamellae reported previously for the healthy cornea (Bergmanson et al., 2005). The exception in the keratoconic group was a cornea that had undergone extreme thinning and was clearly different to the rest of the group, with regards to corneal thickness. Most likely, this cornea was representative of a more advanced stage of the disease process. If the exceptionally thinned cornea is ignored, the average for the keratoconic cornea becomes 360 lamellae, which is a 49% increase over the normal

cornea. This is a perplexing observation considering that the cornea, made thinner by the keratoconus disease, actually contained an elevated number of lamellae. Comparison with control tissue at the same magnification (Figure 4.5) demonstrated that lamellar structure in all of the keratoconic corneas, including the extremely thin cornea, had unraveled into smaller units. Thus, there truly were no more lamellae added to the cornea but rather existing lamellae had broken apart into smaller units.

It is interesting to note that a similar relation between normal and keratoconic corneas was imaged in a recent study (Dawson et al., 2008). This important study did not include a lamellar count, but instead demonstrated, with illustrations, that corneas developing ectasia following post-PRK and -LASIK also had a lamellar fragmentation similar to the keratoconic cornea. The authors did not attempt to quantify the lamellae in the corneas examined but reported a 'loss of lamellar number' in post refractive ectatic corneas. They proposed a phenomenon they likened to 'interlamellar and interfibrillar biomechanical slippage' and that this structural alteration leads to ectasia. The present study confirms and builds on this observation. Our evaluation of the pathological tissue confirmed changes in lamellar organization and our morphometric data revealed the breaking apart of lamellae into smaller units, which, indeed, may have slipped over each other as proposed by Dawson and colleagues (2008). Comparing the post-surgical ectasia with keratoconus in the latter study, it is apparent that the breaking down of normal lamellar structure had occurred in the postsurgical corneas. Corneal ectasia may occur within weeks of refractive surgery or more than a decade later (Binder, 2003; Twa et al., 2004; Holland, 2005; Kim H et al., 2006; Navas et al., 2007; Dawson et al., 2008). When ectasia develops soon after refractive surgery, it is likely that this change in

morphological organization was present prior to the surgery, making these corneas vulnerable to ectasia. In contrast, when ectasia becomes manifest only years after refractive surgery, it appears more likely that lamellar fragmentation had not yet occurred at the time of the surgery. This would suggest that lamellar fragmentation is not itself the cause of ectasia, but when it occurs in conjunction with corneal thinning, surgical or pathological, the cornea becomes ectatic. All keratoconic corneas evaluated in this study had lamellar unraveling, lost anterior stromal lamellae and thinning or missing ALL (Horne et al., 2007) and at the time of the surgery they were all ectatic.

The present study has revealed and quantified a new stromal phenomenon, lamellar fragmentation, associated with corneal ectasia in keratoconus and most likely also in post-refractive corneas. There may be other factors involved in corneal ectasia, but it would seem that lamellar fragmentation and corneal thinning are essential elements of this pathological process.

# Figures and Tables

**Figure 4.1: Number of Lamellae in the Keratoconic Cornea**

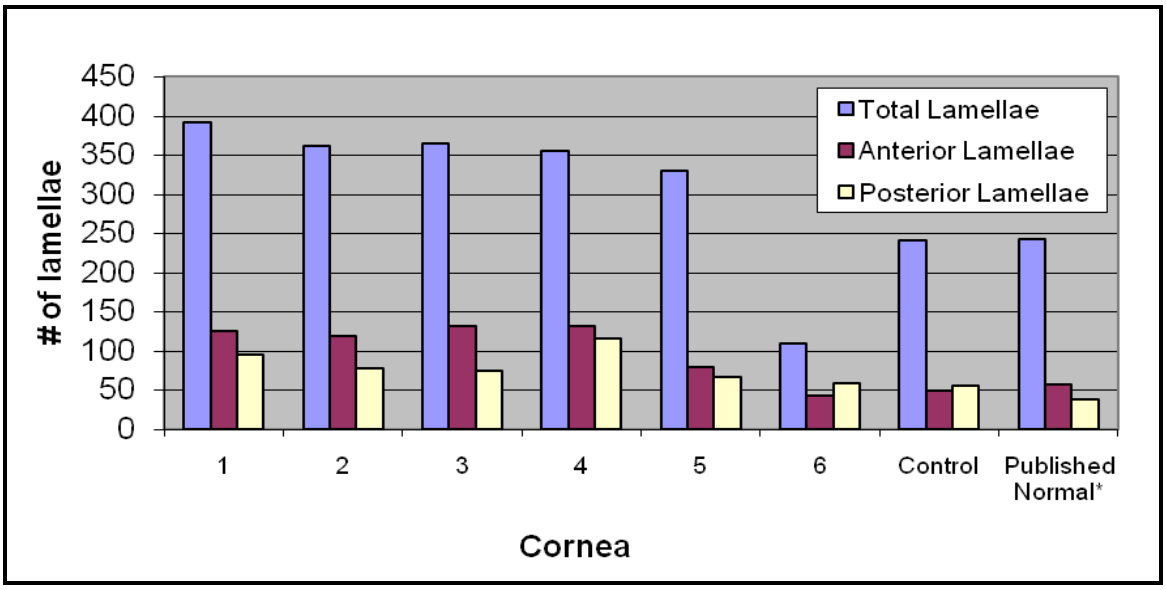


* published data from Bergmanson et al., 2005


**Figure 4.2 A**

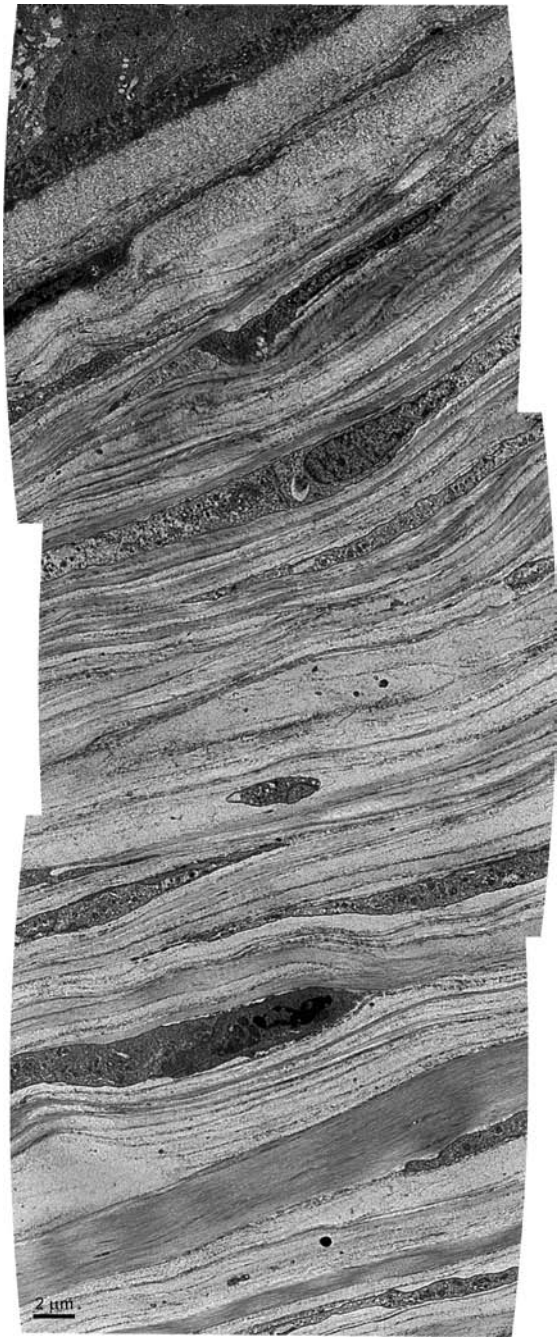


**Figure 4.2 B**

**Figure 4.2: Anterior stromal montage in normal versus keratoconus**

Representative montages from anterior stroma in the human A) normal cornea and B) keratoconic cornea. The keratoconic cornea had numerous lamellae <1µm thick and had a higher incidence of stromal cells. Note the thickened basement membrane, the thinned ALL, and the absence of anterior interweaving stromal lamellae in the keratoconic cornea. Scale bar indicates 2µm. Transmission electron microscopy.

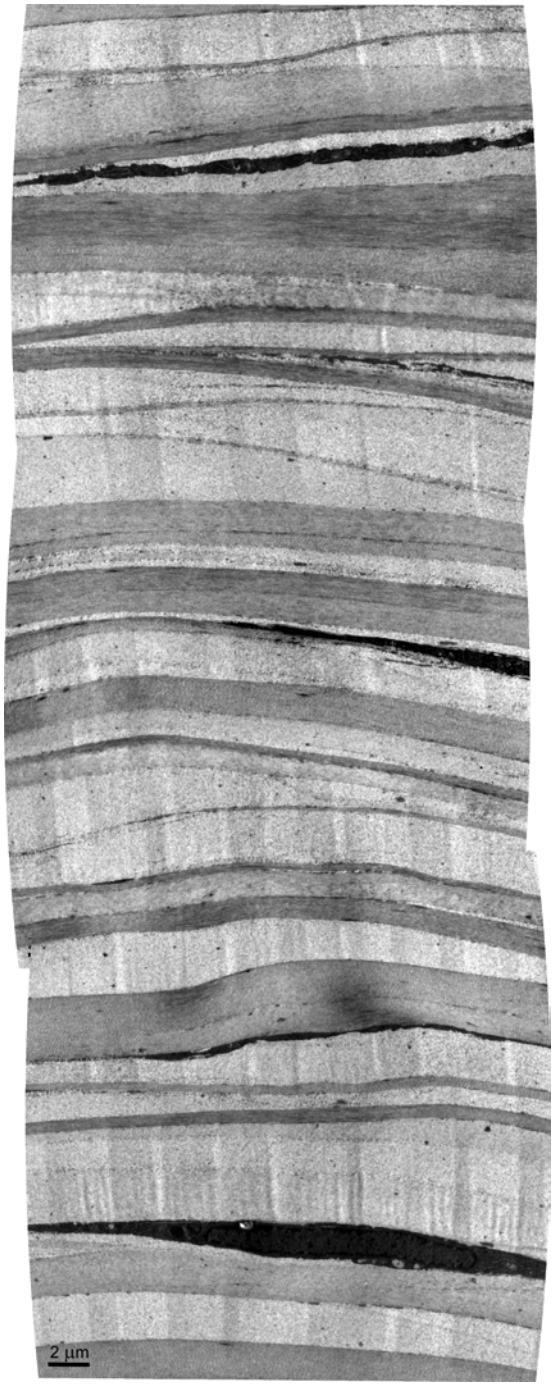


**Figure 4.3 A**


**Figure 4.3 B**

**Figure 4.3: Middle stromal montage in normal versus keratoconus**

Representative montages from middle stroma in the human A) normal cornea and B) keratoconic cornea. In the normal cornea, most lamellae in the middle stroma are 1µm or thicker, while the keratoconic cornea contains numerous lamellae less than 1µm thick Scale bar indicates 2µm. Transmission electron microscopy.

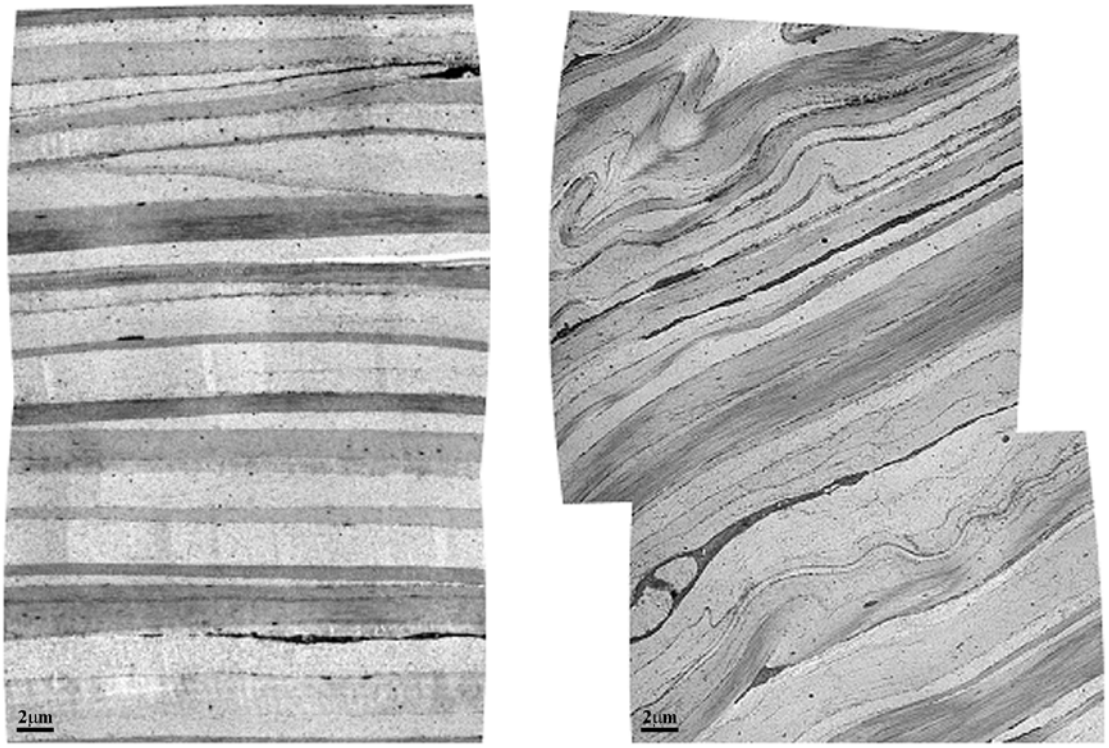


**Figure 4.4: Posterior stromal montage in normal versus keratoconus**

Representative montages from posterior stroma in the human A) normal cornea and B) keratoconic cornea. In normal, most lamellae in the posterior stroma are 1µm or thicker, while the keratoconic cornea contains numerous lamellae less than 1µm thick. Note that some of the lamellae showing fragmentation in the keratoconic cornea are also distorted. Scale bar indicates 2µm. Transmission electron microscopy.

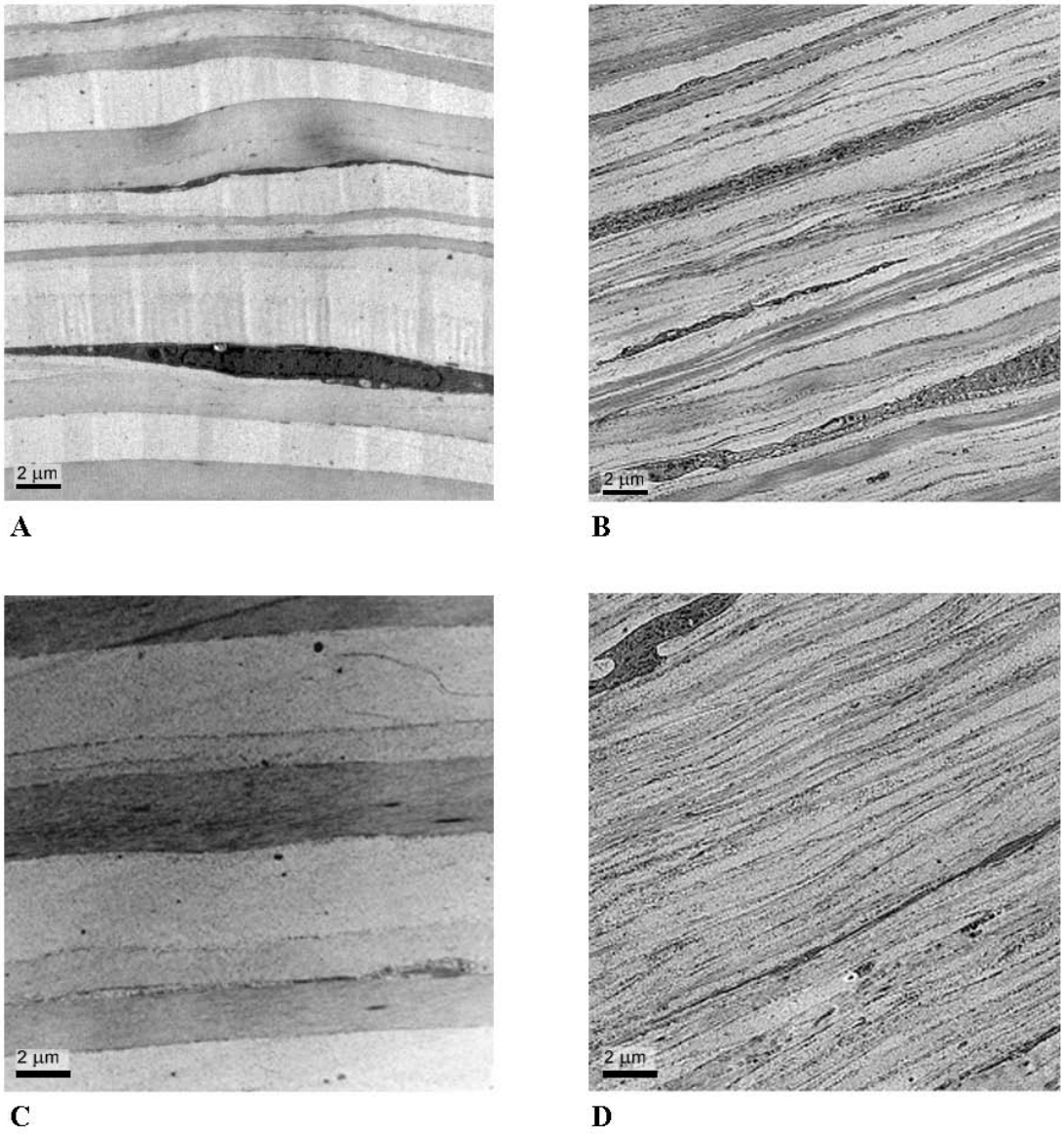


**Figure 4.5: Anterior stromal region of the normal versus keratoconic cornea showing lamellar fragmentation**

Representative micrographs, from the same anterior stromal region, of the normal (A & C) and keratoconic (B & D) cornea. There is an obvious elevation in number of lamellae in the keratoconus vs. normal cornea. Note that these two micrographs are taken at identical magnifications. Scale bar indicates 2µm. Transmission electron microscopy.

# Chapter 5 - Fine structure of the interface between the anterior limiting lamina and the anterior stromal fibrils of the human cornea

This work has been peer-reviewed and published:

Mathew JH, Bergmanson JPG, Doughty MJ. Fine structure of the interface between the anterior limiting lamina and the anterior stromal fibrils of the human cornea. *Invest Ophthalmol & Vis Sci*. 2008; 49(9): 3914-3918.

## Abstract

**Purpose:** To further investigate the ultrastructural details of the collagen fibrils linking the anterior limiting lamina (ALL; Bowman's membrane) of the human cornea to the anterior stromal lamellae, using transmission electron microscopy (TEM).

**Methods:** Six disease-free corneas from donors aged 42 to 82 years were fixed (2% glutaraldehyde in 80mM sodium cacodylate) and processed for TEM in within 72h post-mortem. A series of overlapping images, at 10,240X magnification, of the central corneal ALL/stroma interface were assembled. The features of the terminal ends of fibril bundles at the interface with the anterior stroma were quantitatively assessed.

**Results:** TEM revealed apparently terminating anterior stromal fibril bundles adjacent to ALL. These terminating lamellae (7.8 per 100μm) were embedded in an electron dense material within the surrounding stromal matrix and were termed electron dense formations (EDF's). The mean width of these stromal features was 1.6μm. At intervals, anterior stromal lamellae approached ALL and, in a shallow manner, inserted into ALL. Such projections (5.4 per 100μm) into ALL were, on average, less than 1μm. Numerous fibrils (29.8 per 100μm) extended from ALL into the stroma with a mean length of 0.8μm.

**Conclusions:** The interface the ALL formed with the anterior stroma was complex, and TEM revealed at least three different types of fibrillar arrangements, which may serve optical requirements rather than providing a structural function.

## Introduction

The human cornea is organized into 5 main layers, namely the outer epithelium, the anterior limiting lamina (ALL), the collagen lamellae and keratocyte matrix of the stroma, the posterior limiting lamina and the inner corneal endothelial cell layer (Bergmanson et al., 2005). While this essential organization has been well known for many years (Clareus, 1857; Duke-Elder, 1961; Hogan et al., 1971; Salzmann 1912; Thomas, 1955) increasing attention has been given more recently to the lamellar organization of the anterior corneal stroma and its role in the mechanical properties related to the maintenance of the shape of the anterior surface of the cornea (Bron, 2001; Muller et al., 2001; Pinsky et al., 2005).

A structural aspect of the anterior cornea that has received recent attention is the ALL (often referred to under its eponymous name Bowman's membrane) and, in particular, how this layer is linked to the anterior stromal lamellae. Special features of this interface were first noted by light microscopy methods by Bowman (Bowman, 1847), who considered that there were fibers (from the ALL) that “penetrate the (anterior) lamellae, divide and expand in such a manner as to take a firm hold on them…”. Clareus (1857) noted that unlike at the interface with the PLL, there was no clear borderline between the ALL and anterior stroma, but rather they were continuous with each other. Duke-Elder (1961) summarizes many older ideas by stating that the posterior boundary of the ALL “appears to send prolongations into the substantia propria so that the fibrillar systems of the two are continuous”. In contrast, early transmission electron microscopy (TEM) studies on human cornea noted that the posterior border of the ALL was “marked

by well defined bands of oriented fibers entering an area of unoriented fibers". It was also noted that these fibers, from the anterior stroma, were sometimes parallel to the corneal surface and sometimes almost at right angles to the surface (Kayes & Holmberg, 1960). For chicken corneas, which also possess a fairly well defined ALL, the conclusion drawn from TEM studies was that some fibril bundles were derived from the ALL and projected into the anterior lamellae, while a small contribution came from some terminal ends of anterior lamellae inserting into the ALL particularly in proximity to anteriorly-located keratocytes (Pouliquen et al., 1966). Studies using scanning electron microscopy (SEM) of freeze-fractured corneal specimens revealed the presence of perpendicular coarse fibril bundles at the ALL-stroma interface, and it was concluded that these fibril bundles merged into the ALL and that the ALL was actually a "condensation of the superficial layers of the stroma" (Jacobsen et al., 1984). Recently, second harmonic imaging microscopy has been used to demonstrate the presence of anterior lamellar and fibril bundles that appeared to insert into the ALL (Morishige et al., 2007).

Whether from the earliest light microscopy observations (Bowman, 1847) or much later assessments with TEM (Kayes & Holmberg, 1960; Pouliquen et al., 1966) there is still considerable uncertainty about the fine structure of the interface between the anterior stroma and the ALL. The intent of the present study was to better define the ultrastructure of the ALL/stromal interface at the resolution of the electron microscope to assess details not resolved in recent second harmonic laser imaging studies of this interface (Morishige et al., 2007). This higher resolution imaging is needed to identify the nature of the terminal ends of these collagen fibril bundles, and indicates that there are

distinct differences that could be related to the structural roles that this interface might play.

## Material and Methods

Corneas, with a scleral rim, were obtained from the National Disease Research Interchange (NDRI; Philadelphia, PA) and Lions Eye Bank (Houston and Dallas, Texas, USA) and were handled in accordance with the guidelines of the Declaration of Helsinki regarding research on human tissue. The eyes were from six individuals, aged 42 to 82 years, but had been rejected for use in corneal transplantation for reasons other than corneal disease or previous ocular surgery.

The eyes were delivered to the laboratory within 72h after death, in an iced container and individually immersed in an eye bank storage medium (Optisol GS; Bausch and Lomb, Irvine, CA). Following a previously established protocol developed to minimize tissue distortion and dimensional change (Bergmanson et al., 2005; Doughty et al., 1997; Doughty et al., 2001), the preparations were first thoroughly rinsed with 0.1M sodium cacodylate buffer (pH 7.4), and then immersed overnight at $4^{o}$C in a fixative solution of 2% glutaraldehyde in 80mM sodium cacodylate (pH 7.4, 320 to 340 mOsm/kg). After primary fixation, small analogous pieces (1 x 3 mm) were cut from the central region of the cornea and then rinsed in cacodylate buffer at room temperature, and subsequently post-fixed by immersion for 1h, under subdued lighting, in a freshly prepared 1% solution of osmium tetroxide ($OsO_4$) in 0.1M cacodylate buffer. The samples were again washed in buffer and then dehydrated through a graded alcohol series (30% to 100% in 6 steps) at room temperature. Then the samples were infiltrated with propylene oxide (3 changes at 10 min intervals) and then with a 3:1 v/v mixture of propylene oxide and Spurr's resin (product number 4300, Electron Microscopy Sciences,

Fort Washington, PA, USA) for 3 hours. This was followed by overnight immersion in a 1:1 v/v mixture of propylene oxide and Spurr's resin, followed by transfer to 100% Spurr's resin overnight. The tissue samples were then oriented in embedding molds and left for overnight polymerization at 60$^{o}$C.

The corneal samples were prepared for light microscopy by first cutting thick transverse sections (0.5-1μm) and then staining with toluidine blue. For electron microscopy, parallel bar copper grids (SPI Supplies, West Chester, PA, USA; product number 2415C-XA) with a 125μm spacing were used, and the ultrathin sections (approx. 60-90nm) were stained first in 3.5% uranyl acetate (dissolved in water) for 20min at 60$^{o}$C, followed by Reynold's lead citrate for 10min at room temperature. The grids were examined in a Jeol 100C transmission electron microscope (Jeol USA Inc) operating at 60kV. A sequence of slightly overlapping micrographs was taken at 6600X magnification along the ALL/stroma interface. Sections free of gross sectioning artifacts were selected as suitable for such a montage where the epithelial basement membrane formed a flat and uninterrupted interface with the basal cells.

The negatives were printed to a final magnification of 10,204X, and then assembled to form a continuous montage from each cornea that was then placed on a flat surface and viewed under cool white fluorescent lighting. The corneal montages measured between 115cm and 259cm in width and represented a tissue range of 125μm to 280μm. Detailed measurements were taken, with a ruler placed directly on the prints, of the cross-section length and width of fibril features and relevant lamellar characteristics in five representative locations of each montage. The total number of fibrillar bundles (lamellae terminating intrastromally, stromal lamellar projections into

ALL, and extensions from ALL into stroma) per montage was also counted. All of the data were entered into a statistics software package (Systat, v. 8.0, Systat Inc, Evanston, IL) for generation of descriptive statistics and graphical output. Data sets were checked for normality using the Lilliefors variant of the 1 sample Kolmogorov-Smirnov as included in Systat, and then appropriate parametric or non-parametric tests used to compare measures. A level of statistical significance was set at $p=0.05$.

## Results

### *General features of the fine structure of the ALL / stroma interface as viewed by transmission electron microscopy*

For all six specimens, TEM showed the ALL to be a well defined and uniformly staining amorphous zone immediately under the basement membrane of the corneal epithelium (Figure 5.1). The anterior margin of the ALL appeared smooth, while the posterior edge was irregular. This appearance is primarily explained by the fact that the anterior ALL lines the flat, epithelial basement membrane, while its posterior extreme borders to the anterior stroma with its interwoven, banding and terminating lamellae which harbors anterior keratocytes, predominantly between the lamellae (Figure 5.1).

Large stretches of the ALL/stromal interface followed an irregular outline because of the fibrillar interaction and overlapping between these two layers at this central location. A narrow transect along this interface, between the posterior aspect of the ALL and the anterior stroma, indicated a substantial number of crossings of fibril bundles in both directions, but fibrils predominantly originated from the ALL, with some emanating from terminating anterior stromal lamellae. However, despite the numerous crossings, the true overlap between these two corneal layers appeared to be slight and less than 1µm in either direction (Figure 5.2).

### *Detailed analysis of projections from the ALL and lamellar insertions into the ALL*

Many of these fibril bundles in the interface region stained relatively intensely and were usually oriented obliquely or tangentially but sometimes almost perpendicularly

to the main bulk of the ALL. These rather numerous but finer bundles of fibrils were clearly distinct from the thicker, but still densely staining, lamellae of the most anterior stroma.

Some of the most anterior lamellae had an orientation that was essentially parallel to the ALL. However, other anterior lamellae appeared to have both branched into thinner lamellae and then approached the ALL at a slight angle before apparently coming to an abrupt end near the posterior boundary of the ALL in the central corneal region. This was consistently observed in all samples. These apparent terminal lamellae were embedded in an electron dense, granular material resident in the surrounding stromal matrix, and, will here be described as electron dense formations (EDF's) (Figure 5.3). The width of these terminal ends appeared to be substantial, indicating that they were not just occasional and/or spurious splayed ends of lamellae. In each montage, there was a reasonably consistent incidence of EDF's (average 7.8 $\pm$ 1.3 per 100μm) (Table 5.1). Measures of the width of these EDF's showed a range of values from 0.25 to 2.75μm (Figure 5.4), and across the 6 corneal samples the group mean width was 1.56 ± 0.55μm.

Anterior lamellae approaching the ALL, at intervals, leveled off and minimally engaged with the ALL at a shallow angle. These lamellae were not surrounded by electron dense material as were the EDF's and did not project beyond 1μm into the ALL. These were considered to be lamellar projections or insertions into the ALL (Figure 5.5). The lamellar projections were present at a slightly lower frequency than the EDF's with an average incidence of 5.4 $\pm$ 0.8 insertions per 100μm (Table 5.1). The broad endings on the fibril insertions appeared somewhat stubby and measures of the length for these stroma-originating insertions across the 6 corneas yielded an average value of 0.52 ±

0.38μm (median 0.29μm). Many of these stromal insertions were only 0.25μm in length, and the median value was just 0.29μm (Figure 5.6).

Many of the other fibril bundles that crossed this zone had a distinctly different configuration suggesting that these emanated from the ALL (Figure 5.7). These latter bundles had a wide profile to their posterior aspect and were generally splayed out. The splayed ends were located close to the amorphous aspect of the ALL, and were characteristically very fine, indeed, as they appeared to approach the anterior lamellae of the stroma. The splayed portions of these fine fibril bundles, which were considered to be ALL-originating extensions (and referred to as ALL extensions), were generally oriented at a large angle to the plane of anterior lamellae, sometimes all but perpendicularly. These ALL extensions occurred at a frequency of 29.8 $\pm$ 15.6 per 100μm (Table 5.1). Measures of the overall length of these finer fibril extensions gave a mean value of 0.81 ± 0.58μm (median 0.64μm), but with some as long as 2.65μm (Figure 5.6). Overall, these ALL projections were slightly longer than the stubby lamellar extensions from the stroma (Figure 5.6), and this difference was statistically significant (p=0.031).

## Discussion

The intent of the present study was to better define the fine structure of the ALL/stromal interface at the resolution of the electron microscope, while trying to further investigate the issue of lamellar organization, continuity and discontinuity in the central cornea just under the ALL. As viewed by TEM, the ALL has long been noted to be formed by a dense network of fine, randomly oriented collagen fibers, which are slightly smaller in cross section than the underlying stromal collagen (Kayes & Holmberg, 1960). Such general features have also been noted in more contemporary TEM studies of the ALL (Hayashi et al., 2002) yet provide few clues as to the orientation and/or origin of various fibril bundles. This was more the goal in the present study. In initial ultrastructural observations using TEM (*Horne J, et al. IOVS 2003;44:ARVO E-Abstract 885),* different types of terminal endings for these anterior lamellae were noted. The present report is a completion of the first stage of these analyses which are presented as further evidence for there being both insertions into the ALL as well as extensions from the ALL to the anterior stroma. The TEM methodology, with its associated ultrathin sectioning, has the resolution to demonstrate the existence of the fibrillar overlapping occurring at this interface but cannot reliably reveal the total length of the fibrillar projections from either the ALL or the stroma into its neighboring tissue. High voltage TEM (HVTEM) or TEM with a goniometer may provide a better view of the extent of projection. Using the former (HVTEM), thicker fibrils crossing this interface have been observed that “could be followed for up to 1.5 μm” (Binder et al., 1991) but it is, as yet, unclear if these images represent the total length of such fibrils. In recent second

harmonic laser imaging of the same region of cornea, it was concluded that prominent lamellae appeared to insert into the ALL (Morishige et al., 2007), but such imaging does not have the resolution to see the detail observable with TEM. Notwithstanding, the laser imaging of what appears to be lamellar insertions do show similar features to those seen in light microscopy (not shown), very low magnification TEM images (e.g. Figure 5.1 of this paper) or even scanning electron microscopy (SEM) (Jacobsen et al., 1984), as well as showing remarkable similarity to the diagrams provided by Sir William Bowman based on light microscopy (Bowman, 1847).

At the present time, it is only possible to speculate on the possible origins and/or functions of the insertions into the ALL. The present TEM imaging suggests that some of these insertions arise from branches of anterior lamellae and this then raises the important issue of the course and orientation of any of the lamellae in the anterior stroma. A perspective of the corneal lamellae is that they are essentially flat and very elongated bundles that follow a course from one side of the cornea to the other. However, it was long ago considered and in quite some detail, that some lamellae may well bridge the maximum diameter of the cornea while others can be arranged across much shorter distances (Krauss, 1937). More recent observations have indicated that the anterior lamellae actually also overlap each other quite extensively, and the extent of this so-called inter-lacing between the most anterior lamellae can be more substantial than in the mid- or posterior stroma (Muller et al., 2001; Hayashi et al., 2002; McTigue, 1967; Radner et al., 1993). In addition, evidence has been presented that the lamellae can also branch and even insert through one another (Radner et al., 1998).

At least in the normal human cornea, there appear to be stromal fibril projections into the ALL that are associated with slender ends or branches of anterior lamellae. Such branches, rather than following a course parallel to the ALL interface, are clearly oriented anteriorly. Some appear to broaden out as they become immersed in the network of very fine fibrils that make up the ALL, while others terminate in characteristic electron dense structures (EDF's) that are located posteriorly to the main elements of the ALL (i.e. they do not enter the ALL in a substantial fashion). Since these insertions do appear to arise from a subgroup of anterior lamellae, it is possible that these lamellae are those that do not cross the entire cornea but essentially terminate in the central region of the cornea. The electron dense material, in which the collagen fibers were embedded, may provide the means for securely anchoring down the anteriorly terminating lamellae. This lamellar arrangement and configuration is consistent with a report that there are fewer lamellae in the central region of the cornea compared to the most peripheral regions (Bergmanson et al., 2005; Hamada et al., 1972). In addition to these special configurations of anterior lamellae, a unique group of splayed fibrils appear to originate within the ALL, are directed towards the branched anterior lamellae, but are clearly separated and distinct from these.

The ALL/stromal interface is complex involving multiple fibrillar arrangements each showing a different incidence but together occurred at a relatively high density of 43 per 100µm. The combined structural and mechanical effects of these three types of fibrillar organizations at the posterior aspect of the ALL (that can only be seen at the resolution of the TEM), presumably account for the anecdotal observations that the ALL cannot be detached from the anterior stroma in the normal healthy cornea (Clareus, 1857;

Duke-Elder, 1961; Salzmann, 1912; Thomas, 1955; Bowman, 1847). Logically, such a continuity or shallow blending between the two corneal layers not so much provides structural strength to the most anterior part of the cornea, but rather serves an optical function. For instance, the gradual transition of one tissue into the other would serve optical transparency better than a distinct interface. In addition, we propose that the aspheric curvature of the corneal surface may be explained by the lamellar organization of the central anterior stroma where lamellae appear to terminate rather than stretching from limbus to limbus. The present observations and data will help define the normal morphology of this region and will be most helpful in assessing the pathological consequences of corneal thinning diseases such as keratoconus and pellucid marginal degeneration.

# Figures and Tables

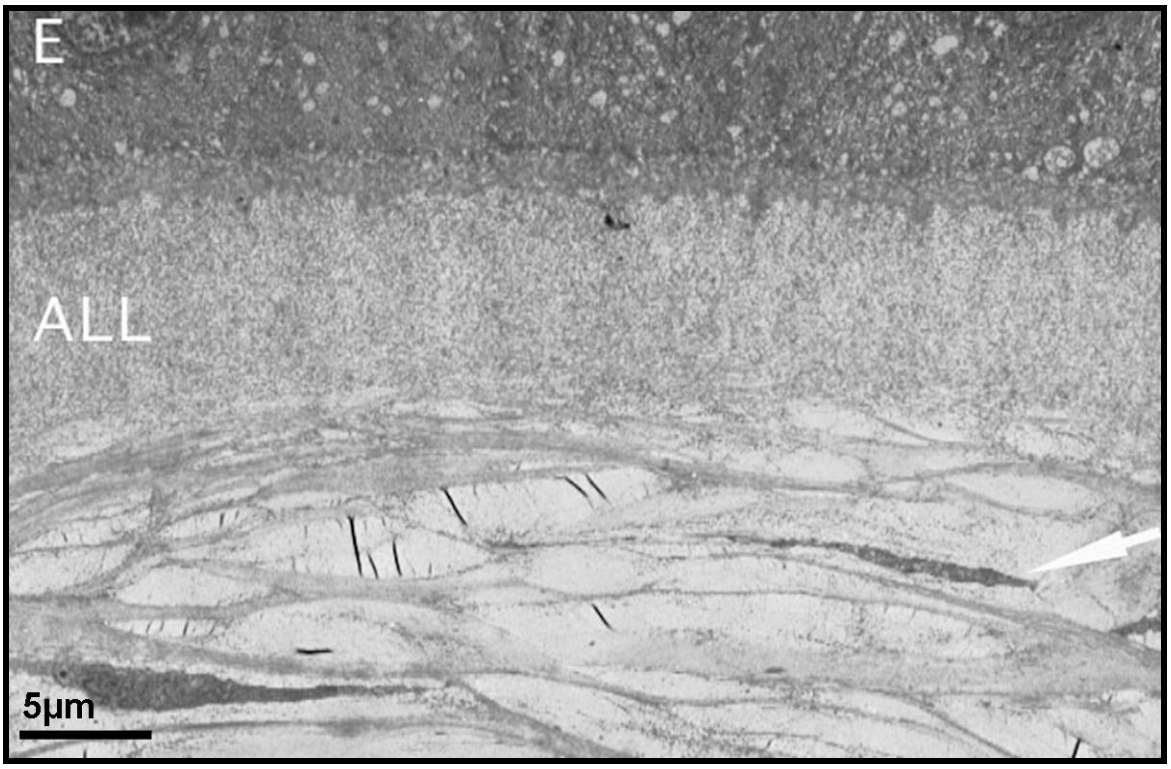


**Figure 5.1: Low magnification of the normal anterior cornea**

Low magnification of anterior cornea showing, basal epithelial cells (E), anterior limiting lamina (ALL) and anterior stroma with regions of flattened, stellate keratocytes (arrow).

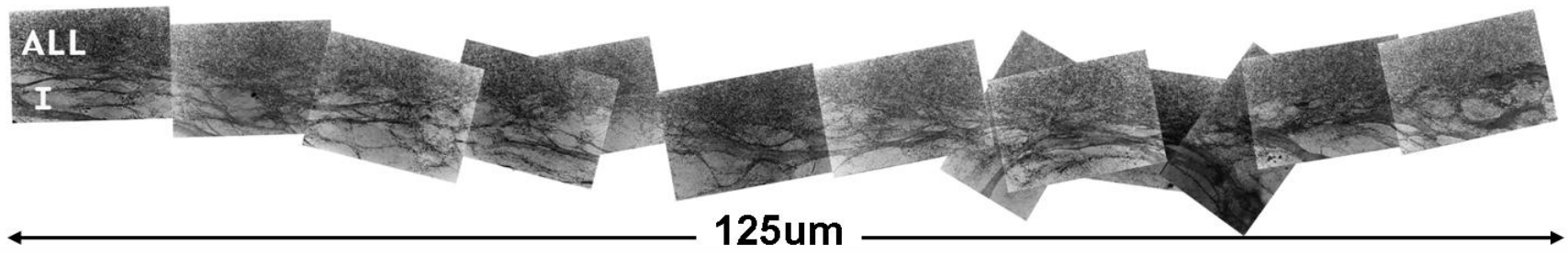


**Figure 5.2: Assembled panoramic montage of ALL/stromal interface in the normal central cornea**

Example of a montage from the central region, approximately 125μm in length, of a cornea showing the anterior liming lamina (ALL) / stromal interface (I).


**Figure 5.3: Terminating anterior lamella in an electron dense formation**

Example of the terminal end of a branch from an anterior lamella in an electron-dense formation (arrow).

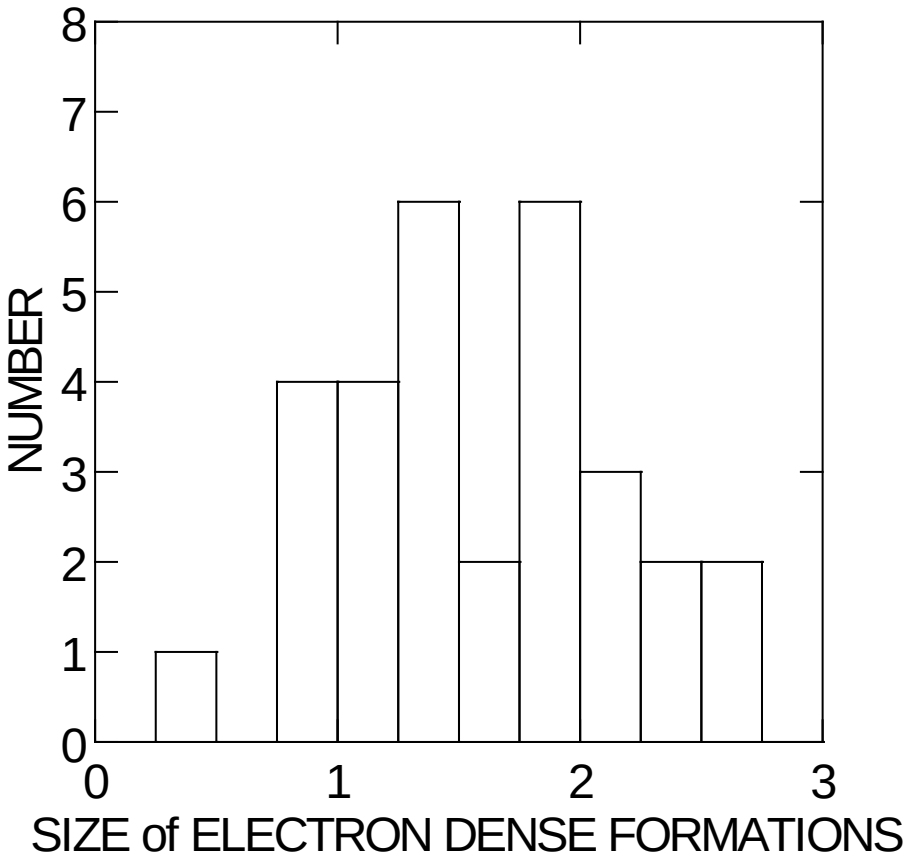


**Figure 5.4: Histogram of electron dense formation size distribution**

Histogram to show distribution of sizes, in μm, for the electron dense formations noted at the posterior boundary of the anterior limiting lamina.

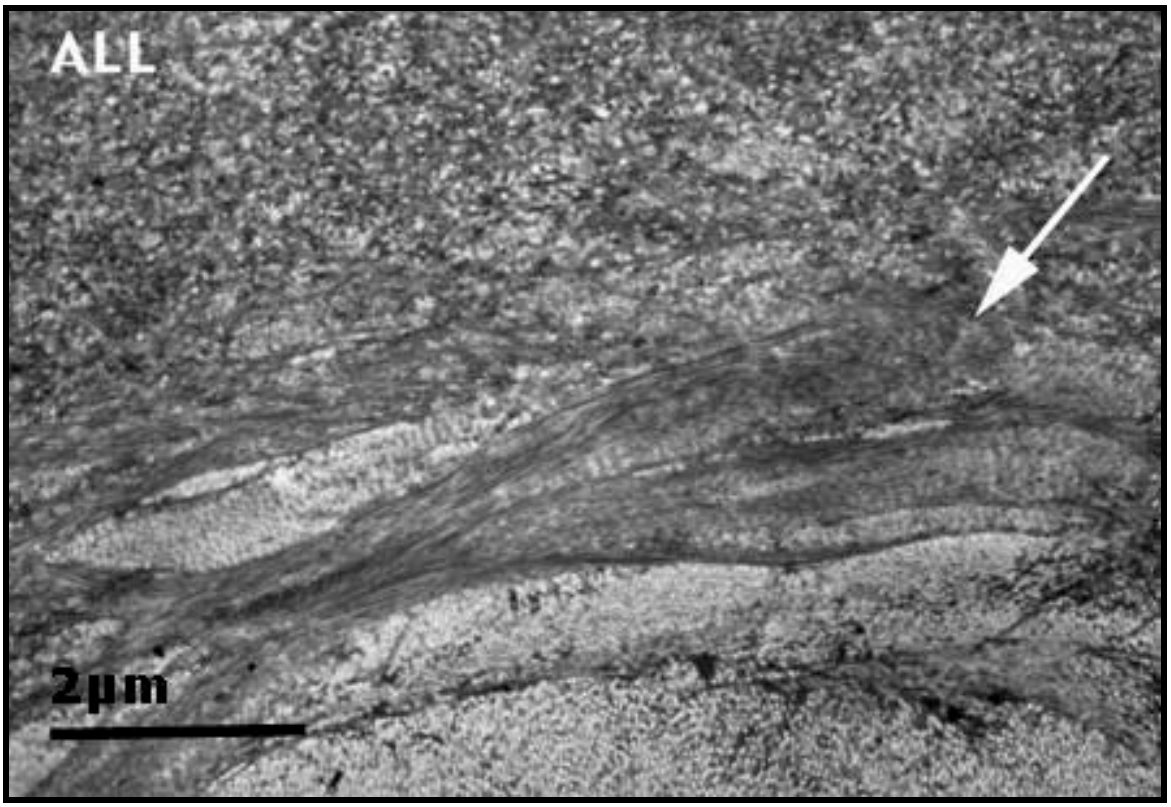


**Figure 5.5: Stromal lamellar insertion into ALL**

Example of a stromal lamellar projection / insertion (arrow) into anterior limiting lamina (ALL) without a terminal electron dense formation.

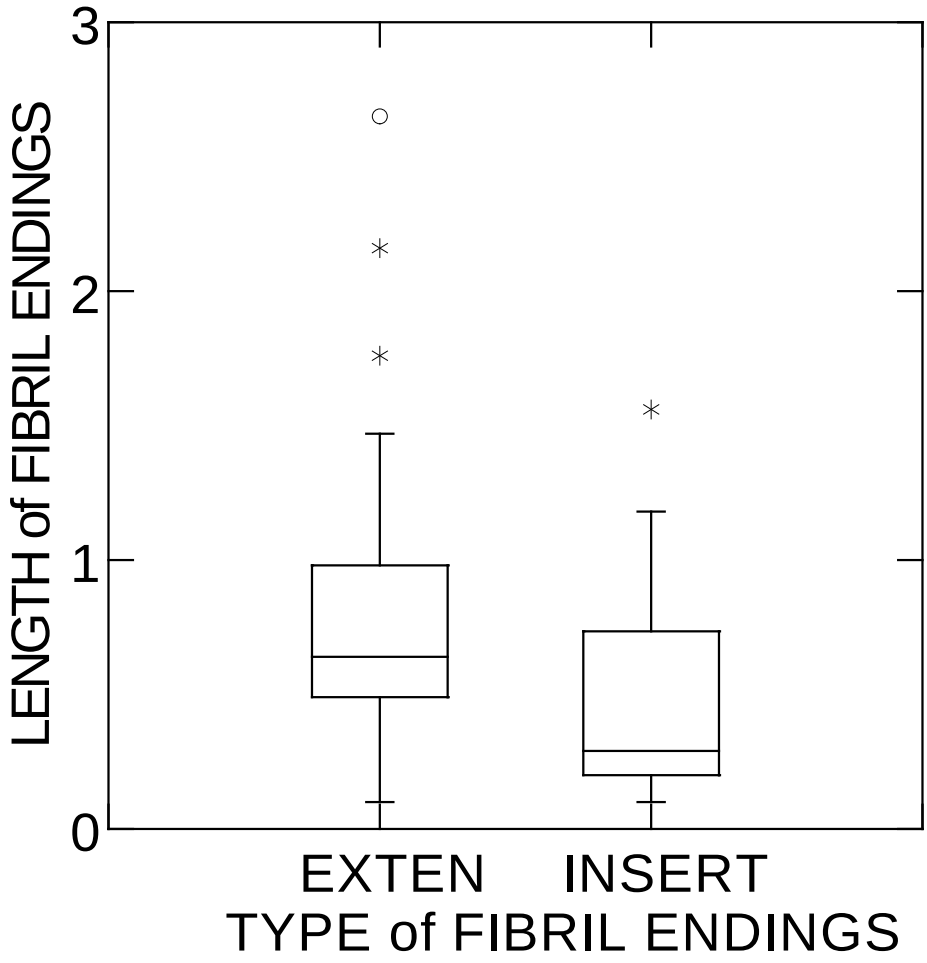


**Figure 5.6: Box plot of difference lengths for stromal insertions vs ALL fibril extensions**

Box plot to show the difference lengths, in μm, for the fibril bundles that make up the lamellar stromal insertions (INSERT) versus those that constitute fibril extensions (EXTEN) from the anterior limiting lamina.

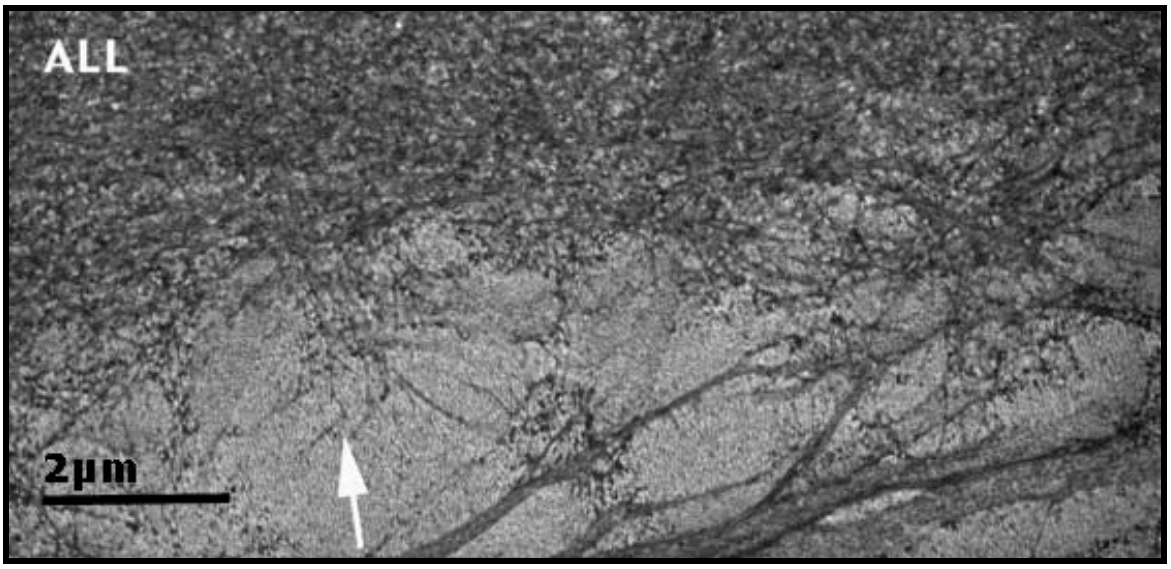


**Figure 5.7: ALL fibril extension into anterior stroma**

Example of a fine fibrillar extension (arrow) from anterior limiting lamina (ALL) into anterior stroma.

**Table 5.1: Incidence of Fibrillar Features at the ALL/stromal Interface (# of fibrils per 100µm)**

| Montage | Electron Dense Formation (EDF) | Stromal Lamellar Projection/Insertion into ALL | ALL Extension into Stroma |
|---|---|---|---|
| **1** | 8 | 4.8 | 61 |
| **2** | 6.1 | 5 | 21.4 |
| **3** | 6.6 | 6.1 | 21 |
| **4** | 7.6 | 5.6 | 22.2 |
| **5** | 9.6 | 6.4 | 23.2 |
| **6** | 8.9 | 4.5 | 30 |
| **Average $\pm$ SD** | 7.8 $\pm$ 1.3 | 5.4 $\pm$ 0.8 | 29.8 $\pm$ 15.6 |

Incidence of fibrillar features at the ALL/stromal interface showing the number of fibrils per 100µm of tissue. The data was collected utilizing montages from 6 separate corneas.

# Chapter 6 - Quantified Histopathology of the Keratoconic Cornea

## Abstract

**Purpose:** The present study systematically investigated and quantified histopathological changes in a series of keratoconic corneas utilizing a physiologically formulated fixative to not further distort the already distorted diseased corneas.

**Methods:** Twelve surgically removed keratoconic corneal buttons were immediately preserved and processed for light and transmission electron microscopy using an established corneal protocol, to minimize tissue shrinkage and distortion. Measurements were taken from the central cone and peripheral regions of the host button. Sample size ranged in overall length from 390-2608µm centrally, while peripherally from 439-2242µm.

**Results:** The average corneal thickness was 437µm centrally and 559µm peripherally. Epithelial thickness varied centrally from 14-92µm and peripherally from 30-91µm. A marked thickening of the epithelial basement membrane was noted in 58% of corneas. Centrally, anterior limiting lamina (ALL) was thinned or lost over 60% of the area examined, while peripheral cornea was also affected, but to a lesser extent. Posterior cornea remained undisturbed by the disease. Anteriorly in the stroma, an increased number of stromal cells and tissue debris were encountered and some of these cells were clearly not keratocytes.

**Conclusion:** It is concluded that keratoconus, at least initially, has a distinct anterior focus involving the epithelium, ALL and anterior stroma. The epithelium had lost its cellular uniformity and was compromised by the loss or damage to ALL. The presence and activity of the hitherto unreported recruited stromal cells may be to break down and

remove ALL and anterior stromal lamellae leading to the overall thinning that accompanies this disease.

## Introduction

Keratoconus is a non-inflammatory condition characterized by corneal ectasia, steepening, thinning and scarring (Rabinowitz, 1998; Zadnik et al., 1998; Barr et al., 2000). Reports in literature have described a number of pathological changes within the keratoconic cornea. Featured prominently in these reports are observations of "breaks/interruptions/fragmentations/dehiscences/ruptures" of the anterior limiting lamina (ALL) (Duke-Elder & Leigh, 1965; Chi et al., 1956; McPherson & Kiffney, 1968; Shapiro et al., 1986; Kaas-Hansen, 1993; Arffa, 1997; Leibowitz & Morello, 1998; Maquire, 1998; Sawaguchi et al., 1998; Eagle, 1999; Sugar, 2004; Feder & Kshettry, 2005; Nakamura et al., 2005; Rabinowitz, 2005; Krachmer & Palay, 2006; Yanoff & Sassani, 2009; Teng, 1963). This observation shared by many, appears to describe a 'crack' or brief discontinuity of the ALL. Although most sources agree that keratoconus is a disease of the stromal layer, Chi et al. (1956) presented some evidence of an epithelial contribution to this ocular pathology. Teng (1963) even postulated that the origin of this disease was to be found in the epithelium (Teng, 1963), and this hypothesis has later received further scientific support from others (McPherson & Kiffney, 1968; Shapiro et al., 1986; Sawaguchi et al., 1998; Tsubota et al., 1995; Wilson et al., 1996; Rorbach et al., 2006).

Stromal changes in the keratoconic cornea have been noted in literature but in limited detail. Leibowitz and Morello (1998) states that, "collagen fibers are said to be normal, with thinning attributable to a decrease in the number of collagen lamellae". The loss of lamellae as an explanation to corneal thinning is also proposed by other sources

(Sugar, 2004; Apple & Rabb, 1998; Morishige et al., 2007, Dawson et al., 2008). In addition, and according to Morishige (2007), the keratoconic cornea showed "less lamellar interweaving and marked reduction or loss of [anterior] inserting lamellae".

Most corneal alterations reported appear to have an anterior location, although histopathological changes can occur in the posterior cornea in this condition as a result of hydrops. However, hydrops are viewed as an uncommon complication in this disease (Thota et al., 2006). Rupture of the posterior limiting lamina (PLL), leading to a discontinuity of endothelial cell coverage of the posterior corneal surface, allows fluid free entry into the corneal stroma (Sugar, 2004; Apple & Raab, 1998; Morishige et al., 2007; Thota et al., 2006). Although the induced corneal edema mostly clears up, resultant scarring may prevent victims of hydrops from regaining acceptable visual acuity (Thota et al., 2006).

It follows that the current understanding of the pathophysiology of keratoconus is incomplete. Eyecare practitioners managing keratoconic patients would greatly benefit from improvement of our knowledge base. Detailed information on tissue changes within the cornea may provide indications on the ability of the unhealthy cornea to handle the presence of a contact lens or where lens bearing is undesirable. More precise knowledge of the location and focus of the disease may better direct the surgeon to the optimal choice of procedure, which, in transplant surgery, may be lamellar or penetrating keratoplasty.

Literature contains only a modest number of histopathological reports on keratoconus involving multiple cases. However, with few exceptions, they lack morphometry and in some cases, are limited to light microscopy and a protocol using a

high osmolality fixative that further distorts an already distorted cornea (McPherson et al., 1968; Scroggs & Proia, 1992; Kaas-Hansen, 1993; Sawaguchi et al., 1998; Rohrbach et al., 2006). The purpose of this study was to systematically investigate and quantify pertinent histopathological changes in a series of keratoconic corneas, in both the central cone area and in the adjacent mid-peripheral corneal region, using an established fixative with physiological osmolality.

## Material and Methods

Twelve keratoconic corneal buttons were surgically removed by one author (JG), with eight corneas removed by penetrating keratoplasty (PKP) and four by deep lamellar keratoplasty (LKP). The corneas were from 12 different individuals, aged 18 to 70 years, and all manifested at least one clinical sign for keratoconus, such as Fleischer ring, Vogt striae, Munson sign, and had vision compromised by the disease. Four apparently disease free corneas obtained from eye banks and the National Disease Research Interchange, were utilized as control tissue. All corneas were handled in accordance with the guidelines of the Declaration of Helsinki regarding research on human tissue. Informed consent was obtained from all subjects after first explaining that there was no risk involved in donating their tissue. This study received appropriate institutional review board approval.

Immediately following the removal of the keratoconic corneal button, the surgeon placed the tissue into a fixative solution of 2% glutaraldehyde in 80mM sodium cacodylate (pH 7.4, 320 to 340 mOsm/kg). Control eyes were stored in the eye bank medium (Optisol GS, Bausch & Lomb, Irvine, CA) and arrived on ice. These corneas were fixed within 72 hours after death. For all corneas, the fixative and tissue preparation followed an established protocol developed to minimize tissue distortion and dimensional change (Doughty et al., 1997; Bergmanson et al., 2005). Small analogous pieces (1 x 3 mm) were cut from the central cone, within the Fleischer ring, and the periphery, opposite to the cone, of each corneal button and placed in a freshly prepared 1% solution of osmium tetroxide ($OsO_4$) in 0.1M cacodylate buffer for post-fixation in subdued

lighting. Thereafter, the samples were washed in buffer and then dehydrated through a graded alcohol series (30% to 100% in 6 steps) at room temperature. Then the samples were infiltrated with propylene oxide (3 changes at 10 min intervals) and subsequently with a 2:1 v/v mixture of propylene oxide and Araldite resin (product number 4300, Electron Microscopy Sciences, Fort Washington, PA, USA) for 3 hours. This was followed by overnight immersion in a 1:1 v/v mixture of propylene oxide and Araldite resin, followed by 4-8 hours in 1:3 v/v mixture of propylene oxide and Araldite resin and then transferred to 100% Araldite resin overnight. The tissue samples were oriented in embedding molds and left for overnight polymerization at 60$^{o}$C.

The corneal samples were prepared for light microscopy by first cutting thick (0.5-1μm) transverse sections and then staining with toluidine blue. Centrally, tissue samples ranged in overall length from 389.6μm to 2607.9μm and measured on average 1363.0μm, while peripherally these measurements were 439.3μm, 2242.3μm and 1182.0μm, respectively. For electron microscopy, parallel bar copper grids (SPI Supplies, West Chester, PA, USA; product number 2440C-XA) with a 80 μm spacing were used, and the ultrathin sections (approx. 60-90nm) were stained first in 3.5% uranyl acetate (dissolved in water) for 20min at 60$^{o}$C, followed by Reynold's lead citrate for 10min at room temperature. The tissue was examined ultrastructurally in a Tecnai G2 12 twin transmission electron microscope (FEI Company, Hillsboro, OR) operating at 100kV.

Using light microscopy (Olympus BX51 digital light microscope), a variety of measurements were taken from keratoconic corneas in two different transverse sections, separated by at least 200-300μm, and then averaged. These measurements were taken at three locations (central and at each extreme) along the tissue length and included:

epithelial thickness (both LKP & PKP), epithelial cell layer counts (both LKP & PKP), ALL pathological involvement (both LKP & PKP), stromal thickness (only PKP), and total corneal thickness (only PKP). Length measurements were obtained using the NIH image software at the light microscope.

Tissue from PKP corneas was also evaluated ultrastructurally utilizing transmission electron microscopy for general and high-resolution observations, photography and measurement of epithelial basement membrane thickness. Control tissue was used for general observations and epithelial basement membrane (BM) measurements but could not be utilized for other length or thickness measurements because of post-mortem tissue swelling. For obvious reasons, the eye bank eye almost invariably has ocular surface defects and, therefore, could not be used in the epithelial thickness and cell layer counts.

## Results

Total keratoconic corneal thickness and stromal thickness could only be measured in those corneas removed by PKP (n=8). Central stromal thickness was, on average, 379.2µm and ranged from 236.2µm to 633.1µm. Total corneal thickness centrally averaged 436.5µm and peripherally averaged 558.6µm (Table 6.1, 6.2). Epithelial thickness was quite variable for both the central cone region and the peripheral region, ranging from 13.5µm to 91.6µm (avg: 42.2µm) and from 29.8µm to 90.9µm (avg: 54.5µm), respectively (Figure 6.1). There were, on average, 6 epithelial cell layers centrally (range: 4-9), and 7 cell layers peripherally (range: 5-8) (Table 6.1, 6.2). The epithelium also showed both elongated and compressed basal cells and granular deposits within the cytoplasm (Figure 6.2, 6.3). Frequently epithelial cells had not taken up the stain in a characteristically uniform manner with some cells appearing strikingly densely stained while others were pale. Light microscopically, it was recorded that 7 of the 12 corneas had developed a noticeably thickened BM (Figure 6.2). Ultrastructural observations of the PKP central buttons (n=8) confirmed an extremely abnormal basement membrane thickness, which averaged 1.46µm and ranged from 0.05-3.67µm. It was often stratified and contained large cracks on the side facing the basal epithelial cells (Table 6.3). In contrast, the control corneas (n=4) were thinner with more uniform BM's measuring 0.05-0.65µm with an average of 0.41µm.

Large areas of ALL were thinned or completely missing centrally, in the central cone region, in all keratoconic corneas except two, but peripherally only half of the corneas manifested abnormalities in this respect (Table 6.4, 6.5). Four keratoconic

corneas had completely lost ALL over significant areas centrally, while peripherally, only two corneas exhibited such a loss. In these corneas, the center of the cone showed that ALL was affected over 60% of tissue examined. ALL was only affected peripherally if it was also affected centrally. In no instance was the peripheral corneal portion of the button affected without central involvement. In the central cone region, areas of extensive ALL loss ranged in length from 31.4µm to 790.0µm and areas of thinned ALL ranged from 32.4µm to 2602.4µm. Peripherally, areas of lost ALL and thinned ALL ranged from 16.28 to 363.9 and 53.0 to 767.9, respectively. Control tissue had ALL of uniform thickness and no areas with ALL missing.

In all specimens examined, a striking feature of the disease was its anterior corneal focus. Other than the already mentioned epithelial changes and the gradual destruction of ALL, the anterior stroma, immediately posterior to ALL, was severely affected and in places even lost. An increased number of stromal cells and tissue debris were typically observed in this region and clearly some of these cells were not keratocytes, showing lighter stained cytoplasm (Figure 6.4, 6.5). These cells appeared to be involved in the removal of corneal tissue. None of these features were recorded in the control tissue.

Interestingly, we did not observe the clinically well-established phenomenon of prominent nerves in the central keratoconic tissue. However, the button contained, on occasion, slender stromal unmyelinated fiber bundles that were abnormal in shape (Figure 6.6).

Posteriorly, the corneal morphology of the keratoconic buttons examined were similar to normal control tissue. On occasion, an abrupt kink was observed in the

keratoconic lamellar outline. Physical trauma to the tissue and its handling during the surgical procedure produced endothelial damage, but away from such areas the endothelial cells appeared healthy and similar to those of the control corneas. The overall impression was that this disease does not involve the endothelium and its BM until a more advanced stage that results in hydrops.

## Discussion

This study attempted to morphometrically characterize keratoconic-induced pathological changes in a case series of 12 corneas from 12 patients. Furthermore, our data were generated from tissue that was preserved in a fixative formulated to better match corneal physiology (Doughty et al., 1997). Our keratoconic tissue protocol, together with the immediate post-surgical fixation, avoided the dilemma of further distortion of an already pathologically distorted tissue. Therefore, it is here argued that the data and observations presented are accurate and generally free of artifacts. In the present study, control tissue was utilized for general observations and comparison with keratoconic specimens, but with the limitation of eye bank corneas, they could not be assessed for many of the measurements carried out on the keratoconic corneas. Further work on the normal human cornea conducted in our laboratory has been published separately (Bergmanson et al., 2005; Mathew et al., 2008).

The ALL is intimately related to the epithelium and provides the foundation that the epithelium needs to remain firmly attached to the cornea (Gipson et al., 1987; Bergmanson, 2010). In the absence of ALL, it is not surprising that the epithelium becomes irregular and less well organized, as was noticed in the present study. In our samples, the central keratoconic cornea showed an almost 80µm (range: 13.5-91.6µm) variation in epithelial thickness. Indeed, this variation was greater than the normal thickness (50µm) of the epithelium, which typically has an extremely uniform outline (Duke-Elder & Leigh, 1965; Bergmanson, 2010; Hogan et al., 1971; Li et al., 1997; Nishida, 2005). In PRK, where ALL invariably is ablated, similar variations in the

epithelial thickness have been described (Waring, 1998). The peripheral cornea also showed epithelial thickness variations, but to a lesser extent. Somewhat surprisingly, the observed thickness variation was not explained by a simple variation in layers of cells. On average, the epithelium was formed by 6 layers of cells, which is within the normal range (Bergmanson, 2010), but where the epithelium was thick, cells were also relatively taller. This observation suggested that pathological epithelial thickness changes in keratoconus were the result of changes in size rather than cellular proliferation.

Contact lens (CL) wear, which with keratoconic patients is typically of the gas permeable variant, may have exaggerated intra-corneal epithelial thickness variation. For visual reasons, some patients may have worn their CL's sufficiently close to the surgery date to have had an effect on the tissue examined histopathologically. Indeed, patients, who were CL wearers, were not discouraged to wear their lenses prior to the surgery. However, most patients had become intolerant to their CL's and were not wearing them. Therefore, we would argue that the observed intra-corneal epithelial thickness variations were mainly a product of the disease itself and to a lesser extent, a result of CL wear.

Although epithelial thickness variation may, to a degree, be the result of an adaptation to a pathological relationship with underlying tissue, there was still distinct evidence of abnormal epithelial behavior. Especially the basal cells often stained densely and had adopted peculiar stances or positions, which is an observation also reported by earlier literature (Teng, 1963; Rabinowitz, 2005). Interestingly, the BM, which should be up to 0.20µm in the healthy eye (Alvarado et al., 1983), and measured 0.4µm in our control tissue, was in some of our keratoconic specimens substantially thicker measuring up to 3.67µm in thickness and occurred without the presence of scar tissue. Others have

made similar observations ultrastructurally, reporting BM thickening and fragmentation, but offering no measurements (Teng, 1963; Brewitt & Reale, 1981; Akhtar et al., 2008). Teng (1963), in observing basal cell and BM pathological changes, arrived at the conclusion that keratoconus had an epithelial etiology. The findings in the present study cannot confirm Teng's hypothesis. However, the epithelium clearly appeared to be an involved participant in the keratoconus disease process, but it was not apparent whether it is an instigator or a passive responder.

A striking and consistent finding was the involvement of ALL in the disease process in all central keratoconic corneas except two. In the majority of the keratoconic corneas examined, ALL was affected in more than 50 percent of the area assessed (Table 6.4). In four of the twelve keratoconic corneas evaluated, ALL was completely missing in places. The variation between the individual corneas is most likely due to a combination of factors, such as disease severity and different disease expressions or types. Furthermore, the area, from which the data was collected, may not have been from the corneal region most severely afflicted, although central cornea tissue sampling came from within the Fleischer ring, when it could be observed under the dissection microscope.

The discovery of the significant and widespread effect of the disease on the ALL is in contrast to the common belief that keratoconus leads to breaks, ruptures, cracks, etc (Duke-Elder & Leigh, 1965; Chi et al., 1956; McPherson & Kiffney, 1968; Shapiro et al., 1986; Kaas-Hansen, 1993; Arffa, 1997; Leibowitz & Morello, 1998; Maquire, 1998; Sawaguchi et al., 1998; Eagle, 1999; Sugar, 2004; Feder & Kshettry, 2005; Nakamura et al., 2005; Rabinowitz, 2005; Krachmer & Palay, 2006; Yanoff & Sassani, 2009; Teng,

1963). This observation, supported by the accompanying morphometry, clearly uncovered more extensive pathological changes than simple breaks or ruptures of ALL. The removal of parts or all of ALL, often together with loss of anterior stromal tissue, may contribute to the weakening of the cornea leading to subsequent corneal ectasia. However, there must be other factors involved in the provocation of corneal ectasia since photorefractive keratectomy, which invariably removes ALL, only rarely leads to ectasia. As mentioned above, the effect of a defective or removed ALL also has epithelial consequences, which includes deficient adhesion and inability to maintain a normal, uniform thickness. Clinically, it is known that the epithelium in keratoconus is more fragile and more often will show surface defects (Young et al., 2005). Interestingly, Akhtar et al. (2008) reported that as keratoconus progresses, the collagen fibril diameter decreases while the proteoglycan content of the stroma increases. It was proposed that these pathological changes were related to the structural weakening of the cornea in keratoconus.

An increased number of cells, compared to control corneas, were noted in the keratoconic anterior stroma, often adjacent to ALL. Many of these cells were clearly not keratocytes, but were cells that had either been differentiated or were of an entirely different lineage. They could be recognized primarily on their lighter staining cytoplasm, but also on their organelle content. These stromal cells, not present in the control corneas, appeared to be involved in the removal or destruction of ALL and anterior stromal lamellae but did not share cytological characteristics with inflammatory cells. Typically these cells were agranular, contained lysosomes and mitochondria and often were intimately aligned to a keratocyte. Furthermore, surrounding stromal tissue harbored a

large amount of debris. We postulate that these cells are involved in the breaking down and phagocytosis of corneal tissue (Figure 6.5). An elevation in cells in keratoconic stroma has been reported and it was postulated that this abnormal cell behavior may be related to the ALL defects (Kenney et al., 1997; Kenney et al., 1994; Brown et al., 1993). The prominent nerve fibers often described as a keratoconus clinical hallmark (Arffa, 1997; Leibowitz & Morello, 1998; Rabinowitz, 2005; Casey & Sharif, 1991), were conspicuously absent in our keratoconus specimens. These nerve fibers have not been described in the histopathological literature concerning this disease. The nerve trunks encountered in our keratoconic corneal button specimens showed signs of abnormalities such as abnormal Schwann cell and axon relationship. They were no larger than nerve fibers normally seen in central cornea. Perhaps the prominent nerves are a feature of more peripheral corneal regions. The abnormal neurology of the keratoconic cornea appears to explain the reduced corneal sensitivity in patients with this pathology (Young, 2005; Bleshoy, 1986).

The peripheral region of the host keratoconic button examined was closer to the mid-peripheral cornea and, therefore, was not representative of the extreme peripheral cornea. However, the peripheral button examined did show similar changes as seen in the central samples, but to a much lesser extent. This observation suggested that this disease involves corneal regions beyond the ectatic cone portion, which may provide an explanation to recurrence of keratoconus reported in literature (Abelson et al., 1980; Nirankari et al., 1983; Bechrakis et al., 1994; Kremer et al., 1995; Bourges et al., 2003; Brookes et al., 2009; Patel et al., 2009). However, with an incidence of one in 2000 (Rabinowitz, 1998), keratoconus is hardly a rare disease, and together with the existence

of form fruste keratoconus, an alternative explanation to disease recurrence may well be found in the laws of probability dictating the frequency with which the donor cornea will have an undetected or form fruste keratoconus.

In summary, the present and first morphometric approach to characterize keratoconus histopathologically has strongly established keratoconus as an anterior corneal disease that, in mild to modest cases, leaves the posterior portions apparently structurally unharmed. The epithelium appears to be involved in the pathophysiology of keratoconus, but it remains uncertain whether this corneal layer is the origin of the disease. Keratoconus severely affects the ALL and the anterior stroma to a greater degree than earlier descriptions suggested. Recruited cells, not normally residents of the stroma, are apparently involved in the breakdown and removal of ALL and anterior stromal lamellae. Future research directed towards determining the exact origin of this disease and the true nature of invading stromal cells, would be most welcome.

# Figures and Tables

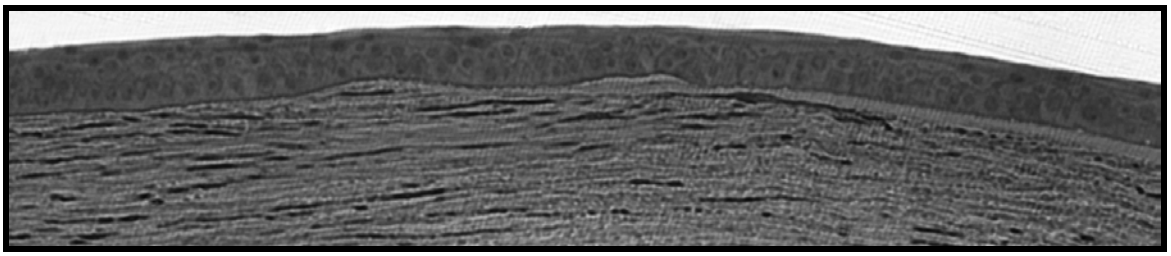

**Figure 6.1: Epithelial thickness variation in the keratoconic cornea**

Anterior keratoconic cornea with distinct epithelial thickness variations. Approximate magnification 100X. Light micrograph. Stained with toluidine blue.

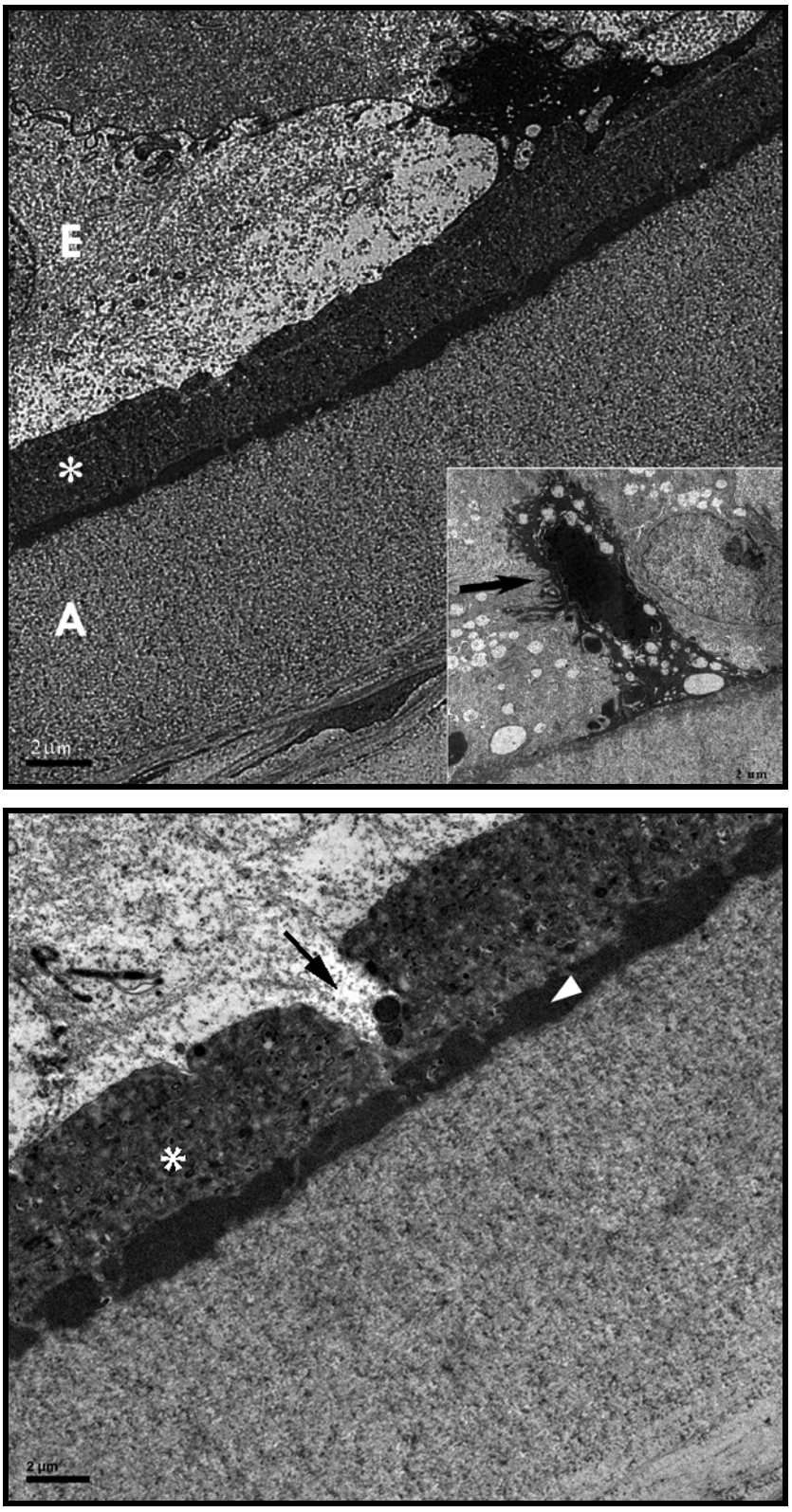


**Figure 6.2 A & B**

**Figure 6.2: Epithelial, ALL and stroma interface of the keratoconic cornea**

The epithelial, anterior limiting lamina (ALL) and stroma interface. **A)** The grossly thickened BM (*) is prominently evident. In this view, the ALL (A) and the anterior stroma appears normal and unaffected by the disease. The epithelium (E) consists of apparently normal and abnormal cells that produced an electron dense substance (arrow). Inset: an extremely distorted vacuolated and electron dense basal cell (arrow) is lodged between two neighboring basal cells, which are not of normal appearance either. **B)** High magnification of the abnormal epithelial BM (*), which shows partial discontinuities (arrow) and granular material (*) laid down on top of an irregular, electron dense layer (triangle). Electron micrograph. Stained with uranyl acetate and Reynold's lead citrate. Scale bars = 2µm

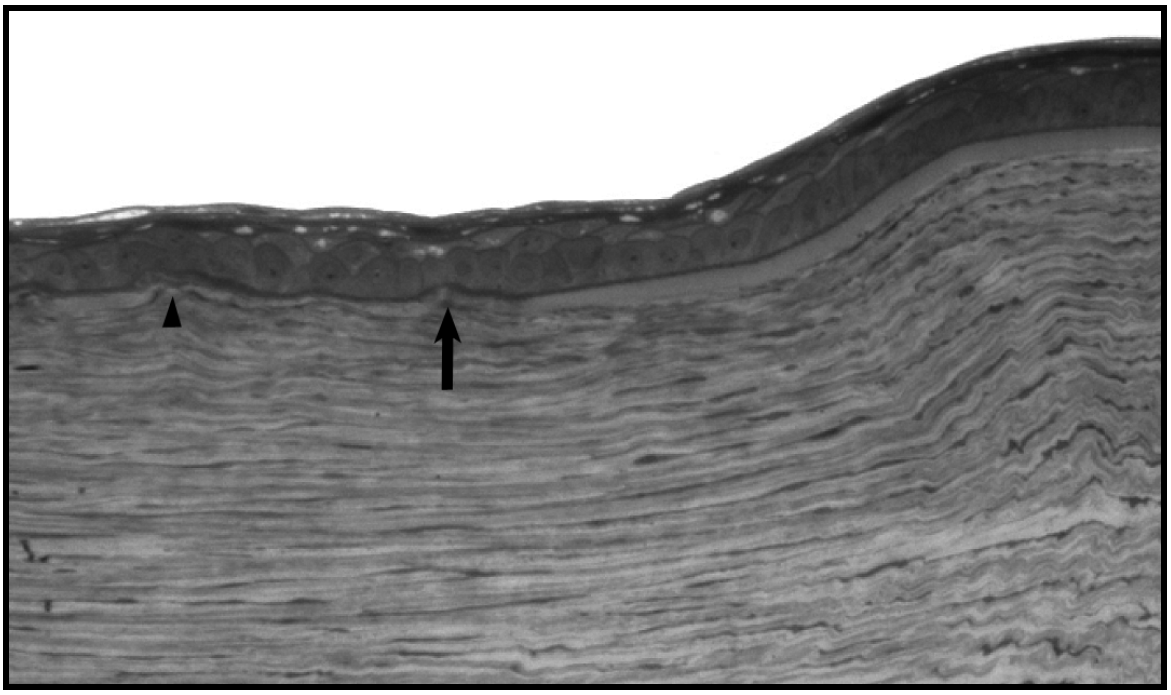

**Figure 6.3: Epithelial irregularities and loss of ALL in keratoconus**

Anterior keratoconic cornea showing modest epithelial irregularities and loss of anterior limiting lamina (ALL). The ALL (arrow) is seen to become thinner and eventually lost (arrowhead). Approximate magnification 100X. Light micrograph. Stained with toluidine blue.

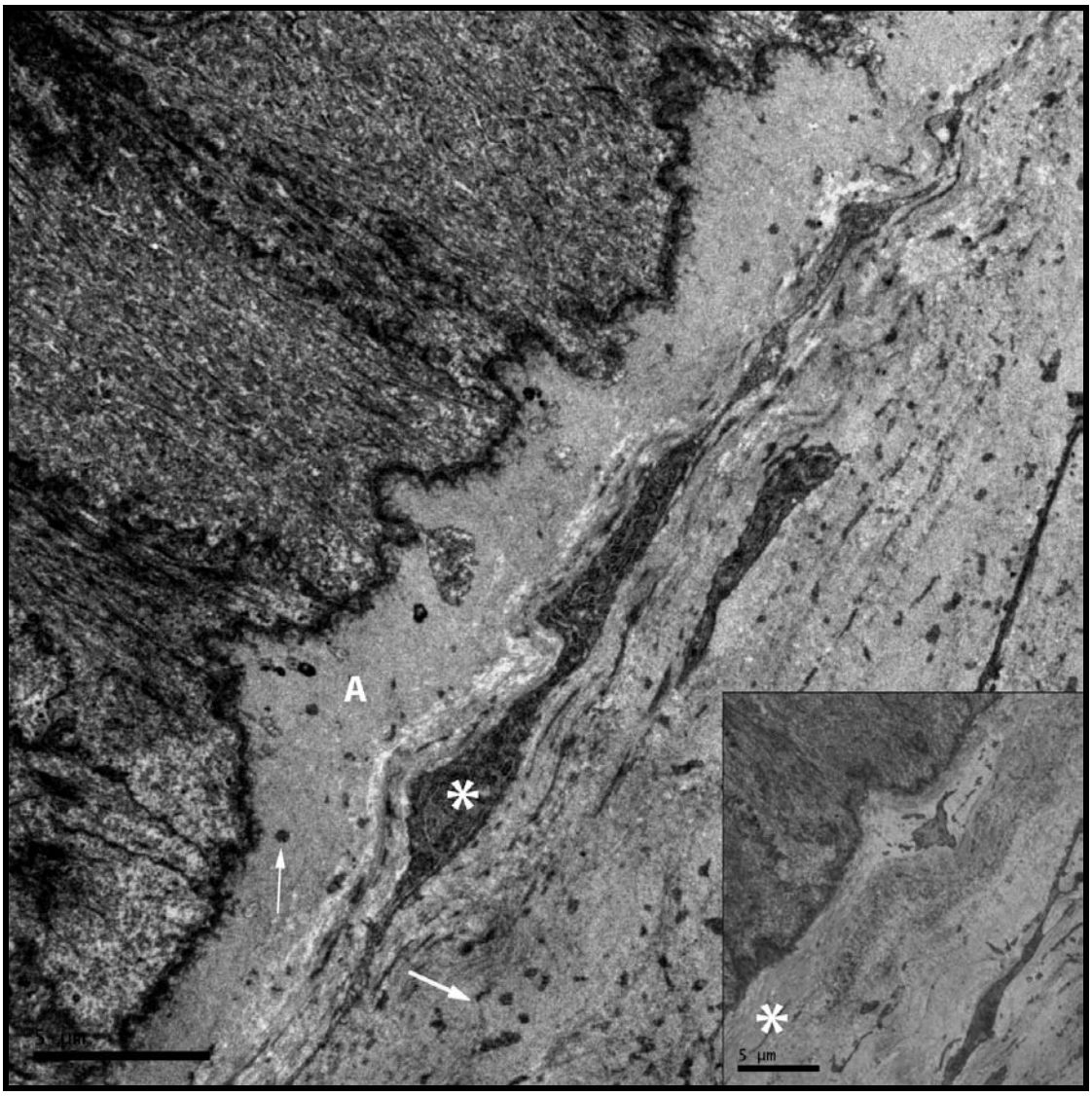


**Figure 6.4: Thinning of ALL in keratoconus**

Thinning of anterior limiting lamina (ALL). The ALL (A) is less than half its normal thickness and immediately adjacent are activated stromal cells (*). Material debris are scattered across ALL and anterior stroma (arrows). Inset: Area with ALL loss. A thin strand of ALL (arrow) is projecting to an area of complete ALL loss (*). Transmission electron micrograph. Stained with uranyl acetate and Reynold's lead citrate. Scale bars = 5µm

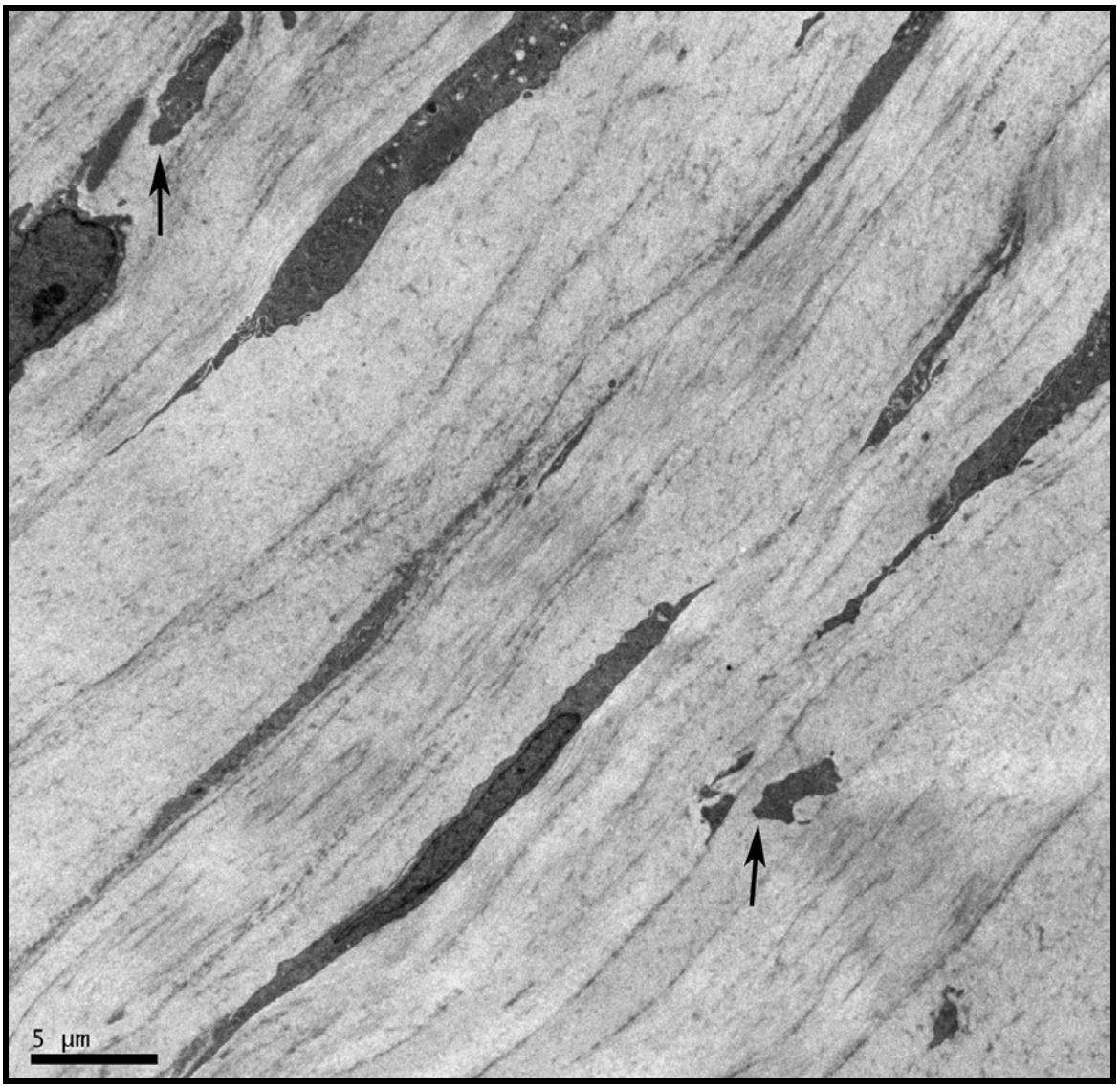


**Figure 6.5: Mid stroma showing elevated cells numbers in the keratoconic cornea**

Mid stroma with elevated number of cells. An increased number of cells were present in mid and anterior stroma. Many of them appeared activated or showed signs of fragmentation (arrows). Electron micrograph. Stained with uranyl acetate and Reynold's lead citrate.

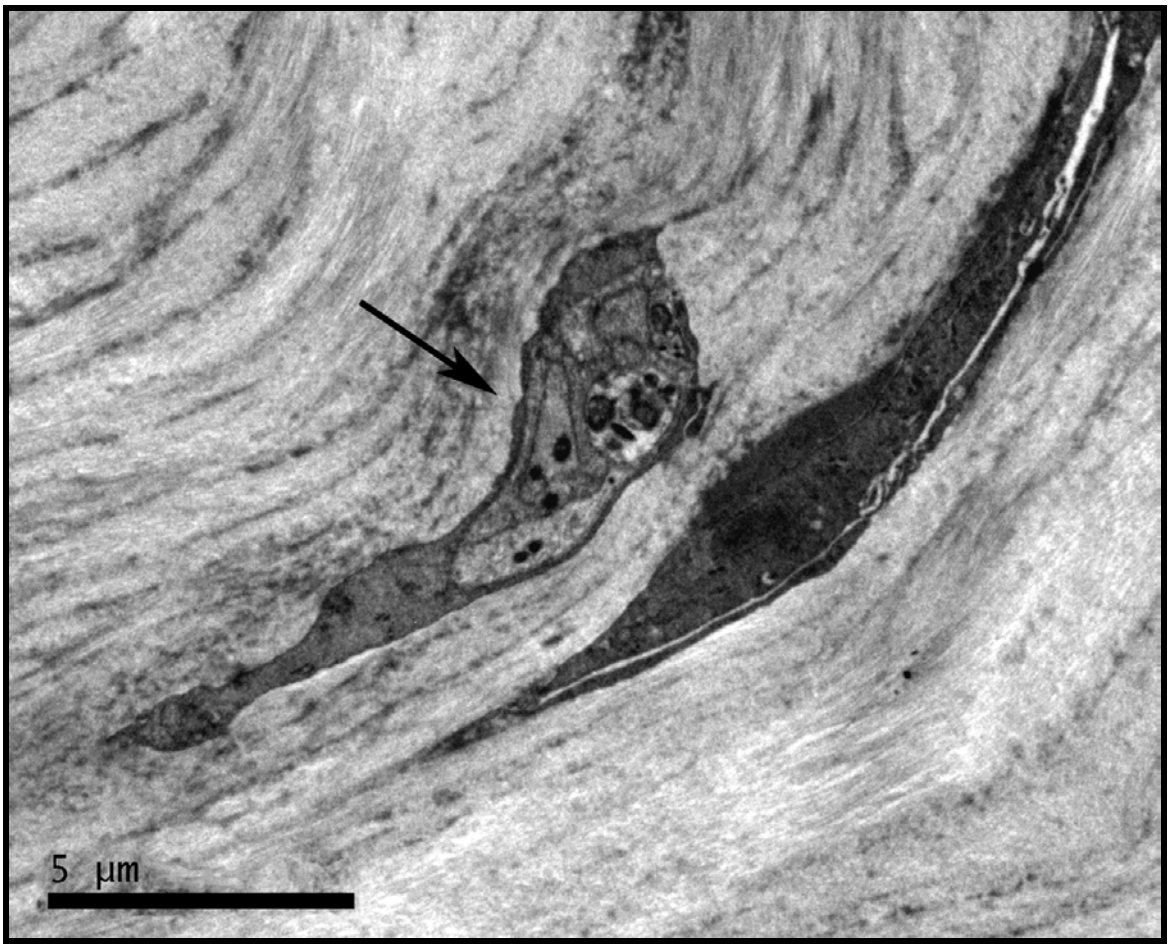


**Figure 6.6: Stromal terminal nerve fiber in the keratoconic cornea**

Stromal terminal nerve fiber. A single unmyelinated nerve fiber bundle (arrow) embedded in the stromal tissue contains terminal axon varicosities containing electron dense bodies. Multiple axons, with varying degrees of electron dense axoplasm, are enclosed by the Schwann cell in an atypical manner. Electron micrograph. Stained with uranyl acetate and Reynold's lead citrate.

**Table 6.1: Average Central Corneal Thickness & Epithelial Morphometry in Keratoconus**

| Cornea | Tissue Length (um) | Full Thickness (um) | Epithelial Thickness (um) | Epithelial Cell Layer Count | Stromal Thickness (um) |
|---|---|---|---|---|---|
| **1** | 1176 ± 15 | 406 ± 59 | 50 ± 9 | 5.5 ± 0.5 | 338 ± 61 |
| **2** | 1010 ± 44 | 380 ± 24 | 32 ± 7 | 5.2 ± 0.6 | 328 ± 16 |
| **3** | 860 ± 5 | LKP | 48 ± 4 | 6.6 ± 0.5 | LKP |
| **4** | 1212 ± 51 | 451 ± 31 | 36 ± 12 | 6.2 ± 1.1 | 383 ± 20 |
| **5** | 2005 ± 23 | 414 ± 6 | 46 ± 2 | 6.0 ± 0.0 | 339 ± 4 |
| **6** | 1364 ± 23 | 650 ± 103 | 39 ± 14 | 5.5 ± 0.9 | 598 ± 83 |
| **7** | 2193 ± 349 | 434 ± 44 | 52 ± 23 | 7.4 ± 1.0 | 368 ± 56 |
| **8** | 2602 ± 8 | 387 ± 71 | 42 ± 16 | 5.5 ± 1.3 | 377 ± 31 |
| **9** | 2465 ± 32 | 370 ± 20 | 49 ± 6 | 7.3 ± 0.6 | 303 ± 21 |
| **10** | 633 ± 2 | LKP | 49 ± 5 | 6.4 ± 0.5 | LKP |
| **11** | 391 ± 3 | LKP | 46 ± 7 | 6.5 ± 0.7 | LKP |
| **12** | 444 ± 20 | LKP | 18 ± 4 | 4.1 ± 0.3 | LKP |

**Table 6.2: Average Peripheral Corneal Thickness & Epithelial Morphometry in Keratoconus**

| Cornea | Tissue Length (um) | Full Thickness (um) | Epithelial Thickness (um) | Epithelial Cell Layer Count | Stromal Thickness (um) |
|---|---|---|---|---|---|
| **1** | 1009 ± 29 | 656 ± 158 | 60 ± 4 | 6.0 ± 0.6 | 598 ± 197 |
| **2** | 1267 ± 87 | 485 ± 5 | 62 ± 4 | 6.8 ± 0.5 | 398 ± 9 |
| **3** | 910 ± 2 | LKP | 54 ± 4 | 7.4 ± 0.5 | LKP |
| **4** | 1233 ± 11 | 560 ± 66 | 57 ± 10 | 7.1 ± 1.0 | 488 ± 76 |
| **5** | 2068 ± 30 | 476 ± 66 | 45 ± 2 | 6.8 ± 0.4 | 414 ± 67 |
| **6** | 768 ± 11 | 914 ± 94 | 64 ± 29 | 6.3 ± 0.9 | 738 ± 26 |
| **7** | 1309 ± 1 | 509 ± 18 | 54 ± 2 | 5.9 ± 0.3 | 426 ± 22 |
| **8** | 2209 ± 48 | 443 ± 37 | 40 ± 12 | 6.0 + 0.0 | 369 ± 38 |
| **9** | 1433 ± 24 | 427 ± 16 | 58 ± 4 | 7.9 ± 0.7 | 346 ± 15 |
| **10** | 807 ± 7 | LKP | 59 ± 14 | 6.0 ± 1.0 | LKP |
| **11** | 729 ± 10 | LKP | 49 ± 1 | 6.5 ± 0.5 | LKP |
| **12** | 443 ± 5 | LKP | 52 ± 2 | 6.8 ± 0.6 | LKP |

**Table 6.3: Basement Membrane (BM) Morphometry in Keratoconus**

| Cornea | BM Thickness (um) |
|---|---|
| **1** | 0.6 ± 0.2 |
| **2** | 1.933 ± 0.115 |
| **3** | LKP |
| **4** | 3.667 ± 0.305 |
| **5** | 0.863 ± 0.180 |
| **6** | 2.933 ± 0.503 |
| **7** | 0.05 ± 0 |
| **8** | 1.608 ± 0.378 |

**Table 6.4: Central Anterior Limiting Lamina (ALL) Morphometry in Keratoconus**

| Cornea | Average Tissue Length (um) | Area Affected (um) | % of Total Area Examined | ALL Lost (um) | % of Area Examined |
|---|---|---|---|---|---|
| **1** | 1176 | 0 | 0 | 0 | 0 |
| **2** | 1010 | 832 | 82 | 443 | 44 |
| **3** | 860 | 177 | 21 | 0 | 0 |
| **4** | 1212 | 1176 | 97 | 0 | 0 |
| **5** | 2005 | 2005 | 100 | 0 | 0 |
| **6** | 1364 | 1002 | 74 | 574 | 42 |
| **7** | 2193 | 2193 | 100 | 1458 | 67 |
| **8** | 2602 | 2602 | 100 | 364 | 14 |
| **9** | 2465 | 622 | 25 | 0 | 0 |
| **10** | 633 | 410 | 65 | 0 | 0 |
| **11** | 391 | 0 | 0 | 0 | 0 |
| **12** | 444 | 256 | 58 | 0 | 0 |

**Table 6.5: Peripheral Anterior Limiting Lamina (ALL) Morphometry in Keratoconus**

| Cornea | Average Tissue Length (um) | Area Affected (um) | % of Total Area Examined | ALL Lost (um) | % of Area Examined |
|---|---|---|---|---|---|
| **1** | 1009 | 0 | 0 | 0 | 0 |
| **2** | 1267 | 283 | 22 | 0 | 0 |
| **3** | 910 | 210 | 23 | 0 | 0 |
| **4** | 1233 | 89 | 7 | 0 | 0 |
| **5** | 2068 | 67 | 3 | 0 | 0 |
| **6** | 768 | 768 | 100 | 66 | 9 |
| **7** | 1309 | 0 | 0 | 364 | 28 |
| **8** | 2209 | 389 | 18 | 0 | 0 |
| **9** | 1433 | 0 | 0 | 0 | 0 |
| **10** | 807 | 162 | 20 | 0 | 0 |
| **11** | 729 | 0 | 0 | 0 | 0 |
| **12** | 443 | 0 | 0 | 0 | 0 |

# Chapter 7 - General Discussion

## General Discussion

This research on the corneal pathology of keratoconus was preceded by an extensive study of the normal healthy cornea to advance our understanding of the corneal stromal architecture so that the often subtle changes occurring during the disease process may be identified and precisely and morphmetrically defined. The subsequent study of pathological tissue, obtained from surgically removed corneas during transplant surgery by a single surgeon, involved observations and digital imaging at light microscopical and ultrastructural levels. This research on the normal and keratoconic cornea represents the first extensive case series to be conducted using systematic morhometry at light and electron microscopical levels.

This research entails a few limitations that may have had an influence on the measurement outcomes and comparisons conducted. The fixation of the keratoconic cornea was instantaneous following removal from the eye, while the control tissue was fixed hours to days post-mortem. There was modest age difference between the eye bank and keratoconic corneas with the control group having an average age of 59, while the average age of the keratoconic group was 47. In determining whether to follow a LKP or PKP protocol, the surgeon considered the patient's age and thickness of the cornea, which implies that there may have been differences between these two surgical groups. However, in this study the LKP and PKP corneas were considered the same.

The ultrastructural, histopathological approach used in this research ensured sufficient resolution for the detailed observations to be made. While studies on the features of keratoconic corneas exist in literature, most accounts are only descriptive and involve a limited sample size (n=1-8) and often no controls (Iwamoto & DeVoe, 1976;

Kaas-Hansen, 1993; Tsubota et al., 1995; Meek et al., 2005; Nakamura et al., 2005). Most importantly, however, most of these studies do not utilize the high resolution of the TEM (McPherson et al., 1968; Scroggs et al., 1992; Kass-Hansen, 1993; Meek et al., 2005; Nakamura et al., 2005; Hayes et al., 2007, Morishige et al, 2007). Perhaps, even more importantly, the fixation methods used in current literature have high osmolality of up to 930mOsm/kg (Chi et al., 1956; Teng, 1963; McPherson et al., 1968; Iwamoto & DeVoe, 1976; Scroggs & Proia, 1992; Kaas-Hansen, 1993; Sturbaum & Peiffer, 1993; Nakamura, 2005), which causes substantial shrinkage of the tissue during processing (Doughty et al., 1997). This is of particular importance in the keratoconic cornea because these pathological tissues are easily distorted further by processing for histology. The fixation method used in our laboratory has an isotonic osmolality of 320–340 mOsm/kg and pH of 7.4, making it much closer to the normal physiology of the eye (310mOsm/kg, pH of 7.6) (Bergmanson, 2010) and will "more faithfully preserve the overall architecture" (Doughty et al., 1997) without further distorting an already distorted tissue, as in the case of keratoconus.

This series of morphometric, ultrastructural studies provides strong evidence for the anterior focus of keratoconus, including the involvement of epithelial, ALL and anterior stromal layers, as described below.

*Epithelium*

The microscopic evaluation of 15 keratoconic corneas demonstrated that the epithelium is clearly and important site of pathological structural changes in the disease process. The wide range in thickness variation (13.5-91.6µm) of the keratoconic epithelial layer was in contrast to the uniform epithelial thickness (50µm) of the normal

cornea (Bergmanson, 2010). This extreme variation was not explained by the number of epithelial cell layers, but rather changes in cell size.

Further involvement of the epithelium in this disease process was seen in the thickened basement membrane, which averaged 1.46µm, and in some cases, measured up to 3.67µm thick. Others have made similar observations ultrastructurally, reporting BM thickening and fragmentation (Teng, 1963; Brewitt & Reale, 1981; Akhtar et al., 2008). However, to my knowledge, a quantitative description of this observation has never been made.

As mentioned previously (in the General Methods) the age of the corneas received for use in this research was not controlled for. Because the basement membrane of the normal human cornea shows thickening with age, it was important to take this into consideration to be sure that the thickening observed was pathological and not simply the result of aging. The normal human corneal basement membrane for a 20 year old is approximately 0.23µm and increases by 0.003µm per year (Alvarado et al., 1983). Even if this calculation is applied to the oldest keratoconic cornea used in this research (70 yo), the basement membrane thickness of 3.67µm is still >10X thicker than the normal cornea. When applied to the average keratoconic basement membrane thickness (1.46µm), it is a 4X increase. Therefore, this thickening of the basement membrane in keratoconus cannot be explained by aging alone and is most certainly a pathological change resulting from the disease process. Given that the basement membrane is synthesized by epithelial cells, this thickening is indicative of an abnormally functioning epithelium. The abnormal basement membrane serves as evidence for an epithelial

involvement in keratoconus, and future research may be useful in exploring this feature to gain further insights into the role of the epithelium in this disease.

The ALL provides the foundation that the epithelium needs to remain firmly attached to the underlying cornea (Gipson et al., 1987; Bergmanson, 2010). This data showed significant thinning or complete loss of the ALL in 10 out of 12 corneas and these defects were considerably larger than the small breaks, ruptures and cracks that have been previously reported in literature (Chi et al., 1956; Teng, 1963; Duke-Elder & Leigh, 1965; McPherson et al., 1968; Shapiro et al., 1986; Kaas-Hansen, 1993; Arffa, 1997; Leibowitz & Morello, 1998; Maquire, 1998; Sawaguchi et al., 1998; Eagle, 1999; Sugar, 2004; Feder & Kshettry, 2005; Nakamura et al., 2005; Rabinowitz, 2005; Krachmer & Palay, 2006; Yanoff & Sassani, 2009). This loss of ALL over large areas, effectively removes the foundation for the epithelium since the anchoring plaques needed for this attachment, which are located within the ALL, are eliminated as well. The thickened basement membrane likely contributes to a loss of adhesion, making it harder for the anchoring fibrils to span across the added thickness. The basement membrane also had an abnormal composition, which may have further compromised the ability to provide a firm attachment. A similar variation in epithelial thickness is also noted in PRK, where the ALL is essentially removed (Waring, 1998). The loss of epithelial anchorage to the ALL also has clinical importance. It is well known and accepted that keratoconic patients clinically exhibit a higher incidence of NaFl staining on the cornea (Young et al., 2005), which can be explained by the weak attachment of this layer to the underlying stroma.

*ALL*

As outlined above, extensive areas of the ALL are involved in the keratoconic disease process, contributing to its anterior focus. The normal cornea showed numerous fibrillar crossings between the ALL and extensive network of anterior interweaving and branching lamellae of the stroma. However, the overlap between these two corneal layers was slight and less than 1μm in either direction (Figure 7.1). This finding was in contrast to other recent accounts in literature that described fibril insertions and crossings at this interface (Binder et al., 1991; Bron, 2001; Morishige et al., 2007). Furthermore, as previously mentioned, Bron (et al., 2001) proposed that keratoconus is a case of lamellar disinsertion from the ALL, suggesting that the breakdown of this interface is an important aspect of the keratoconus disease process. Therefore, it is important to consider whether this interface normally provides structural strength, and if so, whether this contributes to the structural loss in keratoconus.

The gradual transition of one layer into the other, as seen in our research, likely serves an optical function, contributing to the transparency of the cornea, rather than providing structural strength. Furthermore, if this layer largely contributed to the overall architectural strength of the cornea, removal of the ALL would certainly cause a structural weakening resulting in ectasia. However, as seen with PRK, where this layer and the underlying anterior stroma are removed, resultant ectasia does not typically occur and, in fact, appears to be an uncommon complication. Although it does not appear that this layer provides the strength that others have suggested (Bowman, 1847; Clareus, 1857; Duke-Elder, 1961; Salzmann, 1912; Thomas, 1955) the amount of transparency this layer contributes to the overall transparency of the cornea is likely minimal. In the

case of PRK, removing the ALL does not cause the cornea to become opaque. However, it is well established that patients who have undergone this procedure experience certain amounts of corneal haze, halos and glare (Zhao et al., 2010) providing evidence of loss of overall corneal transparency.

*Stroma*

My research on the normal cornea demonstrates the presence of a network of anterior interweaving lamellae in the stroma, which is consistent with previous reports (Radner et al., 1993; Bron, 2001; Morishige et al., 2006). In addition to the relationship these lamellae maintain with the overlying ALL (Figure 7.1), some anterior stromal lamellae (in the central cornea) appeared to terminate into an electron dense, granular material resident in the surrounding stromal matrix. This is not a feature described in literature and are described here as electron dense formations (EDF's) (Figure 7.1).

Accounts in literature have proposed that stromal lamellae extend from limbus to limbus without terminating along the way (Krauss, 1937; Duke-Elder, 1943; Maguire et al., 1998). In contrast, these findings, for central cornea, show that the anterior interweaving stromal lamellae demonstrate fine branching and, in some cases termination into EDF's. These findings provide further evidenced that stromal lamellae do, in fact, terminate in the central anterior normal cornea as proposed by others **(**Bowman, 1847; Bron, 2001; Morishige, 2007). These characteristic features of the normal central corneal stroma - anterior interweaving lamellae with EDF's - were absent in all keratoconic corneas examined and this loss corresponds with the corneal thinning observed clinically in this disease.

Lamellar counts on normal and keratoconic corneas were accomplished using high resolution, full thickness corneal montages. The number of lamellae were counted across the entire thickness of the stroma in the central normal cornea and the central cone region of keratoconic corneas using an established set of criteria to define individual lamellae. Lamellar numbers for the normal human cornea have been reported in literature, although most accounts were not clear about the methods used to arrive at their conclusion. The systematic accounts available (as discussed in Chapter 3) either did not use the resolution of TEM (Hamada et al., 1972; Pouliquen, 1985) or made a count on a small region of the cornea and extrapolated the data to get a full thickness count (Takahashi et al., 1990). As a consequence the number of lamellae varies in literature from 60 to 500, with no consensus reached. Our lamellar count on the normal human central cornea showed an average number of 242$\pm$4. The fact that our counts were performed by three separate individuals, not influenced by each other and with a coefficient of variation of 1.08%, shows that the criteria developed, together with training, allowed for a repeatable and standardized way of counting lamellae. These results also suggested that there is not a great deal of individual variation in numbers of lamellae forming the cornea. The closeness in counts among the corneas signifies that we can be fairly certain that the number of lamellae found in the research presented here is representative of the normal cornea.

Due to the stromal thinning associated with keratoconus, lamellar counts on the keratoconic cornea were expected to show a decrease in number. However, using the same criteria as for normal, these corneas showed a paradoxical increase in the number of lamellae. It is important to recognize that there were not actually more lamellae added to

the cornea but instead, lamellae had unraveled or fragmented into smaller units. This observation could not have been established without first determining the normative data. Interestingly, a recent study showed images of normal and keratoconic corneas where this lamellar phenomenon could be viewed but was not recognized (Dawson et al., 2008). This important study did not include a lamellar count, but instead demonstrated, with illustrations only, that ectasia following post-PRK and -LASIK also had a lamellar fragmentation similar to the keratoconic cornea. They did not attempt to quantify the lamellae in these corneas but they did report a 'loss of lamellar number', which they contributed to 'interlamellar and interfibrillar biomechanical slippage'.

Corneal thinning is associated with corneal ectasia, but lamellar fragmentation appears to be an equally important factor for ectasia to occur. In other words, to provoke ectasia, both thinning and lamellar fragmentation must take place. The effect of lamellar unraveling has been likened to the weakening of a rope that has become frayed (Figure 7.2).

Ultrastructurally, the normal corneal stroma contained only one cell type, the keratocyte, except for the occasional Schwann cell and neuron. In contrast, all keratoconic corneas showed an elevated number of cells in the stroma, especially anteriorly, when compared to the normal corneas. Some of these cells were, indeed, keratocytes. However, others showed a different morphology than the keratocyte consisting of lighter cytoplasm, increased organelles and varying in nuclear staining. These cells were often present in areas where lamellar fragmentation occurred and sometimes were abutting areas of thinning ALL and encroaching onto this layer. The cells tended to align closely with resident keratocytes, although the purpose or

consequence of this behavior was not clear. Increased amounts of membrane bound fragments of cellular origin were surrounding these non-keratocyte cells and it appeared that the cells were somehow involved in disassembling the ALL and stromal lamellae. It appeared that these cells may have been recruited from outside of the cornea, although investigation of this and the origin of these cells is an ongoing effort of my current and future research. Initial efforts have commenced using immunofluorescent techniques to better understand and identify the origin of these specific cells.

Based on observations made in this research study, it has become evident that keratoconus is an anterior corneal disease, at least until its end stage when hydrops occurs. This may be important to surgeons and supports the use of the nonconventional LKP surgical approach, rather than the traditional PKP procedure. The use of the LKP on corneas afflicted by keratoconus only removes the anterior, affected part of the cornea, leaving the posterior cornea intact. Other advantages of the LKP over the PKP include: less graft rejections, maintained global strength, and quicker post-surgical recovery (Goosey & Sturbaum, 2005). However, PKP may still be the best solution for older patients with extremely thin corneas (personal communication, John Goosey, MD, 2010).

## *Final Summary of Original Observations and Findings*

Normal Human Cornea:

- Not all anterior lamellae span limbus to limbus. This is an observation that contradicts the majority of the literature.
- Lamellae terminating in central cornea were embedded in electron dense bodies and were give the name, electron dense formations (EDF's).
- The minimal overlapping of bordering tissues at the ALL/stromal interface was defined.
- The first full stromal thickness, anterior to posterior lamellar count of the central cornea was performed to provide normative data.

Keratoconic Human Cornea:

- The epithelial involvement in keratoconus was confirmed and the grossly thickened basement membrane was quantified.
- The destruction of and intermittent loss of ALL over large areas was quantified using morphometric methods and these finding contrasted with current literature, which only reports breaks, interruptions, tears and ruptures.
- The anterior, branching, and interweaving stromal lamellae were lost providing an explanation for the clinically observed cornel thinning associated with keratoconus.
- Lamellar fragmentation, or breaking down into thinner units, leading to an increased count of stromal lamellae, was reported for the first time.

- A change in the stromal cellular population, with potentially other cells than keratocytes present, was reported.
- Prominent nerve fibers often described clinically in keratoconus were not part of the central cone region. Instead, superficial stromal nerve fibers were thin and contained a small number of axons that had an abnormal relationship with its associated Schwann cell.
- The evidence provided, demonstrated the anterior focus of keratoconus, at least until its end stage when hydrops occurs, and supported the notion that LKP, rather than PKP, may be an ideal surgical option for many keratoconic patients in need of keratoplasty.

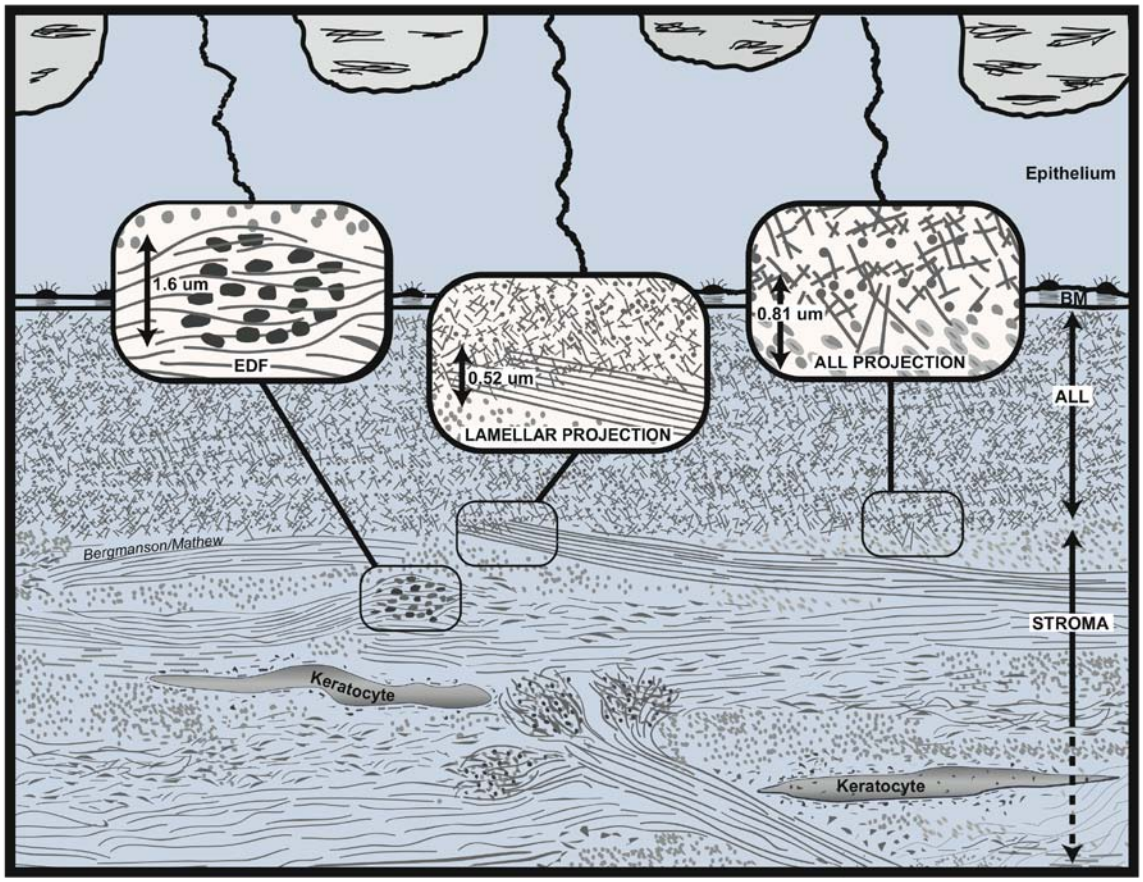


**Figure 7.1: ALL/stromal interface diagram of the normal cornea**

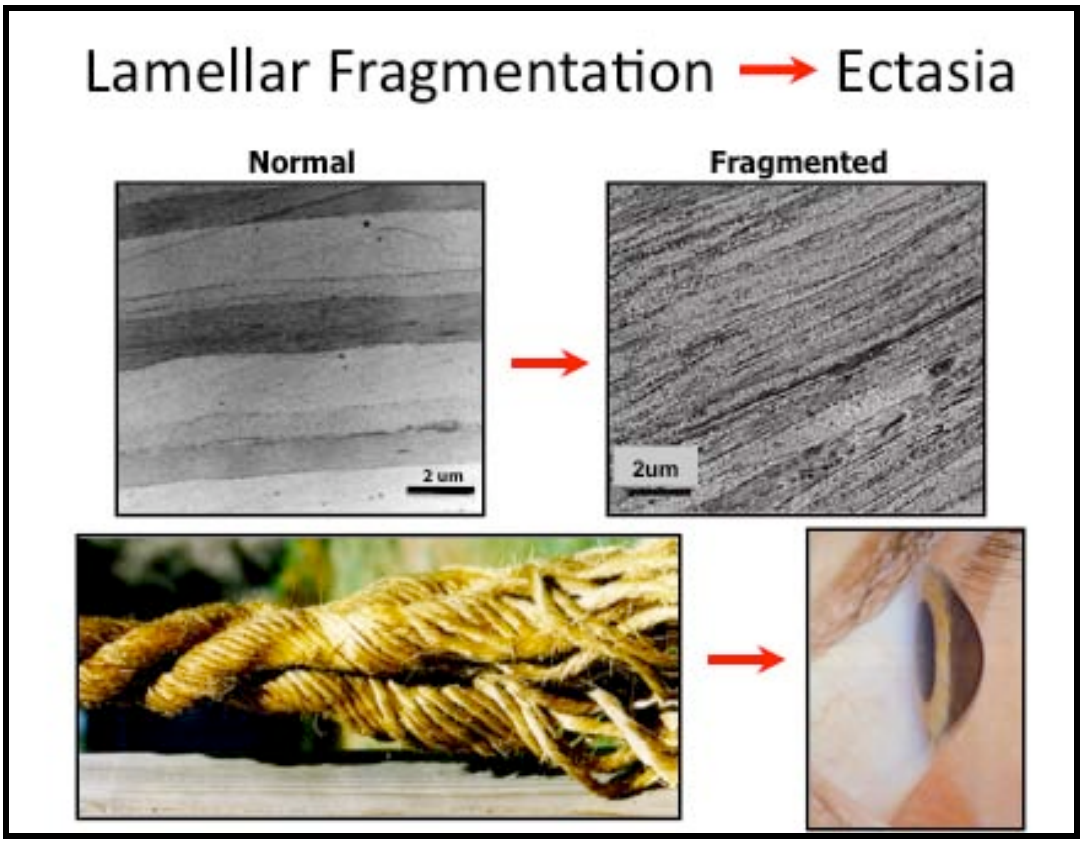


**Figure 7.2: Ectasia caused by lamellar fragmentation – histopathological evidence and an analogy.**

# References

1. Abelson MB, Collin HB, Gillette TE, Dohlman CH. Recurrent keratoconus after keratoplasty. *Am J Ophthalmol*. 1980; 90(5):672-676.
2. Akhtar S, Bron AJ, Salvi SM, Hawksworth NR, Tuft SJ, Meek KM. Ultrastructural analysis of collagen fibrils and proteoglycans in keratoconus. *Acta Ophthalmol*. 2008; 86(7):764-772.
3. Albert DM. Ocular Refraction and Development of Spectacles. In: Albert DM, Edwards DD, eds. *The History of Ophthalmology*. Cambridge, MA: Blackwell Science. 1996:107-123.
4. Alvarado J, Murphy C, Juster R. Age related changes in the basement membrane of the human corneal epithelium. *IOVS*. 1983; 24(8):1015-1028.
5. Apple DJ, Rabb MF. *Ocular Pathology: Clinical Applications & Self Assessment*. 2nd ed. St. Louis: Mosby; 1998:85-86.
6. Arffa, RC. *Grayson's Diseases of the Cornea*. 4th ed. St. Louis, MO: Mosby. 1997: 446-454.
7. Barr J, Wilson B, Gordon M, Rah M, Riley C, Kollbaum P, Zadnik K, CLEK study group. Estimation of the incidence and factors predictive of corneal scarring in the Collaborative Longitudinal Evaluation of Keratoconus (CLEK) study. *Cornea.* 2006; 25(1):16-25.
8. Barr JT, Zadnik K, Wilson BS Edrington TB, Everett DF, Fink BA, Shovlin JP, Wissman BA, Siegmund K, Gordon MO, CLEK Study Group. Factors associated with corneal scarring in the Collaborative Longitudinal Evaluation of Keratoconus (CLEK) Study. *Cornea*. 2000;19(4):501-507.

9. Bechrakis N, Blom ML, Stark WJ, Green WR. Recurrent keratoconus. *Cornea*. 1994; 13(1):73-77.

10. Bergmanson JPG, Doughty MJ. Anatomy, morphology and electron microscopy of the cornea and conjunctiva. In: Bennett E, Weissman BA. *Clinical Contact Lens Practice.* Philadelphia: Lippincott-Williams & Wilkins; 2005;11-39.

11. Bergmanson JPG, Horne J, Doughty MJ, Garcia M, Gondo M. Assessment of the number of lamellae in the central region of the human corneal stroma, at the resolution of the transmission electron microscope. *Eye Contact Lens.* 2005; 31(6): 281-287.

12. Bergmanson JPG. *Clinical Ocular Anatomy & Physiology*. 17th ed. Houston: Texas Eye Research & Technology Center; 2010:69-96.

13. Berman E. *Biochemistry of the Eye*. New York: Plenium Press, 1991.

14. Binder PS, Rock ME, Schmidt KC, Anderson JA. High-voltage electon microscopy of normal human cornea. *Invest Ophthalmol Vis Sci.* 1991; 32(8): 2234-2243.

15. Binder PS. Ectasia after laser in situ keratomileusis. *J Cataract Refract Surg*. 2003; 29(12):2419-29

16. Bleshoy H. Corneal sensitivity in keratoconus. *Transactions BCLA Conference*. 1986:9-12.

17. Boote C, Dennis S, Huang Y, Quantock AJ, Meek KM. Lamellar orientation in human cornea in relation to mechanical properties. J Struct Biol. 2005; 149(1):1-6.

18. Bourges JL, Savoldelli M, Dighiero P, Assouline M, Pouliquen Y, BenEzra D, Renard G, Behar-Cohen F. Recurrence of keratoconus characteristics: a clinical

and histologic follow-up analysis of donor grafts. *Ophthalmology*. 2003; 110(10):1920-1925.

19. Bowman W. General View of the Eyeball. Lectures delivered at the Royal London Ophthalmic Hospital, Moorfields. *London Medical Gazette*. 1847; 5:743-753.
20. Brachner A. Hundertjahre Kontaktlinse. Vom Lesestein zur Kontaktlinse. *Vereinigung Deutscher Contactlinsenspezialisten*. Munchen, 1988.
21. Brewitt H. Reale E. The basement membrane complex of the human corneal epithelium. *Albrecht von Graefes Arch Klin Ophthalmol*. 1981; 215:223-231.
22. Bron AJ, Tripathi RC, Tripathi BJ. The cornea and sclera. In: Wolff's Anatomy of the Eye and Orbit, 8th ed. London, Chapman & Hall Medical, 1997, p 247.
23. Bron AJ. The architecture of the corneal stroma. *Br J Ophthalmol*. 2001;85:379-383.
24. Brookes NH, Niederer RL, Hickey D, McGhee CN, Sherwin T. Recurrence of kertaoconic pathology in penetrating keratoplasty buttons originally transplanted for keratoconus. *Cornea*. 2009; 28(6):688-93.
25. Brown D, Chwa MM, Opbroek A, Kenney MC. Keratoconus corneas: increased gelatinolytic activity appears after modification of inhibitors. Current Eye Research. 1993; 12(6):571-581.
26. Casey TA, Sharif KW. *Color Atlas of Corneal Dystrophies & Degenerations*. St. Louis: Mosby; 1991:71-80.
27. Chi HH, Katzin HM, Teng CC. Histopathology of Keratoconus. *Am. J. Ophthalmol*. 1956; 42:847-860.

28. Cintron C. The Molecular Structure of the Corneal Stroma in Health and Disease. In: Chandler JW, Sugar J, Edelhauser HF, eds. *External Diseases: Cornea, Conjunctiva, Sclera, Eyelids, Lacrimal System*. London: Mosby, 1994: 5.1-5.14.

29. Clareus F. *Hornhinnans histologi.* Thesis, Upsala University Medical School. Westrell, Stockholm, 1857.

30. Clarke JI. Fourier and power law analysis of structural complexity in cornea and lens. *Micron* 2001;32:239–249.

31. Dawson DG, Randleman JB, Grossniklaus HE, O'Brien TP, Dubovy SR, Schmack I, Stulting RD, Edelhauser HF. Corneal ectasia after excimer laser keratorefractive surgery: histopathology, ultrastructure, and pathophysiology. *Ophthalmology*. 2008;115(12):2181-2191.

32. Doughty MJ, Bergmanson JPG, Blocker Y. Shrinkage and distortion of the rabbit corneal endothelial cell mosaic caused by a high osmolality glutaraldehyde-formaldehyde fixative compared to glutaraldehyde. *Tissue & Cell.* 1997;29(5):533-547.

33. Doughty MJ, Bergmanson JPG. Collagen fibril characteristics at the cornea-scleral boundary and rabbit corneal stroma swelling. *Clin Exp Optom.* 2004; 87(2):81–92.

34. Doughty MJ, Seabert W, Bergmanson JPG, et al. A descriptive and quantitative study of the keratocytes of the corneal stroma of albino rabbits using transmission electron microscopy. *Tissue & Cell.* 2001; 33(4):408–422.

35. Doughty MJ, Zaman ML. Human corneal thickness and its impact on intraocular pressure measures: A review and meta-analysis approach. *Surv Ophthalmol* 2000;44:367–408.

36. Doughty MJ. A physiological perspective in the swelling properties of the mammalian corneal stroma. *Contact Lens Anterior Eye* 2003;26:117–129.

37. Duke-Elder S, Leigh AG. *System of Ophthalmology, Vol. VIII: Diseases of the Outer Eye: Part 2*. St. Louis, MO: Mosby; 1965: 964-976.

38. Duke-Elder S, Wybar KC. The eye. In: *System of Ophthalmology. Vol. II. The Anatomy of the Visual System.* London: Henry Kimpton; 1961;92-131.

39. Duke-Elder, S. *Textbook of Ophthalmology, Vol. 2: Diseases of the inner eye*. 1943; 2027-34.

40. Eagle RC. *Eye Pathology: An Atlas and Basic Text*. Philadelphia: WB Saunders Company, 1999: 91.

41. Edelhauser HF, Ubels JL. The cornea. In: Kaufman PL, Alm A, eds. Adler's Physiology of the Eye. St. Louis, CV Mosby, 2003, p 56.

42. Fatt I, Weissman BA. Cornea. In: Physiology of the Eye, 2nd ed. Boston, Butterworth-Heinemann, 1992, p 101.

43. Feder RS, Kshettry P. Noninflammatory Ectatic Disorders. In: Krachmer JH, Mannis MJ, Holland EJ, eds. *Cornea, Vol 1: Fundamentals, Diagnosis and Management*. 2nd ed. Philadelphia: Elsevier, 2005: 955-974.

44. Fick AE. A contact-lens. 'Eine Contactbrille' (1888) translated by May CH. *Arch Ophthalmol*. 1988; 106:1373-1377.

45. Freegard TJ. The physical basis of transparency of the normal cornea. *Eye* 1997;11:465–471.

46. Gallagher B, Maurice D. Striations of light scattering in the corneal stroma. *J Ultrastruct Res* 1977;61:100–114.

47. Gipson IK. Spurr-Michaud SJ, Tisdale AS. Anchoring fibrils form a complex network in human and rabbit cornea. *Invest Ophthalmol Vis Sci*. 1987; 28(2): 212-220.

48. Goosey JD and Sturbaum CW. Lamellar Keratoplasty. In: Foster CS, Azar DT, Dohlman CH, eds. *The Cornea: Scientific Founations & Clinical Practice*, 4th ed. Philadelphia: Lippincott Williams & Wilkins, 2005: 1043-1055.

49. Hamada R, Giraud J-P, Graf B, et al. Étude analytique et statistique des lamelles, des kératocytes, des fibrils de collagène de la région centrale de la cornée humaine normale. *Arch Ophtalmol (Paris)* 1972;32:563–570.

50. Hartstein J. Keratoconus that developed in patients wearing corneal contact lenses: Report of four cases. *Arch. Ophthalmol*. 1968; 80:345-346.

51. Hayashi S, Osawa T, Tohyama K. Comparative observations on corneas, with special reference to Bowman's layer and Descemet's membrane in mammals and amphibians. *J Morpholl.* 2002;254:247-258.

52. Hayes S, Boote C, Tuft SJ, Quantock AJ, Meek KM. A study of corneal thickness, shape and collagen organization in keratoconus using videokeratography and X-ray scattering techniques. *Exp Eye Res*. 2007; 84:423-434.

53. Hogan MJ, Alvarado JA, Weddell JE. *Histology of the Human Eye.* Philadelphia: WB Saunders; 1971;55-111.

54. Holland EJ. Ectasia following laser in situ keratomileusis. *J Cataract Refract Surg.* 2005; 31(11):2034.

55. Horne J, Bergmanson JPG, Goosey J. Pathological and Morphometrical alterations in the keratoconic cornea. *Invest. Ophthalmol. Vis. Sci*. 2007; 48: ARVO E-Abstract 1863.

56. Horne J, Fulton J, Gondo M, et al. Stromal lamellar insertions into the anterior limiting lamina—do they exist? *Optom Vis Sci* 2002;79(12 suppl):248.

57. Huff JW. Corneal stroma. In: Bennett ES, Weissman BA, ed. Clinical Contact Lens Practice. Philadelphia, Lippincott-Raven, 1997, p 1.

58. Iwamoto T, DeVoe AG. Electron microscopical study of the Fleischer ring. *Arch Ophthalmol*. 1976 Sep;94(9):1579-84

59. Jacobsen IE, Jensen OA, Prause JU. Structure and composition of Bowman's membrane. Study by frozen resin cracking. *Acta Ophthalmol*. 1984; 62(1):39-53.

60. Kaas-Hansen M. The histopathological changes of Keratoconus. *Acta Ophthalmol.* 1993; 71:411-414.

61. Karseras A, Ruben M. Aetiology of keratoconus. *Brit J Ophthalmol* 1976; 60(7):522-525.

62. Kayes J, Holmberg A. The fine structure of Bowman's layer and the basement membrane of the corneal epithelium. *Am J Ophthalmol*. 1960;50(Pt. 2):1013-1021.

63. Kennedy RH, Bourne WM, Dyer JA. A 48-year clinical and epidemiologic study of keratoconus. Am J Ophthalmol. 1986. 15; 101(3):267-73.

64. Kenney MC, Brown DJ, Rajeev B. Everett Kinsey lecture. The elusive causes of keratoconus: a working hypothesis. *CLAO J.* 2000; 26(1):10-13.

65. Kenney MC, Chwa M, Lin B, Huang GH, Ljubimov AV, Brown DJ. Identification of cell types in human diseased corneas. *Cornea*. 2001; 20(3):309-316.

66. Kenney MC, Chwa M, Opbroek AJ, Brown DJ. Increased gelatinolytic activity in keratoconus keratocyte cultures. *Cornea*. 1994; 13(2):114-124.

67. Kenney MC, Nesburn AB, Bergeson RE, Butkowski RJ, Ljubimov AV. Abnormalities of the extracellular matrix in keratoconus corneas. *Cornea*. 1997; 16(3):345-351.

68. Kikkawa Y, Hirayama K. Uneven swelling of the corneal stroma (preliminary report) [in Japanese]. *Acta Soc Ophthalmol Jpn* 1971;75:134–139.

69. Kim H, Choi JS, Joo CK. Corneal ectasia after PRK: clinicopathologic case report. *Cornea*. 2006; 25(7):845-8.

70. Kim WJ, Rabinowitz YS, Meisler DM, Wilson SE. Keratocyte apoptosis associated with keratoconus. *Exp Eye Res.* 1999; 69(5):475-481.

71. Klyce SD, Beuerman RW. Structure and function of the cornea. In: Kaufmann HE, Barron BA, McDonald MR, eds. The Cornea. Boston, Butterworth-Heinemann, Boston, 1998, p 14.

72. Komai Y, Ushiki T. The three-dimensional organization of collagen fibrils in the human cornea and sclera. *Invest. Ophthalmol. Vis. Sci.* 1991; 32:2244–2258.

73. Krachmer JH, Palay DA. *Cornea Atlas*. 2nd ed. Philadelphia: Elsevier, 2006: 178-185.

74. Krachmer JH. Eye rubbing can cause keratoconus. *Cornea.* 2004; 23(6):539-540.

75. Krauss R. Der konstruktive bau der cornea. *Z Mikrosk.* 1937;53:420-434.

76. Kremer I, Eagle RC, Rapuano CJ, Laibson PR. Histologic evidence of recurrent keratoconus seven years after keratoplasty. *Am J Ophthalmol*. 1995; 119(4):511-512.

77. Kuwabara T. Current concepts in anatomy and histology of the cornea. *Contact Intraocular Lens Med J* 1978;4:101–132.

78. Kymes SM, Walline JJ, Zadnik K, Gordon MO; Collaborative Longitudinal Evaluation of Keratoconus study group. Quality of life in keratoconus. *Am J Ophthalmol*. 2004; 138(4):527-535.

79. Lee D, Wilson G. Non-uniform swelling properties of the corneal stroma. *Curr Eye Res* 1981;1:457–461.

80. Leibowitz HM, Morello S. Keratoconus and Noninflammatory Thinning Disorders. In: Leibowitz HM, Waring GO, eds. *Corneal Disorders: Clinical Diagnosis and Management*. Philadelphia: WB Saunders Company, 1998: 349-374.

81. Li HF, Petroll WP, Moller-Pedersen T, et al. Epithelial and corneal thickness measurements by in vivo confocal microscopy through focusing (CMTF). *Curr Eye Res* 1997; 16:214-221.

82. Maeno A, Naor J, Lee H, Hunter W, Rootman D. Three decades of corneal transplantation: indications and patient characteristics. *Cornea* 2000; 19(1):7-11.

83. Maguire LJ. Ectatic Corneal Degenerations. In: Kaufman HE, Barron BA, McDonald MB, eds. *The Cornea*. 2nd ed. Boston: Butterworth-Heinemann, 1998: 525-537.

84. Mahmoud AM, Robert CJ, Lembach RG, Twa MD, Herderick EE, McMahon TT,

CLEK Study Group. CLMI: The cone location and magnitude index. Cornea. 2008; 27(4):480-487.

85. Marshall J, Grindle CFJ. Fine structure of the cornea and its development. *Trans Ophthalmol Soc UK* 1978;98:320–328.

86. Mathew JH, Bergmanson JPG, Doughty MJ. Fine structure of the interface between the anterior limiting lamina and the anterior stromal fibrils of the human cornea. *Invest Ophthalmol & Vis Sci*. 2008; 49(9): 3914-3918.

87. Mathew JH, Goosey J, Bergmanson JPG. The Undocumented Cells of Keratoconus. *Optometry and Vision Science.* 84(12s); 2009.

88. Maurice DM. The cornea and sclera. In: Davson H, ed. The Eye, 3rd ed. London, Academic Press, 1984, pp 1–158.

89. McMahon TT, Szczotka-Flynn LB. Contact Lens Applications for Ocular Trauma, Disease, and Surgery. In: Bennet ES, Weissman B. eds. *Clinical Contact Lens Practice*. Lippincott Williams and Wilkins: Philadelphia, 2005: 550-575.

90. McMonnies CW. Mechanisms of rubbing-related corneal trauma in keratoconus. *Cornea.* 2009; 28(6):607-615.

91. McPherson SD, Kiffney GT, Hill C. Some histologic findings in keratoconus. *Arch Ophthal*. 1968; 79:669-673.

92. McTigue JW. The human cornea: a light and electron microscopic study of the normal cornea and its alterations in various dystrophies. *Trans Am Ophthalmol Soc.* 1967;65:591-660.

93. Meek KM, Tuft SJ, Huang Y, Gill PS, Hayes S, Newton RH, Bron AJ. Changes in collagen orientation and distribution in keratoconus corneas. *Invest Ophthalmol*

*Vis Sci.* 2005; 46(6):1948-1956.

94. Merindano MD, Canals M, Potau JM, et al. Morphological and morphometric aspects of primate cornea: A comparative study with human cornea. *Eur J Morphol* 1997;35:95–104.

95. Morishige N, Petroll WM, Nishida T, Kenney MC, Jester J. Noninvasive corneal stromal collagen imaging using two-photon-generated second-harmonic signals. *J Cataract Refract Surg*. 2006; 32:1178-1191.

96. Morishige N, Wahlert AJ, Kenney MC, Brown DJ, Kawamoto K, Chikama T, Nishida T, Jester JV. Second-harmonic imaging microscopy of normal human and keratoconus cornea. *Invest. Ophthalmol. Vis. Sci.* 2007; 48(3):1087-1094.

97. Müller LJ, Pels E, Vrensen GFJM. The effects of organ-culture on the density of keratocytes and collagen fibers in human corneas. *Cornea* 2001; 20(1):86–95.

98. Müller LJ, Pels E, Vrensen GFJM. The specific architecture of the anterior stroma accounts for maintenance of corneal curvature. *Br J Ophthalmol*. 2001; 85(4):437-443.

99. Myrowitz EH, Melia M, O'Brien TP. The relationship between long term contact lens wear and corneal thickness. *CLAO J.* 2002; 28(4):217–220.

100. Nakamura H, Riley F, Sakai H, Rademaker W, Yue BYJT, Edward DP. Histopathological and immunohistochemical studies of lenticules after epikeratoplasty for Keratoconus. *Br. J. Ophthalmol*. 2005; 89(7):841-846.

101. Navas A, Ariza E, Haber A, Fermón S, Velázquez R, Suárez R. Bilateral keratectasia after photorefractive keratectomy. *J Refract Surg*. 2007; 23(9):941-3.

102. Newell F. Ophthalmology: Principles and Concepts. St. Louis: CV Mosby, 1982: 9.

103. Nichols JJ, Steger-May K, Edrington TB, Zadnik K; CLEK study group. The relation between disease asymmetry and severity in keratoconus. *Br J Ophthalmol*. 2004 ;88(6):788-91.

104. Nirankari VS, Karesh J, Bastion F, Lakhanpal V, Billings E. Recurrence of keratoconus in donor cornea 22 years after successful keratoplasty. *Br J Ophthalmol*. 1983; 67(1):23-8.

105. Nishida T. Cornea. In: Krachmer JH, Mannis MJ, Holland EJ, eds. *Cornea, Vol 1: Fundamentals, Diagnosis and Management*. 2nd ed. Philadelphia: Elsevier; 2005:3-26.

106. Nottingham J. *Practical observations on Conical Cornea, and on the short sight, and other defects of vision connected with it.* London: Churchill, 1854.

107. Ojeda JL, Ventosa JA, Piedra S. The three-dimensional microanatomy of the rabbit and human cornea. A chemical and mechanical microdissection-SEM approach. *J Anat.* 2001; 199(5):567–576.

108. Oyster CW. The Human Eye. Sunderland, MA, Sinauer Associates, 1999, p 328.

109. Patel SV, Malta JB, Banitt MR, Mian SI, Sugar A, Elner VM, Tester RA, Farjo QA, Soong HK. Recurrent ectasia in corneal grafts and outcomes of repeat keratoplasty for keratoconus. *Br J Ophthalmol*. 2009; 93(2):191-7.

110. Patey A, Savoldelli M, Pouliquen Y. Keratoconus and normal cornea: A comparative study of the collagenous fibers of the corneal stroma by image analysis. *Cornea.* 1984; 3(2):119–124.

111. Pearson RM. Kalt, Keratoconus, and the Contact Lens. *Optom. and Vis. Sci.* 1989; 66(9):643-646.

112. Pinsky PM, Van Der Heide D, Chernyak D. Computational modelling of mechanical anisotropy in the cornea and sclera. *J Cataract Refract Surg*. 2005; 31(1):136-145.

113. Pouliquen Y, D'Hermies F, Peuch M, et al. Acute corneal edema in pellucid marginal degeneration or acute marginal keratoconus. *Cornea.* 1987; 6(3):169–174.

114. Pouliquen Y, Faure JP, Bisson J, et al. La zone fibrillaire acellulaire sous-épithéliale de la cornée de l'embryon de poulet. Ses rapports avec la formation de la membrane basale de l'épithelium et de la membrane de Bowman. *Arch Ophtalmol* (Paris). 1966;26:59-68.

115. Pouliquen Y, Graf B, Hamada R, Giraud JP, Offret G. Fibrocytes in keratoconus. Morphological appearance and change in the extracellular spaces. Optical and electron microscopic study. Arch Opthalmol. 1972; 32(8):571-586.

116. Pouliquen Y. Keratoconus. *Eye* 1987;1:1–14.

117. Pouliquen YJM. Fine structure of the corneal stroma. *Cornea* 1985;3:168–177.

118. Pramanik S, Musch DC, Sutphin JE, Farjo AA. Extended long-term outcomes of penetrating keratoplasty for keratoconus. Ophthalmology. 2006; 113(9):1633-1638.

119. Rabinowitz Y. Ectatic Disorders of the Cornea. In: Foster CS, Azar DT, Dohlman CH, eds. *The Cornea: Scientific Founations & Clinical Practice*, 4th ed. Philadelphia: Lippincott Williams & Wilkins, 2005: 889-911.

120. Rabinowitz YS. Keratoconus: Major Review. *Surv Ophthalmol*. 1998;42(4):297-319.

121. Rabinowitz YS. The Cornea: Scientific Foundations & Clinical Practice 4th ed. ed Foster CS, Azar DT, Dohlman CH. Ch. 49: Ectatic Disorders of the Cornea. P889-911, 2005. Lippincott Williams & Wilkins, Philadelphia.

122. Radner W, Zehetmayer M, Aufreiter R, Mallinger R. Interlacing and cross-angle distribution of collagen lamellae in the human cornea. *Cornea.* 1998; 17(5):537–543.

123. Radner W, Zehetmayer M, Mallinger R, et al. Zur dreidimensionalen Anordnung der kollagenen Lamellen im posterioren Stroma der menschlichen Hornhaut. *Spektrum Augenheilkd.* 1993;7:77-80.

124. Rohrbach JM, Szurman P, El-Wardani M, Grub M. About the frequency of excessive epithelial basement membrane thickening in keratoconus. *Klin Monatsbl Augenheilkd*. 2006; 223(11):889-893.

125. Salzmann M. *The Anatomy and Histology of the Human Eyeball in the Normal State.* Translated by Brown EVL. Chicago: Photopress Inc; 1912;31-35.

126. Sawaguchi S, Fukuchi T, Abe H, Kaiya T, Sugar J, Yue BYJT. Three-dimensional scanning electron microscopic study of Keratoconus corneas. *Arch Ophthalmol.* 1998; 116:62-68.

127. Schwartz W, Keyserlingk DG. Über die Feinstruktur der menschlichen Cornea, mit desorderer Berücksichtigung des Problems der Transparenz. *Z Zellforsch* 1966;73:540–548.

128. Scroggs MW, Proia AD. Histophathological variation in keratoconus. *Cornea*. 1992; 11(6):553-559.

129. Shapiro MB, Rodriquez MM, Mandal MR, Krachmer JH. Anterior clear spaces in Keratoconus. *Ophthalmol*. 1986; 93(10):1316-1319.

130. Simpson GV. Corneal edema. *Trans Am Ophthalmol Soc* 1949;47:692–737.

131. Sturbaum CW, Peiffer RL. Pathology of corneal endothelium in keratoconus. *Ophthalmologica*. 1993; 206(4):192-208.

132. Sugar J. Stromal Corneal Dystrophies and Ectasias. In: Yanoff M, Duker JS, eds. *Ophthalmology*. 2nd ed. Philadelphia, PA: Mosby, 2004: 442-444.

133. Takahashi A, Nakayasu K, Okisaka S, et al. Quantitative analysis of collagen fiber in keratoconus. *Acta Soc Ophthalmol Jpn* 1990;94:1068–1073.

134. Teng CC. Electron microscope study of the pathology of keratoconus: part I. *Am J Ophthalmol.* 1963; 55:18-47.

135. Thomas CI. *The Cornea.* Springfield, IL: Charles C. Thomas; 1955:19.

136. Thota S, Miller WL, Bergmanson JPG. Acute corneal hydrops: A case report including confocal and histopathological considerations. *Contact Lens & Ant Eye*. 2006; 29(2):69-73.

137. Trinkaus-Randall V, Edelhauser HF, Leibowitz HM, et al. Corneal structure and function. In: Leibowitz HM, Waring GO, eds. Corneal Disorders. Clinical Diagnosis and Management. Philadelphia, WB Saunders, 1998, p 16.

138. Tsubota K, Mashima Y, Murata H, Sato N, Ogata T. Corneal epithelium in Keratoconus. *Cornea*.1995;14(1):77-83.

139. Twa MD, Nichols JJ, Joslin CE, Kollbaum PS, Edrington TB, Bullimore MA, Mitchell GL, Cruickshanks KJ, Schanzlin DJ. Characteristics of corneal ectasia after LASIK for myopia. *Cornea*. 2004; 23(5):447-57.

140. Waring GO. Refractive Surgery. In Leibowitz HM, Waring GO eds. *Corneal Disorders: Clinical Diagnosis and Management*. 2nd ed. Philadelphia: WB Saunders; 1998: 1023-1105.

141. Wilson S, Mohan R, Hutcheon A, Mohan R, Ambrosio R, Zieske J, Hong J, Lee J. Effect of ectopic epithelial tissue within the stroma on keratocye apoptosis, mitosis, and myofibroblast transformation. *Exp Eye Res.* 2003; 76(2):193-201.

142. Wilson SE, He YG, Weng J, Li Q, McDowall AW, Vital M, Chwang EL. Epithelial injury induces keratocytes apoptosis: hypothesized role for the interleukin-1 system in the modulation of corneal tissue organization and wound healing. *Exp. Eye Res*. 1996; 62(4):325-337.

143. Woodward EG, Rubinstein MP. Keratoconus. In: Phillips AJ, Speedwell L, eds. *Contact Lenses*, 5th ed. Philadelphia, PA: Elsevier, 2007: 451-467.

144. Yanoff M, Sassani JW. *Ocular Pathology*, 6th ed. China: Mosby, 2009: 302-305.

145. Young C, Miller W, Leach N, Horne J, Busuioc C, Perrigin D, Bergmanson J. Tear, staining and corneal sensitivity profile in keratoconus. What is abnormal? *Optometry and Vision Science* 2005; 82(12s): abstract #055051.

146. Zadnik K, Barr JT, Edrington TB, Everett DF, Jameson M, McMahon TT, Shin JA, Sterling JL, Wagner H, Gordon MO. Baseline findings in the Collaborative Longitudinal Evaluation of Keratoconus (CLEK) Study. *Invest Ophthalmol Vis Sci.* 1998; 39(13):2537-2546.

147. Zhao LQ, Wei RL, Cheng JW, Li Y, Cai JP, Ma XY. Meta-analysis: clinical outcomes of laser-assisted subepithelial keratectomy and photorefractive keratectomy in myopia. Ophthalmology. 2010; 117(10):1912-22.